

NOAA Technical Memorandum NMFS



APRIL 2017

MOBILE ACOUSTIC SAMPLING TO MAP BATHYMETRY AND QUANTIFY THE DENSITIES AND DISTRIBUTIONS OF SALMONID SMOLT PREDATORS IN THE SAN JOAQUIN RIVER

G.R. Cutter Jr., S.C. Manugian, J. Renfree, J. Smith, C. Michel, D. Huff,
T.S. Sessions, B.E. Elliot, K. Stierhoff, S. Mau, D. Murfin, and D.A. Demer

NOAA-TM-NMFS-SWFSC-575

U.S. DEPARTMENT OF COMMERCE
National Oceanic and Atmospheric Administration
National Marine Fisheries Service
Southwest Fisheries Science Center

The National Oceanic and Atmospheric Administration (NOAA), organized in 1970, has evolved into an agency that establishes national policies and manages and conserves our oceanic, coastal, and atmospheric resources. An organizational element within NOAA, the Office of Fisheries, is responsible for fisheries policy and the direction of the National Marine Fisheries Service (NMFS).

In addition to its formal publications, NMFS uses the NOAA Technical Memorandum series to issue informal scientific and technical publications when complete formal review and editorial processing are not appropriate or feasible. Documents within this series, however, reflect sound professional work and may be referenced in the formal scientific and technical literature.

SWFSC Technical Memorandums are accessible online at the SWFSC web site (<http://swfsc.noaa.gov>). Print copies are available from the National Technical Information Service, 5285 Port Royal Road, Springfield, VA22151 (<http://www.ntis.gov>).

NOAA Technical Memorandum NMFS

This TM series is used for documentation and timely communication of preliminary results, interim reports, or special purpose information. The TMs have not received complete formal review, editorial control, or detailed editing



APRIL 2017

**MOBILE ACOUSTIC SAMPLING TO MAP
BATHYMETRY AND QUANTIFY THE DENSITIES AND
DISTRIBUTIONS OF SALMONID SMOLT PREDATORS
IN THE SAN JOAQUIN RIVER**

G.R. Cutter Jr.¹, S.C. Manugian², J. Renfree¹, J. Smith³, C. Michel², D. Huff⁴,
T.S. Sessions¹, B.E. Elliot⁵, K. Stierhoff¹, S. Mau¹, D. Murfin¹, and D.A. Demer¹

¹ NOAA Southwest Fisheries Science Center

² University of California Santa Cruz

³ University of Washington

⁴ NOAA Northwest Fisheries Science Center

⁵ NOAA OMAO

NOAA-TM-NMFS-SWFSC-575

U.S. DEPARTMENT OF COMMERCE

Wilbur L. Ross, Secretary of Commerce

National Oceanic and Atmospheric Administration

Benjamin Friedman, Acting NOAA Administrator

National Marine Fisheries Service

Samuel D. Rauch III, Acting Assistant Administrator for Fisheries

Mobile Acoustic Sampling to Map Bathymetry and Quantify the Densities and Distributions of Salmonid Smolt Predators in the San Joaquin River

G.R. Cutter Jr.¹, S.C. Manugian², J. Renfree¹, J. Smith³, C. Michel², D. Huff⁴, T.S. Sessions¹, B.E. Elliot⁵, K. Stierhoff¹, S. Mau¹, D. Murfin¹, and D.A. Demer¹

¹ NOAA Southwest Fisheries Science Center

² University of California Santa Cruz

³ University of Washington

⁴ NOAA Northwest Fisheries Science Center

⁵ NOAA OMAO

April, 2017

¹ Fisheries Resources Division
Southwest Fisheries Science Center
National Marine Fisheries Service
National Oceanic and Atmospheric Administration
8901 La Jolla Shores Drive
La Jolla, CA 92037, USA

² University of California Santa Cruz
Cooperative Institute for Marine Ecosystems and Climate (CIMEC)
Earth and Marine Sciences Building
Santa Cruz, CA 95064, USA
(Affiliated with Southwest Fisheries Science Center)

³ School of Aquatic and Fishery Sciences
University of Washington
1122 N.E. Boat Street, Box 355020,
Seattle, WA 98195-5020, USA

⁴ Fish Ecology Division
Northwest Fisheries Science Center
National Marine Fisheries Service
National Oceanic and Atmospheric Administration
2725 Montlake Blvd E
Seattle, WA 98112, USA

⁵ Office of Marine and Aviation Operations
National Oceanic and Atmospheric Administration

Suggested citation: G. R. Cutter Jr., S. C. Manugian, J. Renfree, J. Smith, C. Michel, D. Huff, T.S. Sessions, B. E. Elliot, K. Stierhoff, S. Mau, D. Murfin, and D. A. Demer. 2017. Mobile Acoustic Sampling to Map Bathymetry and Quantify the Densities and Distributions of Salmonid Smolt Predators in the San Joaquin River. NOAA Technical Memorandum, NOAA-TM-NMFS-SWFSC-575. 134 pp.

Contents

Mobile Acoustic Sampling to Map Bathymetry and Quantify the Densities and Distributions of Salmonid Smolt Predators in the San Joaquin River	1
Abstract.....	5
Introduction	6
Methods.....	8
Study area.....	8
Vessel and instrumentation.....	11
Riverbed bathymetry	12
Riverbed terrain.....	14
Multibeam detection of fish and submerged aquatic vegetation.....	14
River conditions	14
Acoustic surveys of fish.....	15
Sonar calibration	16
Operational settings	16
Target strength modeling.....	17
Fish target detection	18
Echo track detection.....	18
Spatial transformations	19
Echo-track filtering.....	20
Sampled volume estimation.....	21
Beam sampled volume weighted by target-detection probability.....	22
River segmentation.....	24
Fish target counts, density, and abundance estimates	25
Sizes of detected targets	26
Results and Discussion.....	27
River Bathymetry	27
Riverbed terrain classes	37

Submerged aquatic vegetation.....	40
Fish TS modeling.....	42
Single target detections.....	44
Echo tracks.....	45
Fish density and abundance estimates.....	48
Areas with persistent high densities.....	74
Fish density comparisons.....	76
River conditions.....	91
Target identification and fish species composition	96
Fish habitat associations	98
Conclusion.....	100
Acknowledgements	101
References.....	101
Appendix.....	105

Abstract

Salmon smolt mortality in the Sacramento-San Joaquin River (SJR) system of central California is impacted by predatory fish. To quantify the abundance, distribution, and habitats of these predators, we devised and implemented novel active-acoustic methods to sample the fish and bathymetry in this shallow-water environment. Acoustic surveys using vertically- and horizontally-oriented split-beam and multibeam sonars were conducted between March and May, 2014 and 2015, from the Port of Stockton to Lathrop, California. Individual fish were acoustically detected using single-target detection and echo-track processing methods, and aggregated fish counts were converted to densities and abundances by compensating for the sampled volumes of the acoustic beams, the probability of target detections, and the river volume. Volume was estimated from 1-by-1-m grid-cell bathymetric maps produced from M3 multibeam sonars for the 26-km study area. Bathymetric mapping and target detection efforts were complicated by the low grazing angles, high-reverberation and clutter, and strong second bottom returns induced by the shallow river environment. Riverbed habitats were discriminated by morphology and backscatter intensity, and bathymetry data were used to constrain sonar detections of fish. Additionally, novel signal processing of M3 water-column data was used to map submerged aquatic vegetation (SAV) beds and to detect fish among clutter. Predators were associated with certain riverbed features and SAV along the part of the route that salmon smolt migrate to the ocean. Fish densities were highly variable in both space and time, however, persistently high densities occurred in many deep pools in the bends of the river.

Introduction

For over a century, the rivers of California's Central Valley have been controlled using an assortment of flow-regulated aqueducts, ranging from rim dams to leveed channels. As a result, nearly every aspect of the watershed has been altered from its natural state. Furthermore, numerous predatory fish species have been introduced to the Sacramento-San Joaquin River Delta (e.g., largemouth bass [*Micropterus salmoides*] and striped bass [*Morone saxatilis*]), are abundant (Nobriga et al. 2003, Nobriga and Feyrer 2007), and prey on salmon. Native salmonid populations have declined significantly. For example, three Chinook stocks (*Oncorhynchus* sp.) are now endangered (Chinook winter run) or threatened (Chinook and steelhead spring runs) under the Endangered Species Act. A third Chinook stock (fall run) is still commercially and recreationally harvested. Salmonid smolt predation may increase the risk or rate of potential extinction for some of these stocks (Lindley and Mohr 2003). To mitigate this potential, the initial challenge is to obtain accurate estimates of the distributions and abundances of salmon and predatory fishes throughout the Delta (Michel 2010, Carey et al. 2012). Also needed is detailed information on their riverbed habitats.

Grossman et al. (2013) concluded that there are presently no available methods to assess the populations of fish that prey upon juvenile salmon. Animals in the ocean are routinely surveyed using acoustic methods, but there is additional complexity when those methods are applied to surveys conducted in rivers and estuaries. These additional challenges include detecting and classifying multiple fish species and sizes and that fish can be located near boundaries in shallow reverberant environments (Trevorrow, 1998). Echosounders and imaging sonars can be used to detect fish in streams and rivers, but those deployed in fixed locations may be of little value for studies of non-migratory species. Transducers deployed on mobile platforms are limited by blind spots, low detectability due to reverberation in the stream or river, and poor discrimination among species and non-fish scatterers, particularly in near-boundary habitats occupied by demersal species (Hateley and Gregory 2006). To mitigate these potential errors in detection, researchers increasingly augment data from multi-frequency echosounder surveys with samples from other acoustic instruments such as multibeam echosounders (Cox et al. 2009, Cox et al. 2010, Cutter and Demer 2007), multibeam imaging sonars (Korneliussen et al. 2009, Patel and Ona 2009), and long-range scanning sonars (Bernasconi et al. 2009, Stockwell et al. 2013). These data can be used to model and measure known targets and create "acoustic signatures" (Conti and Demer 2003, Demer and Conti 2003, Graham et al. 2010, Renfree et al. 2009) so echoes from organisms with known signatures can be separated from the "noise" (De Robertis et al. 2010, Demer et al. 2009) and apportioned to target species.

Even without use of multi-frequency echosounders, surveys of fish in shallow rivers and lakes have been successful using non-standard sonar deployments. Horizontal sonar beams have proven effective for detection and enumeration of migrating fish from fixed-location (Steig and Johnston 1996, Tuser et al. 2009) and mobile surveys (Kubecka and Wittingerova 1998, Lyons 1998). The orientation of fish has a strong influence on the echoes received by the sonar and outweighs size effects. By directing beams horizontally normal to the migration direction of fish in restricted passages (Tuser et al. 2009)

orientation effects on target strength (*TS*) may be reduced. However, orienting beams horizontally and directed to the side, whereby fish are more likely to be insonified in side-aspect (Lyons 1996), reduces the number of echoes received and the probability of detection, potentially leading to biased density estimates. Orienting beams directly or diagonally forward increases the number of echoes from targets, the probability of resolving individuals, and detections near normal incidence.

Fish densities may be estimated from acoustic echoes or echo tracks detected along survey transects (Ehrenberg and Lytle 1972) after accounting for sample volumes and probability of detection (Mulligan and Kieser 1996). Fish distributions may be mapped for multiple target species in relation to their acoustically mapped habitats. Fish abundances may be estimated by multiplying their densities by associated habitat areas.

This investigation was conducted in support of a predator-density manipulation study conducted by colleagues at the NOAA Fisheries Santa Cruz Laboratory, in collaboration with the California Department of Fish and Wildlife (CDFW) and funded by the California Department of Water Resources (CADWR) agreement #4600010100. The principal objectives were to:

1. develop and improve methods for acoustically detecting, sizing, and enumerating predators of salmonid smolt in the Delta, and concurrently mapping the riverine bathymetry;
2. survey an approximately 26-km stretch of the San Joaquin River, between Lathrop, near the Head of Old River, and Port of Stockton during spring 2014 and 2015;
3. survey the Clifton Court Forebay and a section of the Deep-water shipping channel near Morrison Island and Vulcan Island during spring 2015;
4. estimate predator densities and sizes, and map their spatial distributions for each survey period;
5. map bathymetry and characterize the habitats of salmon-smolt predators using environmental factors such as tide, water flow and temperature, and locations of river bank, thalweg, and scour holes;
6. explore relationships between salmon-smolt predators and their habitats; and
7. quantify and map the abundances of salmon-smolt predators versus time.

Acoustic methods for surveying fish and bathymetry in the Delta were developed, applied to the San Joaquin River from Port of Stockton to Lathrop, California during spring 2014, and refined and re-applied in the same region during spring 2015. Bathymetry was mapped and classified; fish were detected, classified by their estimated sizes, and enumerated; and time series of fish densities and abundances were created.

Methods

Study area

The main study area included a 26-km portion of the San Joaquin River (SJR), between Port of Stockton and Lathrop (Figures 1 and 2). This area was surveyed during March to June 2014 (Julian day, JD 2014-083 – 2014-142) and April to May 2015 (JD 2015-096 – 2015-140, Table A01). During spring 2015, two additional areas in the vicinity of Stockton, California, were surveyed (Figure 1), including Clifton Court Forebay (CCF; 37.8389° N, -121.5738° W) and a section of the Deep-water shipping channel (DWSC) near Morrison Island and Vulcan Island (37.9958° N, -121.4147° W and 37.9810° N, -121.4049° W).

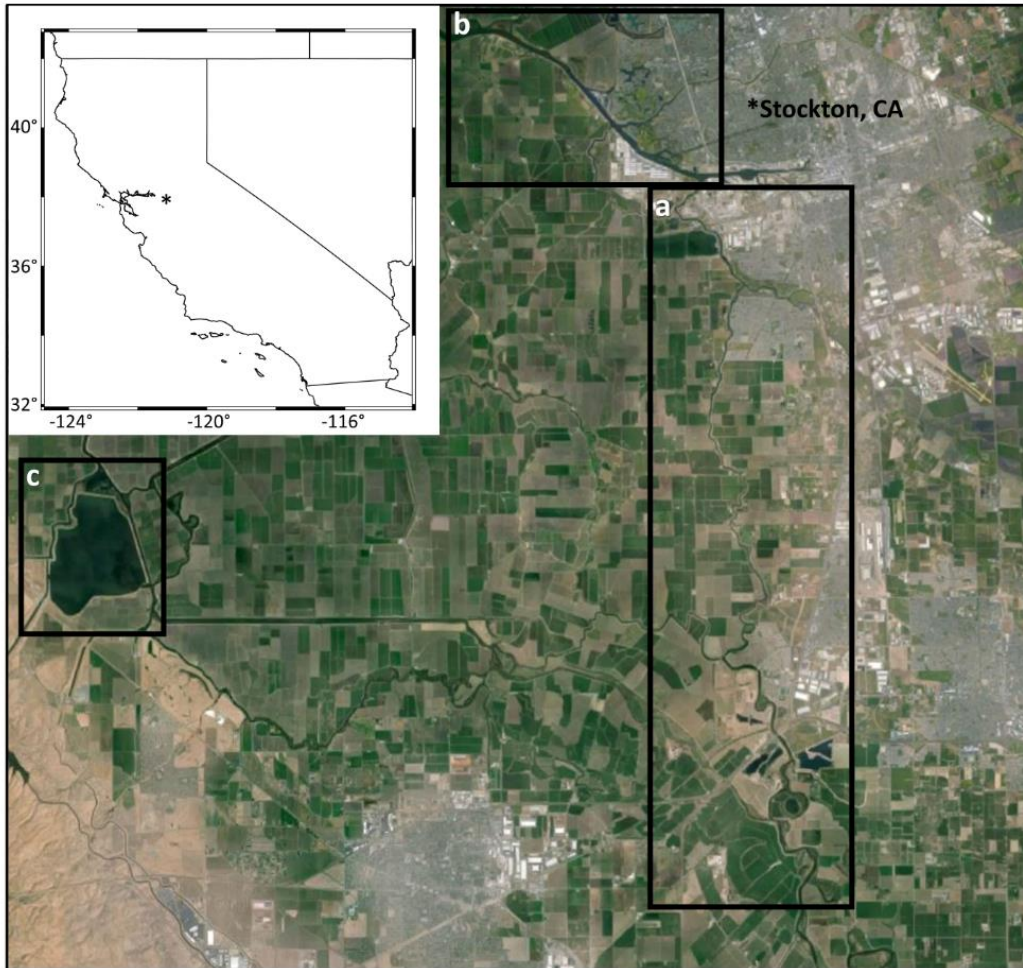


Figure 1. The surveyed areas near Stockton, California, included a) San Joaquin River, from Port of Stockton to Lathrop; b) San Joaquin River deep-water shipping channel; and c) Clifton Court Forebay.

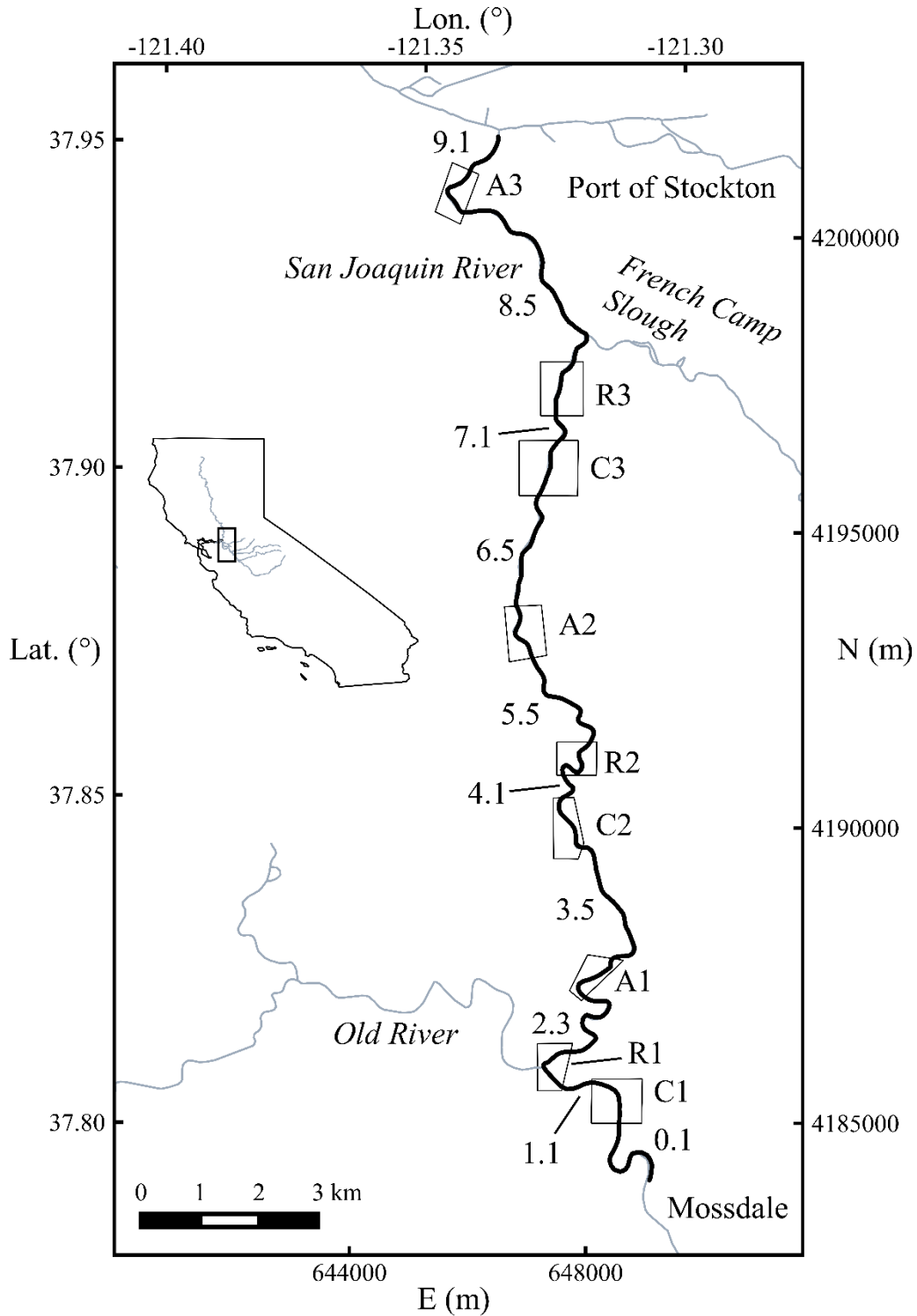


Figure 2. The principal study region in the San Joaquin River, between the head of the Old River and the Port of Stockton, included nine study reaches, evenly divided between three experimental blocks.

The principal study area (Figure 1a) contained three experimental blocks that each included a 1-km long control (C), removal (R), and addition (A) reach (Figure 2, Table A02). During one week each year, fish were removed from the R reaches and relocated to the A reaches within their respective blocks for predator-density manipulation experiments (Smith and Michel, *pers. comm.*).

Vessel and instrumentation

A 6-m long aluminum skiff was used for all of the surveys, but it was equipped differently each year (Figure 3). In 2014, a pole-mounted transducer array included: a single 500-kHz broad-bandwidth, split-beam multibeam sonar (Mesotech M3) to measure bathymetry to the port side of the vessel; a 120-kHz elliptical split-beam sonar (Simrad-Kongsberg EK60) to track and enumerate fishes to the port side of the vessel; and a vertically-oriented 200-kHz conical single-beam echosounder (Simrad-Kongsberg ES15) to measure depth beneath the vessel.

In 2015, a bow-mounted transducer array included: two 500-kHz broad-bandwidth, split-beam multibeam sonars (Mesotech M3) to measure bathymetry and detect fish to both port and starboard; a 120-kHz elliptical split-beam sonar (Simrad-Kongsberg EK60) to track and enumerate fishes in front of the vessel; and a 200-kHz conical split-beam echosounder (Simrad-Kongsberg EK60) to track and enumerate fishes beneath the vessel. A camera was used to concurrently image above the water in the direction of the side- and forward-looking acoustic observations.

Vessel position, motion, and orientation were measured by a position and motion sensor system (Applanix POS-MV Wavemaster V4). With corrections from a differential geographic positioning system (GPS) receiver, position estimates were accurate to ≤ 0.5 m. The GAMS (GNSS Azimuth Measurement System) heading solution provided enhanced heading accuracy ($< 0.1^\circ$).

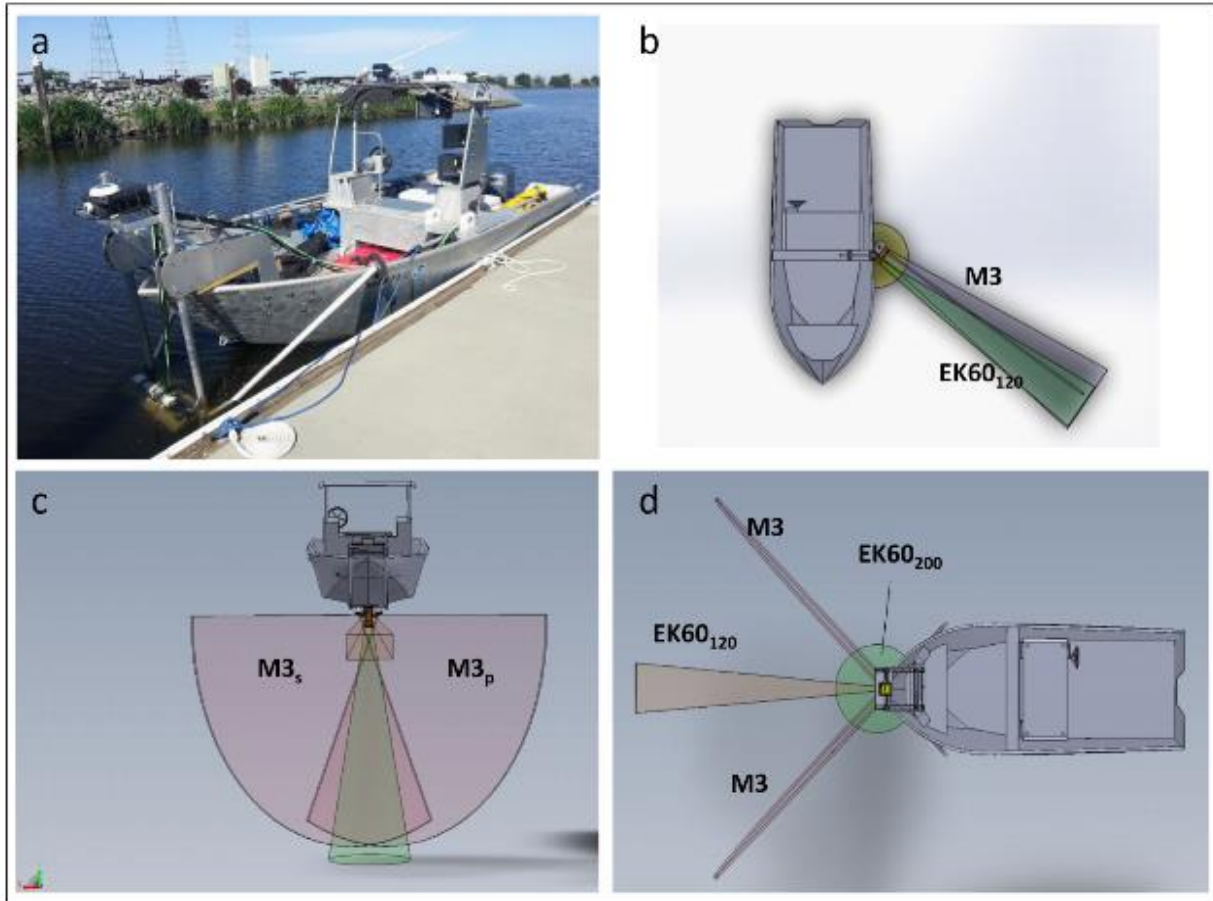


Figure 3. Fish and riverbed bathymetry were acoustically sampled to the port side (in 2014) and both beneath and ahead (in 2015) of the 6-m long survey vessel (a). In spring 2014, a pole-mounted transducer array was deployed from the side of the vessel (b) including a 500-kHz M3 multibeam sonar, a side 120-kHz elliptical split-beam transducer, and a 70-kHz conical split-beam wide-bandwidth transducer. The side sonar beams and the multibeam swath were rotated in azimuth by 45° to increase the potential number of fish detections. In spring 2015, a dual-head M3 multibeam system was deployed from a bow mount (c-d). The EK60-120 kHz beam was directed forward and EK60-200 kHz beam was directed downward.

Riverbed bathymetry

The M3 multibeam sonar was operated in ‘profile mode’ to simultaneously measure riverbed bathymetry and detect fish (Figure 4). The multibeam transducer was rotated 30° from vertical so that the 120° swath would insonify angles spanning from horizontal to 30° past vertical on the opposite side of the vessel, and at 45° from forward to increase target detections from fish (Figure 3). The M3 was operated in ‘fast-profiling mode’ with a ping rate of 5 to 10 Hz, and ‘soundings’ were recorded to Simrad ‘.all’ files and used to map river bathymetry.

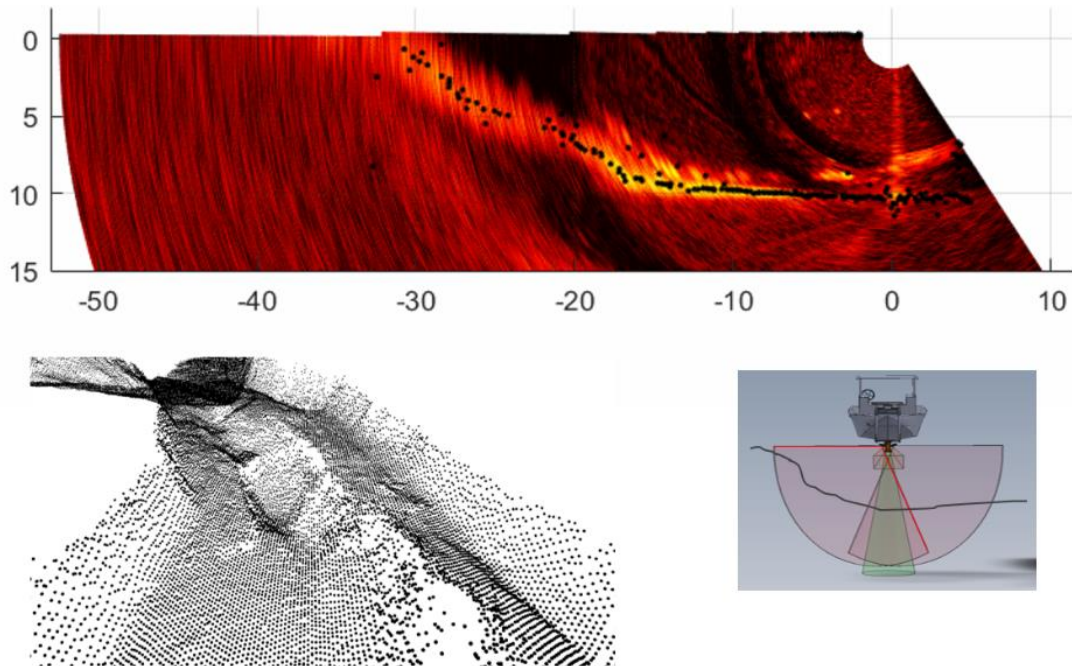


Figure 4. Top: Example echogram from a 500-kHz multibeam sonar used to simultaneously map bathymetry (black soundings) and detect fishes beneath and to the side of the vessel. Backscatter intensity (increasing from red to yellow) is plotted versus range from the transducer (0-50 m) and steering angle (120° swath). Bottom left: Soundings from the M3. Bottom right: Front view of the survey vessel and dual-multibeam swath coverage (M3 beam footprints are red, EK60-200 kHz beam is green).

The multibeam bathymetry data were corrected for water-level elevations and vessel motion using POS-MV data recorded into the .all files. Soundings data were then “cleaned” by removal of outliers using commercial software (CARIS HIPS-SIPS v. 9.0). Static translation and angular offset values were estimated using patch-test data and offset estimation procedures in HIPS & SIPS. Soundings were interpolated as gridded surfaces of various cell sizes (50 cm, 1 m, and 2 m) created using commercial hydrographic software and GIS analysis software (QPS Fledermaus; SAGA-GIS). Bathymetric and derivative products are reported from the 1-m surfaces.

River stage (water level) data from five river monitoring stations within and close to the SJR study area (north to south: RRI, SJG, BDT, SJL/SJD, MSD) were obtained from the California Department of Water Resources (DWR) California Data Exchange Center (water quality sampling stations: <http://www.cd.water.ca.gov/delta/ECstations.cfm>; data: http://cdec.water.ca.gov/cgi-progs/selectQuery?station_id=BDT&sensor_num=1&dur_code=E&start_date=&end_date=now). Using the tide zoning process in HIPS & SIPS, water level was estimated for every survey location and sounding time based on spatial and temporal filtering of data from each of the river monitoring stations, and soundings data were compensated for these zoned water levels.

Soundings and gridded products were referred vertically to the NAVD-1988 datum, and horizontally to the WGS84 ellipsoid and a Universal Transverse Mercator (UTM) zone 10-north projection with Easting and Northing horizontal coordinates in units of meters.

Riverbed terrain

Riverbed terrain classes were derived from the 1-m grid digital elevation model (DEM) of the SJR. Ten standard terrain classes representing categories of slope and local curvature quantities were produced using the method of Iwahashi and Pike (2007) implemented in SAGA-GIS (Conrad et al. 2015). Those ten classes were combined, based on spatial contiguity, to represent five riverbed classes: deep pools, pool margins, channels and runs, channel and bedform margins, and bank edges and steep slopes. These classes were coincident with visually apparent features in the bathymetry.

Multibeam detection of fish and submerged aquatic vegetation

Submerged aquatic vegetation (SAV) and fish were detected in the M3 multibeam sonar data. The detection algorithm used constant false alarm rate (CFAR) target detection techniques (Acosta and Villar 2015) in combination with filtering based on discrete wavelet transforms. Both fish and SAV targets were detected by the CFAR algorithm, and those were separated in post processing based on their spatial aggregation properties and target intensity distributions.

River conditions

River conditions, in addition to water level including flow and velocity, were obtained from the five river monitoring stations previously mentioned (north to south: RRI, SJG, BDT, SJL / SJD, MSD). Daily statistics (mean, standard deviation, minimum, and maximum) were calculated for each variable for each station.

Between 22 April and 21 May 2015, a CTD (Seabird SeaCAT 19plus V2) with a dissolved oxygen sensor (SBE 43) was mounted on the bow of the vessel. These sensors were calibrated by Seabird in 2007. The CTD was operated in 'profile mode' with a 10-s pump delay and averaged every four scans. The result was a sample every 10 s. Raw data were stored internally while filtered and converted data were output to a text log for monitoring during the survey. The CTD-data collection was started and stopped using a magnetic switch. At the beginning of the survey, the CTD clock was synchronized with the clock on the vessel's operating computer (UTC via GPS feed) to allow all data to be indexed by the same time.

The measured conductivity ($S\ m^{-1}$), depth (fresh water, m), temperature (ITS-90, degrees), salinity practical (psu), oxygen SBE 43 ($mg\ l^{-1}$), and oxygen saturation ($mg\ l^{-1}$) were output

from the Seabird terminal program. Other than being modified by calibration coefficients and averaged, no additional processing was done.

Acoustic surveys of fish

Salmon predators and their riverbed habitats were acoustically sampled using a 120-kHz echosounder (Simrad EK60) and an elliptical, split beam transducer (Simrad ES120-4x10) oriented 45° to the side in 2014, and forward in 2015. Fish were detected below the vessel using 200-kHz echosounders: a Simrad ES15 with single-beam transducer in 2014; and a Simrad EK60 with ES200-7C split-beam transducer in 2015 (Figure 5).

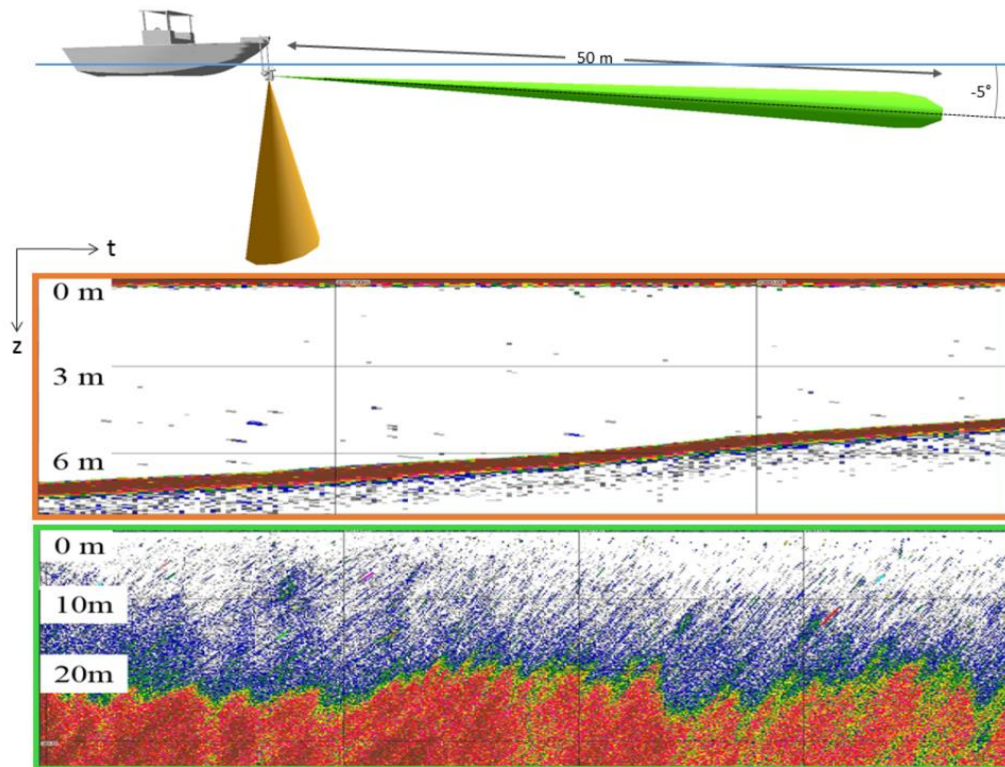


Figure 5. Top: A diagram of the survey vessel and fisheries sonar beams: 200-kHz vertical (orange) and 120-kHz forward (green). Center and bottom: Example echograms showing fish echoes (diagonal streaks) above the riverbed echoes (mostly red) measured using a 200-kHz vertical sonar (center, orange outline), and side (2014) and forward (2015) 120-kHz sonars (bottom, green outline). Vertical axes in the echograms are range (z; m) and horizontal axes are time (t; s).

Sonar calibration

On 14 March 2014, the 120-kHz sonar (Simrad EK60) with elliptical-beam transducer (Simrad ES120-4x10) was calibrated in the Southwest Fisheries Science Center's (SWFSC) Technology Development Tank using a 38.1-mm diameter sphere made of tungsten-carbide with 6% cobalt binder. Calibrations were done for three pulse durations: 256, 512, and 1014 μ s. On 16 April 2015, prior to the 2015 surveys, the 120-kHz and 200-kHz EK60 sonars were calibrated in the SWFSC tank for pulse duration of 128 μ s (Table 1).

Table 1. EK60 calibration parameters for the pulse durations used during survey.

Parameter	2014 side	2015 forward	2015 downward
Frequency (kHz)	120	120	200
Model	ES120-4x10	ES120-4x10	ES200-7C
Transmit Power (W)	250	50	25
Pulse Duration ($s * 10^{-3}$)	0.256	0.128	0.128
Alongship beam angle (deg.)	4.4	4.4	7.0
Alongship offset (deg.)	0	0	0
Athwartship beam angle (deg.)	9.0	9.0	7.0
Athwartship offset (deg.)	0	0	0
EBA (dB)	-17.3	-17.3	-20.8
Athwartship angle sensitivity	18	18	23
Alongship angle sensitivity	36	36	23
Absorption ($dB km^{-1}$)	43.4	3.74	9.8
Transducer Gain, GTS (dB)	25.36	22.50	26.80
Sa Correction (dB)	-0.66	0	0
RMS (dB)	0.26	0.23	0.19

Operational settings

Sonar surveys were conducted using the transmit powers listed in Table 1, and pulse durations of 256- μ s during 2014 and 128- μ s during 2015, to obtain range resolutions of approximately 19 cm and 10 cm, respectively. For all the EK60 sonars, operating range was 50 m, transmit rate was 10 Hz, and all EK60s and M3s were synchronized for simultaneous transmissions.

Target strength modeling

Striped bass (STB) and largemouth bass (LMB) larger than 15 cm, and channel catfish (CHC; *Ictalurus punctatus*) and white catfish (WHC; *Ameiurus catus*) larger than 20 cm are the common predators of salmonid smolts in the Delta (J. Smith & C. Michel, pers. comm.).

X-radiographs of predator-sized STB, LMB, CHC, WHC and black crappie (BLC) were acquired (Figure 6) to define shapes of the fishes' bodies and swim-bladders for use in models of their TS values. TS -model results aid in the differentiation of echoes from fish predators versus other targets such as smaller fish, plants, and floating debris.

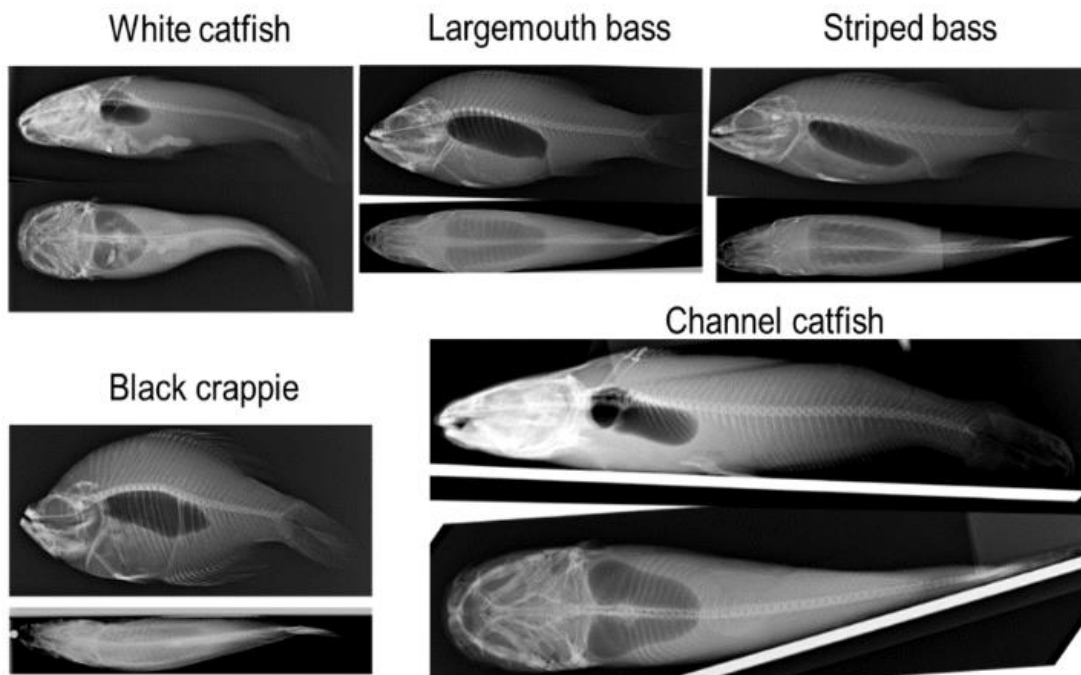


Figure 6. Example X-radiographs of salmon predator species, showing the lateral and dorsal shapes of the fish body and swim bladder.

A Kirchoff Ray-Mode (KRM) model (<http://swfscdata.nmfs.noaa.gov/AST/KRM/krm.html>) was used to predict dorsal and lateral backscattering cross-sectional areas σ_{bs} of fish by size, orientation, and acoustic frequency.

Values of $\sigma_{bs}(f)$ and $TS = 10 * \log_{10}(\sigma_{bs})$ were estimated using the KRM model, fit with fish and swim bladder shapes imaged using X-rays. Values used for impedance contrasts were 0.9146 for water-body and 3927 for body-bladder. Assumed distributions of incidence angle for dorsal were $\sim N(90^\circ, 3^\circ)$ and uniform for lateral. Fish-length distributions were estimated from 2014 and 2015 electro-fishing specimens: WHC $\sim N(230.4, 49.2)$, CHC $\sim N(404.5, 91.8)$, LMB $\sim N(229.7, 87.6)$, STB $\sim N(255.1, 82.1)$, and BLC $\sim N(242.4, 74.8)$.

Additionally, the KRM model was used to estimate *TS* versus a range of incidence angles (65° to 115°) for striped bass.

Minimum-*TS* thresholds, used for detections of single targets and echo-track of fish in EK60 echograms, were based on modeled *TS* values for minimum lengths of known predators.

Fish target detection

Echosounder data were processed using commercial software (Echoview 7.0) to measure and track the *TS* of individual fishes. Received echoes were attributed to fish based on a single-target detection algorithm (Echoview Split-Beam – Method 2; Hartman and Nagy 2005, Kayanda et al. 2012, and Warner et al. 2012) using parameter values in Table 2.

Table 2. Single target detection parameters used in Split-Beam - Method 2 (Echoview) to analyze EK60 data.

	2014 120 kHz (side)	2015 120kHz (forward)	2015 200kHz (downward)
Single target detections			
Minimum <i>TS</i> threshold (dB)	-57	-57	-60
Pulse length determination level (dB)	12	12	9
Minimum normalized pulse length	0.7	0.7	0.65
Maximum normalized pulse length	3	3	1.3
Beam compensation model	Simrad LOBE	Simrad LOBE	Simrad LOBE
Maximum beam compensation (dB)	10	10	12
Maximum stdev of minor-axis angles (°)	1	1	2
Maximum stdev of major-axis angles (°)	1	1	2

Echo track detection

Multiple single-target detections of individual fish were assigned to single echo-tracks using an echo-track detection algorithm (Echoview) and parameter values in Table 3. For data from the 2014 side sonar and 2015 downward sonar, the edited riverbed detection lines were used to limit detections by range. For the 2015 forward sonar, no constraints were placed on echo track detection range for the Echoview processing; spatial constraints and filtering were applied in post processing.

Table 3. Echo-track parameter values used to analyze EK60 sonar data.

Fish track regions	2014 120 kHz (side)	2015 120kHz (forward)	2015 200kHz (downward)
Algorithm, data type	4D	4D	4D
Alpha, major axis	0.3	0.3	0.7
Alpha, minor axis	0.3	0.3	0.7
Alpha, range	0.7	0.3	0.7
Beta, major axis	0.2	0.22	0.5
Beta, minor axis	0.2	0.22	0.5
Beta, range	0.5	0.22	0.5
<i>Target Gates</i>			
Major axis exclusion distance (m)	1	0.85	4
Minor axis exclusion distance (m)	1	0.85	4
Range exclusion distance (m)	0.7	0.85	0.4
Major axis missed ping expansion (%)	0	2.5	0
Minor axis missed ping expansion (%)	0	2.5	0
Range missed ping expansion (%)	0	2.5	0
<i>Weight</i>			
Major axis weight	0%	10%	30%
Minor axis weight	0%	10%	30%
Range weight	30%	10%	40%
TS weight	0%	0%	0%
Ping gap weight	0%	0%	0%
<i>Target Acceptance</i>			
Minimum number of single targets in a track	4	8	3
Minimum number of pings in a track (pings)	4	8	3
Maximum gap between single targets (pings)	2	2	1

Spatial transformations

Riverbed detection defined stop ranges for echo-track analysis were adequate for spatially filtering the 2014 side and 2015 downward sonar data, but weak echoes from the riverbed in the forward-sonar data made standard riverbed detection ineffective. Therefore, in

2015, the bathymetry from the M3s were used to filter the target data from the forward sonar. The range and within-beam angles of each echo track location of the forward sonar were converted to global spatial reference frame (UTM, zone 10 north; EPSG 32610) by compensating for the instantaneous pitch, roll, heave, and heading recorded from the POS-MV and river water elevation data interpolated to the ping location using custom code (written in MATLAB, R, and Python) following the methods described in Conti et al. (2005) and Cutter and Demer (2010).

Echo-track filtering

The river bathymetry data were used to determine if the echo-track positions occurred spatially within the bounds of the river water volume (Figure 7). Echo tracks that occurred below or within 0.5 m of the bathymetric surface were rejected from analysis and not included in counts.

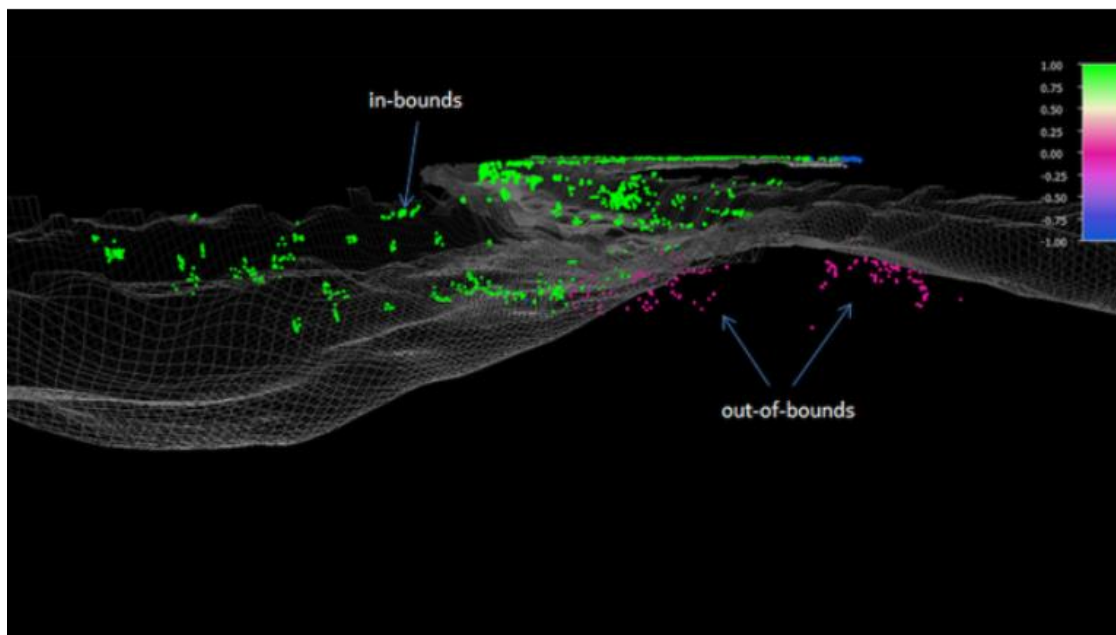


Figure 7. Bathymetric constraints applied to spatially-transformed echo-track data ensured that targets were within the river volume.

The resulting 'in-bounds' echo-track targets were transformed by principal components analysis (PCA) and further refined to eliminate potential inclusion of riverbed-echoes. After rotations of the first three PCA scores in the 3-D space, fish and riverbed target echo groups were divided using a plane. Fish targets were retained and riverbed targets were rejected, producing 'in-bounds' fish targets. This dataset was used in subsequent analyses (Figure 8).

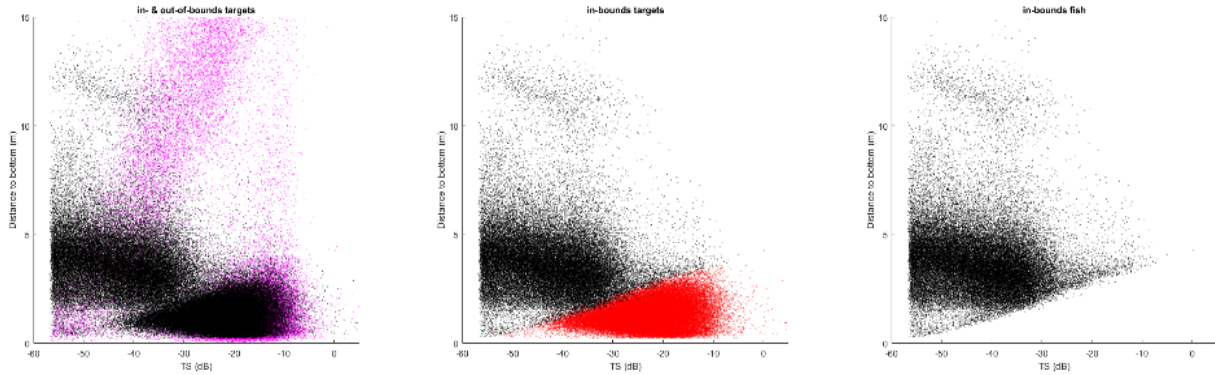


Figure 8. *TS and distance to riverbed for echo-tracks at three stages of filtering: full set of unfiltered echo tracks (left), in-bounds targets (center), and fish only targets (right).*

The *TS* distributions for the full set of unfiltered echo-tracks, the in-bounds targets, and the fish-only targets (Figure 9) show that removal of riverbed echoes by spatial filtering resulted in a narrow, less skewed distribution, as could be expected for fish with modes of -20, -24, and -38 dB, respectively (Figure 9).

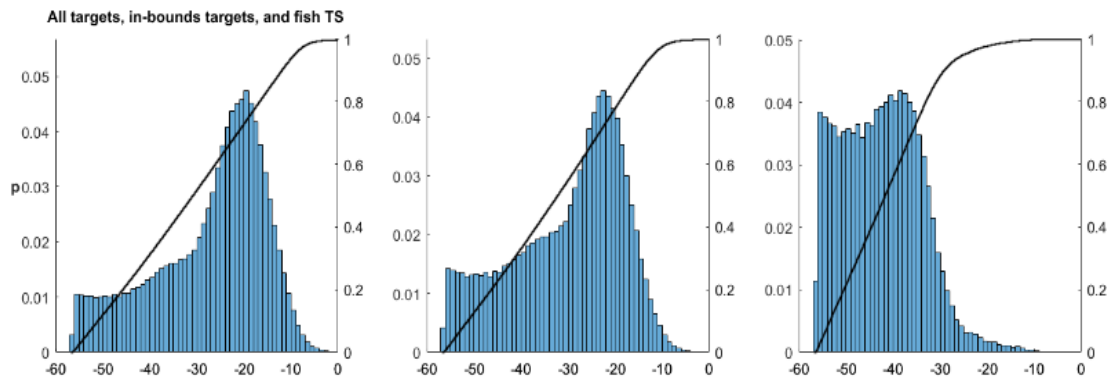


Figure 9. *TS distributions of unfiltered (left), in-bounds (center), and fish echo tracks (right).*

Sampled volume estimation

The sampling range for the downward sonar beam was estimated using the range between the beginning of the far-field region and the minimum range to the riverbed, or the range where the probability of fish detection was < 0.01. The probability of target detection is not constant throughout an echosounder beam, and is higher toward the beam-center (Mulligan and Kieser, 1996). The far-field range for the 200-kHz transducer (ES200-7C) was 1.49 m (Korneliussen et al., 2009). The sampled volume of the downward sonar was estimated as a swept cone or wedge with height equal to the mean sampled range (dz)

within a river segment, length equal to the accumulated river-segment centerline distance, e.g., 10 m, and width defined by a conical model of the beam with opening angle equal to 7.0 degrees (Figure 10).

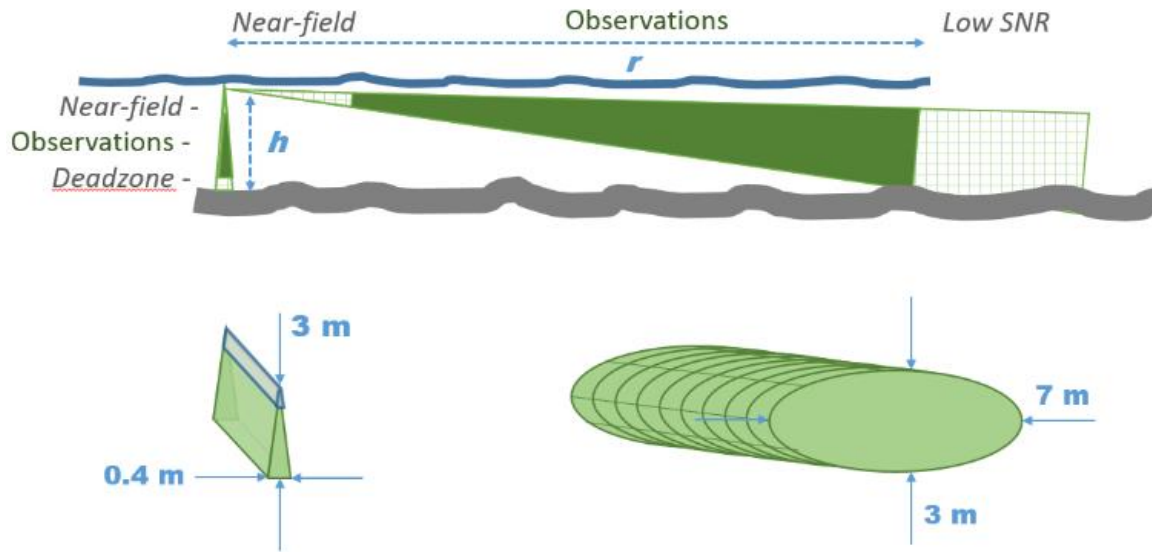


Figure 10. Top: Ideal beam observation volumes. Bottom: The swept cone (left) and ellipse (right) method used to estimate sampled volume; forward range, $r = 40$ m.

Beam sampled volume weighted by target-detection probability

The sampled range of the forward and side sonars was estimated to be 40 m, where the probability of target detection diminished to 0.01 along the beam axis. The effective beam angles encompassing 99% of the target detections (alongship and athwartship) from the forward sonar, defined here as the solid angles within which target detection exceeds 0.01, were 10.7° by 5.2° . These angles are larger than the ideal -3 dB beamwidths, 10° by 4° , and less than the beamwidths which included all target tracks, 11.6° by 5.6° (Figure 11).

The effective sampling volume was estimated as the integral of the volumes of the individual slices of the beam, weighted by the probability of detection of each radial slice (Table 4). The *weighted* effective beamwidths ($\theta_{y,eff,w}$, $\theta_{z,eff,w}$) were 6.0° and 1.6° , when multiplying the incremental beam volume by the probability of detection for each 0.01° angular interval.

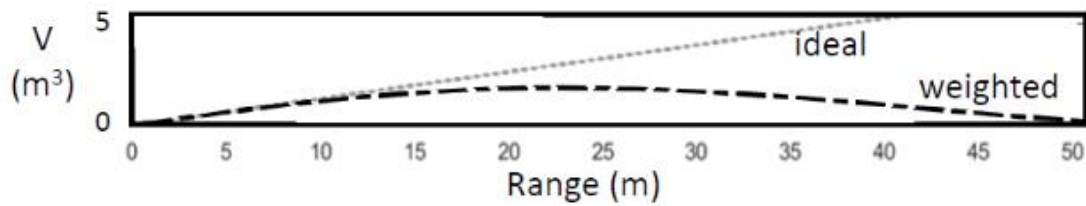
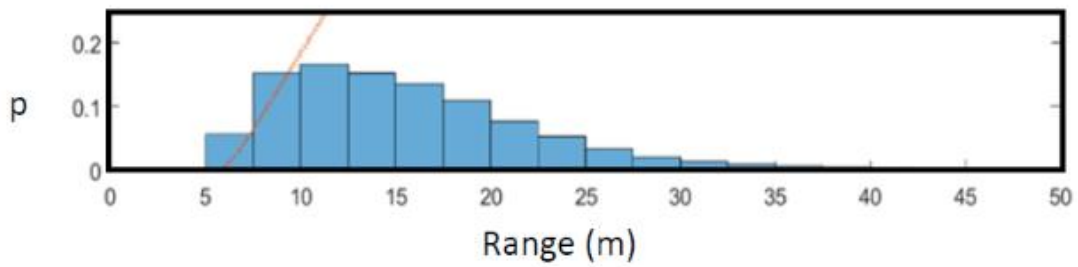
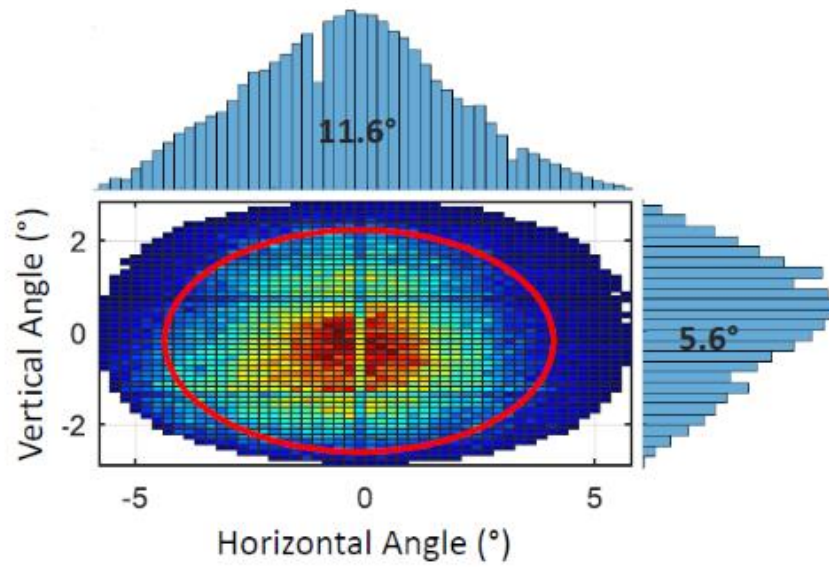


Figure 11. Probability of detection, and the maximum (full grid) and hypothetical effective (red ellipse) beam angles for the forward 120-kHz echosounder (top); probability of detection by range (middle); and effective beam volume by range (bottom).

Table 4. Variables for calculation of sampled volume per river segment and by transducer.

Variable	Downward beam (200kHz)	Side and forward beams (120kHz)
V_{samp}	Sampled volume per river segment	Sampled volume per river segment
V_{samp}	$dx_{segm} * A_c$	$dx_{segm} * A_c$
dx_{segm}	River segment length (centerline)	River segment length (centerline)
A_c	$\frac{(dy * dx)}{2}$	$\pi * dy * dz$
dy	$2 * h_{cl} * \tan(0.5 * \theta_{yd,eff})$	$R_f * \tan(0.5 * \theta_{yf,eff})$
dz	h_{cl}	$R_f * \tan(0.5 * \theta_{zf,eff})$
h_{cl}	Mean water depth, segment centerline	Mean water depth, segment centerline
R_f		$\min(r_{bot-int}, 40)$ (m)
$\theta_{yd,ideal}$	7°	
$\theta_{yf,ideal}$		9.0°
$\theta_{zf,ideal}$		4.4°
$\theta_{yd,max}$	9.8°	
$\theta_{yf,max}$		11.6°
$\theta_{zf,max}$		5.6°
$\theta_{yd,eff}$	7°	
$\theta_{yf,eff}$		10.7°
$\theta_{zf,eff}$		5.2°
$\theta_{yf,eff,w}$		6.0°
$\theta_{zf,eff,w}$		1.6°

River segmentation

The river was segmented every meter along its midline. The sides of these river segments are larger, equal to, or smaller than 1 m where the bank is convex, flat, or concave, respectively (Figure 12). Each segment represents a constant along-river interval but segments do not have equal areas. The 1-m segments were aggregated to create larger segment sizes.

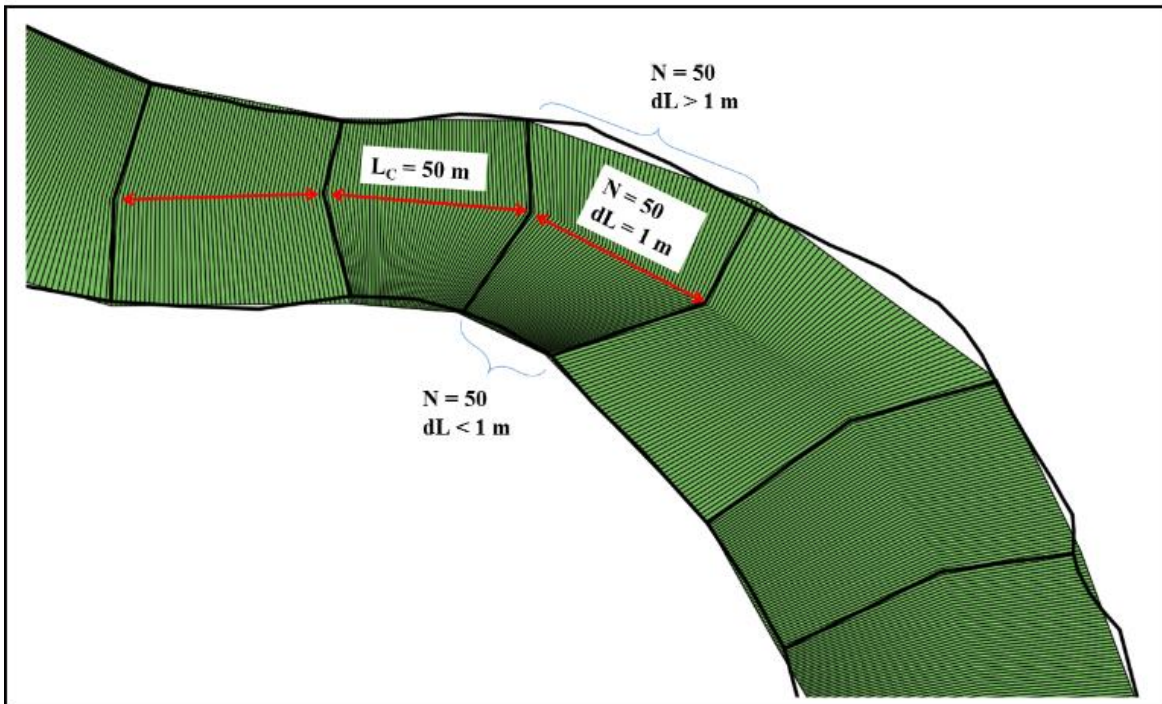


Figure 12. River segmentation: center to bank segments connect center nodes to nearest point on bank. $dL_{50} = 50\text{ m}$, along river center; $dL_1 = 1\text{ m}$ only along centerline.

Fish target counts, density, and abundance estimates

The distance sampling unit used for densities and abundances was defined as a 10-m along river segment, each comprising 10 of the elemental 1-m segments (Figure 12). Counts of fish echo-tracks were summed within each of these river segments for each survey day. Sampled volume was calculated as the integral of the swept-beam volume after compensating for detection probability by angle and limiting by range to the beam-riverbed intersection. Summed counts of echo-tracks were converted to densities by compensating for insonified sampled volume within each segment (Table 5). Fish abundances were estimated from the product of fish densities and integrated river volume within each segment, assuming uniform distribution of fish throughout the volume. Integrated river volumes were based on mean 10-m river-segment depth, relative to the NAVD88 vertical datum, averaged over tidal cycles during the survey period.

Table 5. Conversion of counts to density and abundance.

Variable	Meaning	Expression
N	Count per river segment	$N_{echotracks}$
V_{samp}	Sampled volume per segment	$dx_{segm} * A_c$
D	Density	$\frac{N}{V_{samp}}$
A	Abundance	$D * V_{river(segment)}$

Sizes of detected targets

Length distributions of the main four predator species, channel catfish (CHC), striped bass (STB), white catfish (WHC), and largemouth bass (LMB), were estimated from the combined 2014 and 2015 electro-fishing catch data ($n_{CHC} = 113$, $n_{LMB} = 1620$, $n_{STB} = 407$, $n_{WHC} = 370$). From the seven “fish-community” sampling events which were a subset of electro-fishing efforts when all caught fish were counted and measured (19, 20, and 27 May 2014, and 13-16 April 2015), the lengths of the top four predator species ranged from 54 to 760 mm (Figure 13). Mean sizes of CHC were largest (425 mm), and the other species (WHC, LMB and STB) had mean lengths between 233 and 255 mm. However, sampled length distributions of LMB and STB were bimodal and skewed, with modal lengths near 300 mm and only a few large fish > 450 mm. Most CHC were between 375 and 600 mm, but rarely < 350 mm.

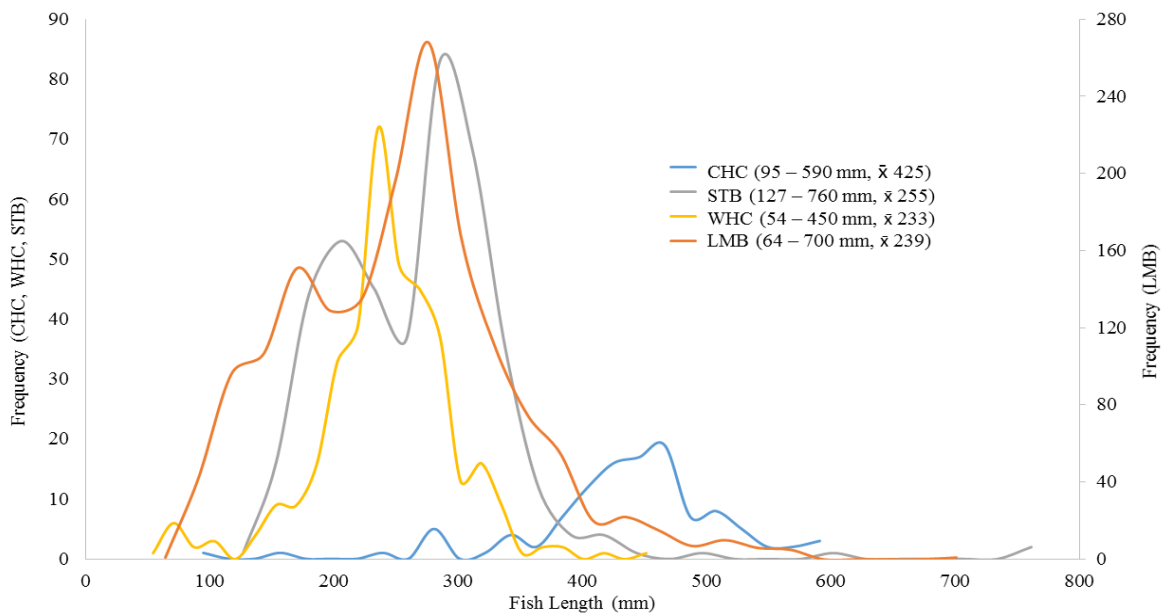


Figure 13. Length distributions for the top predator fish species: channel catfish (CHC), striped bass (STB), white catfish (WHC), and largemouth bass (LMB; right axis).

Results and Discussion

River Bathymetry

Primary study area

Bathymetry (1-m grid) of the San Joaquin River within the study area, between Port of Stockton and Lathrop, ranged in depth from < 1 m near Lathrop to > 12 m near the deep-water shipping channel (Figure 14 and Figures A01-A26). Scour holes in the river bends have depths ranging from 7.5 to 10 m which deviate from the trend of the profile (Figure 15) characterized by mean depths of 2 m to 5 m from south to north.



Figure 14. Riverbed bathymetry for the primary study area between the Port of Stockton and Lathrop, a) northern (downstream), b) central, and c) southern (upstream) sections.

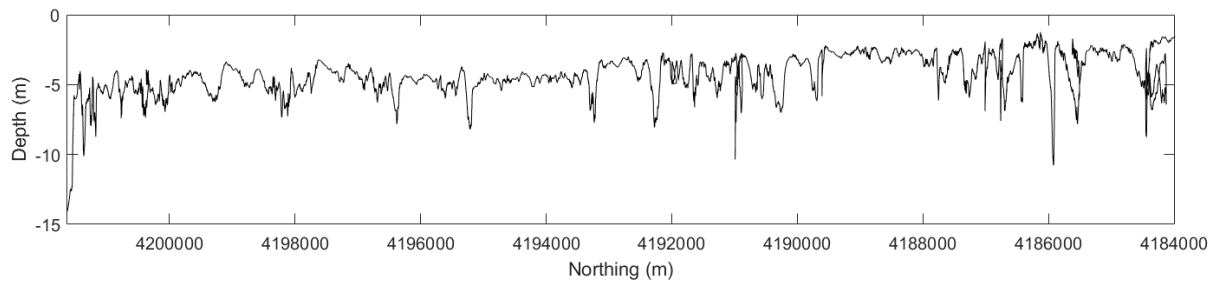


Figure 15. Mean depth (referred to the NAVD88 vertical datum) of the San Joaquin River between Port of Stockton and Lathrop by Northing (numbered north to south from left to right).

Perspective views and cross-sectional profiles of the river bathymetry (Figures 16 and 17) show the complexity of this river environment, the sinuosity of the river, and variability of morphological features that are potentially important to salmonid smolt migration and predator habitats. Cuts and channels occur in the north, near Port of Stockton, and in study reach A3 (Figure 16).

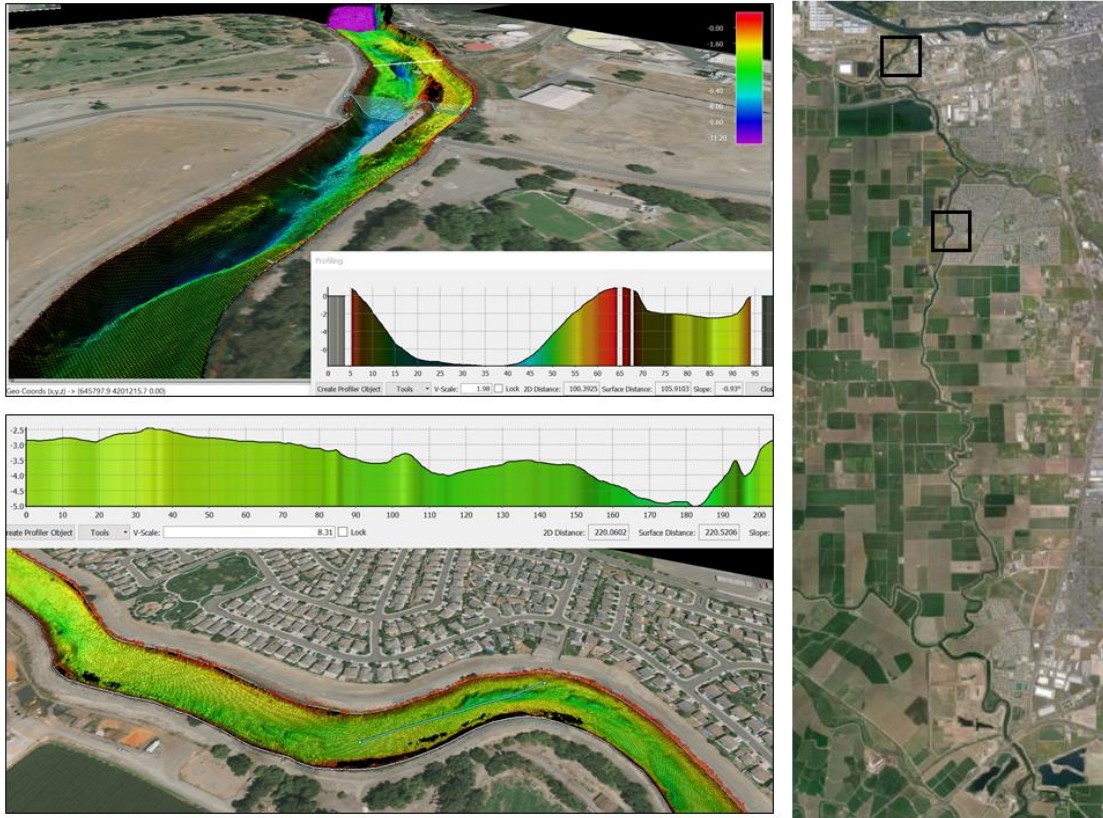


Figure 16. Perspective views of San Joaquin River bathymetry for two northern sections.

Shallow (<1 m), meandering stretches with migratory sedimented bedforms occur in the south, and a deep (9 to 10 m) scour hole occurs just north of the head of Old River (Figure 17).

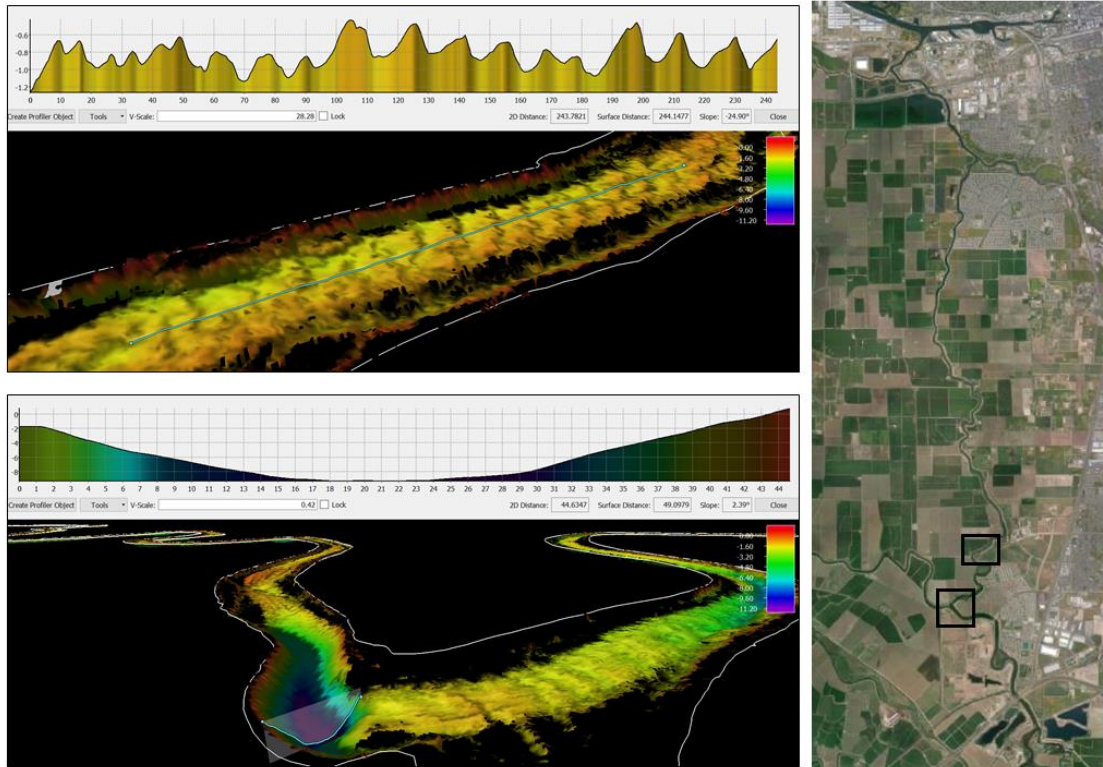


Figure 17. Perspective views of San Joaquin River bathymetry for two southern sections.

Stockton Deepwater Shipping Channel

In 2015, two additional areas were surveyed including portions of the Stockton deep-water shipping channel (Figure 18) and Clifton Court Forebay (Figure 19). The deep-water shipping channel was typically 11 to 12 m deep, apparently dredged for ship traffic.

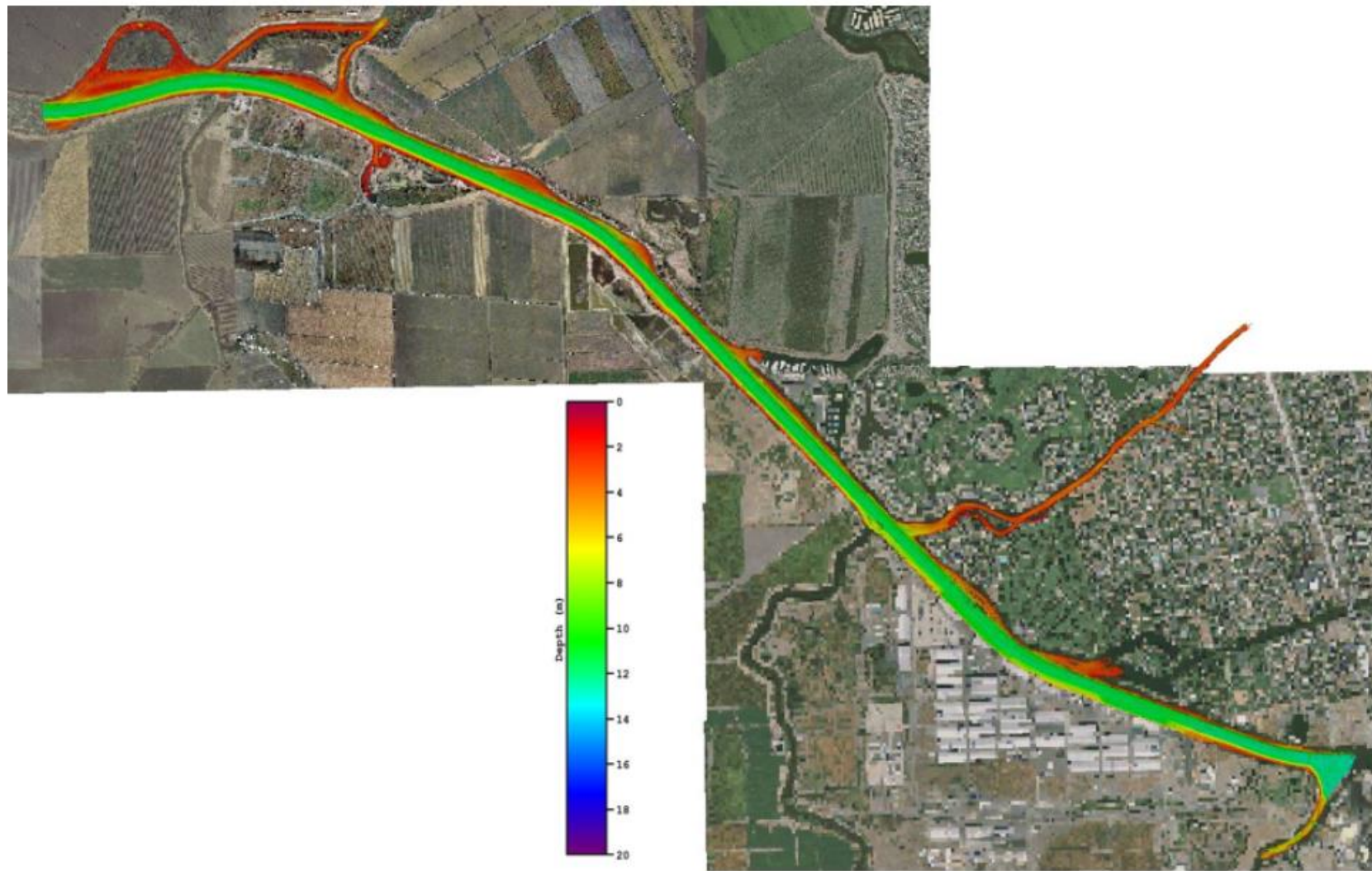


Figure 18. Bathymetry map for of the Stockton deepwater shipping channel portion of the San Joaquin River.

Clifton Court Forebay

The intake canal of Clifton Court Forebay ranged from 3 m deep, just north of the opening between the jetties, to 9 m deep in the south near the pumping facility (Figure 19). Near the radial gates of Clifton Court Forebay was a scour hole approximately 20 m deep surrounded by sedimented flats less than 2 m deep (Figures 19 and 20).

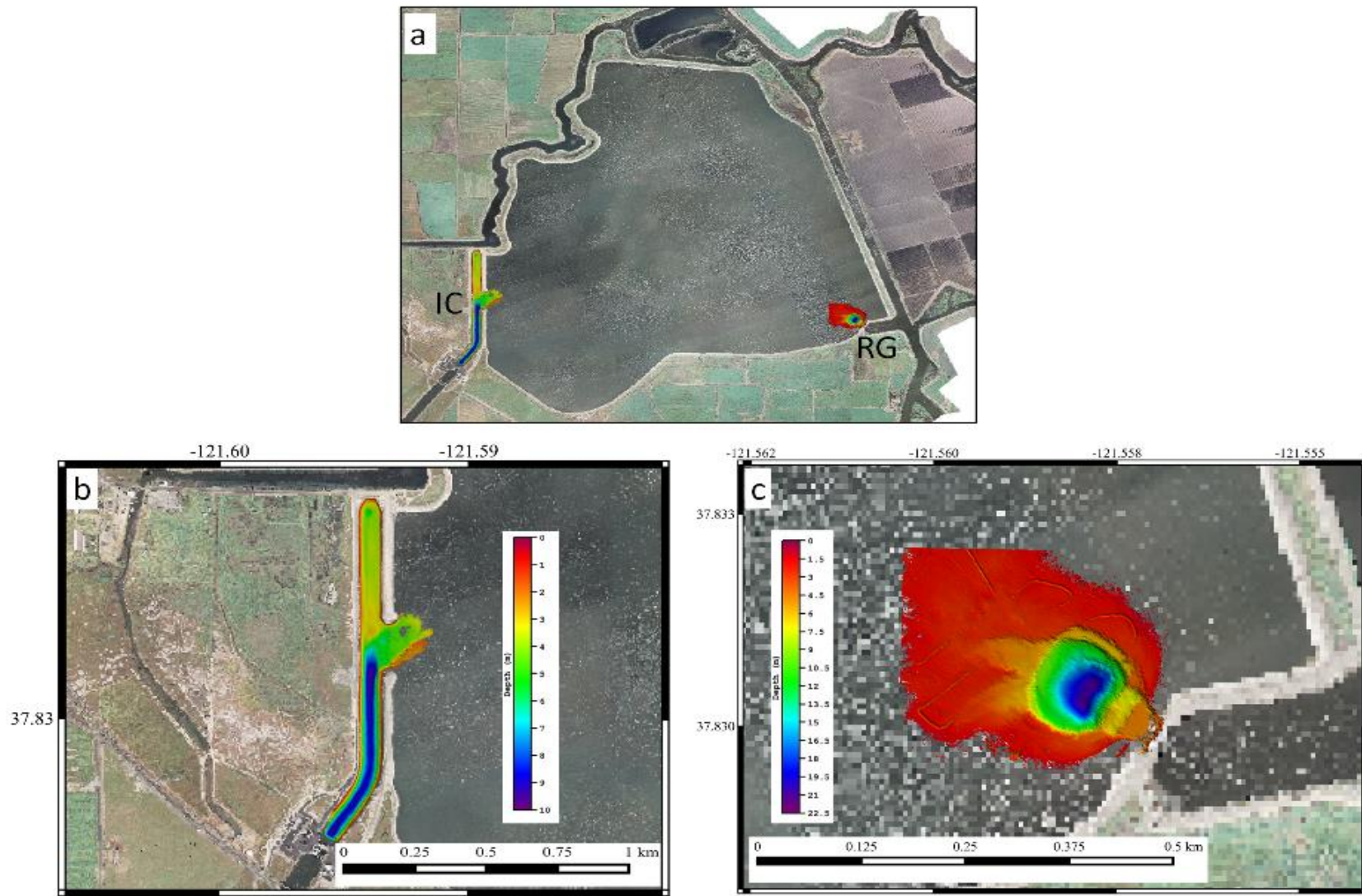


Figure 19. Bathymetry map for 2015-surveyed portions of a) Clifton Court Forebay: b) intake canal (IC), c) radial gates (RG) scour hole.

The terracing of the 20-m deep scour hole near the radial gates, with ledges near 4 and 8 m, is evident from the perspective view of the bathymetry (Figure 20). In this scour hole, several species of predatory fish including striped bass, largemouth bass, and catfish were abundant.

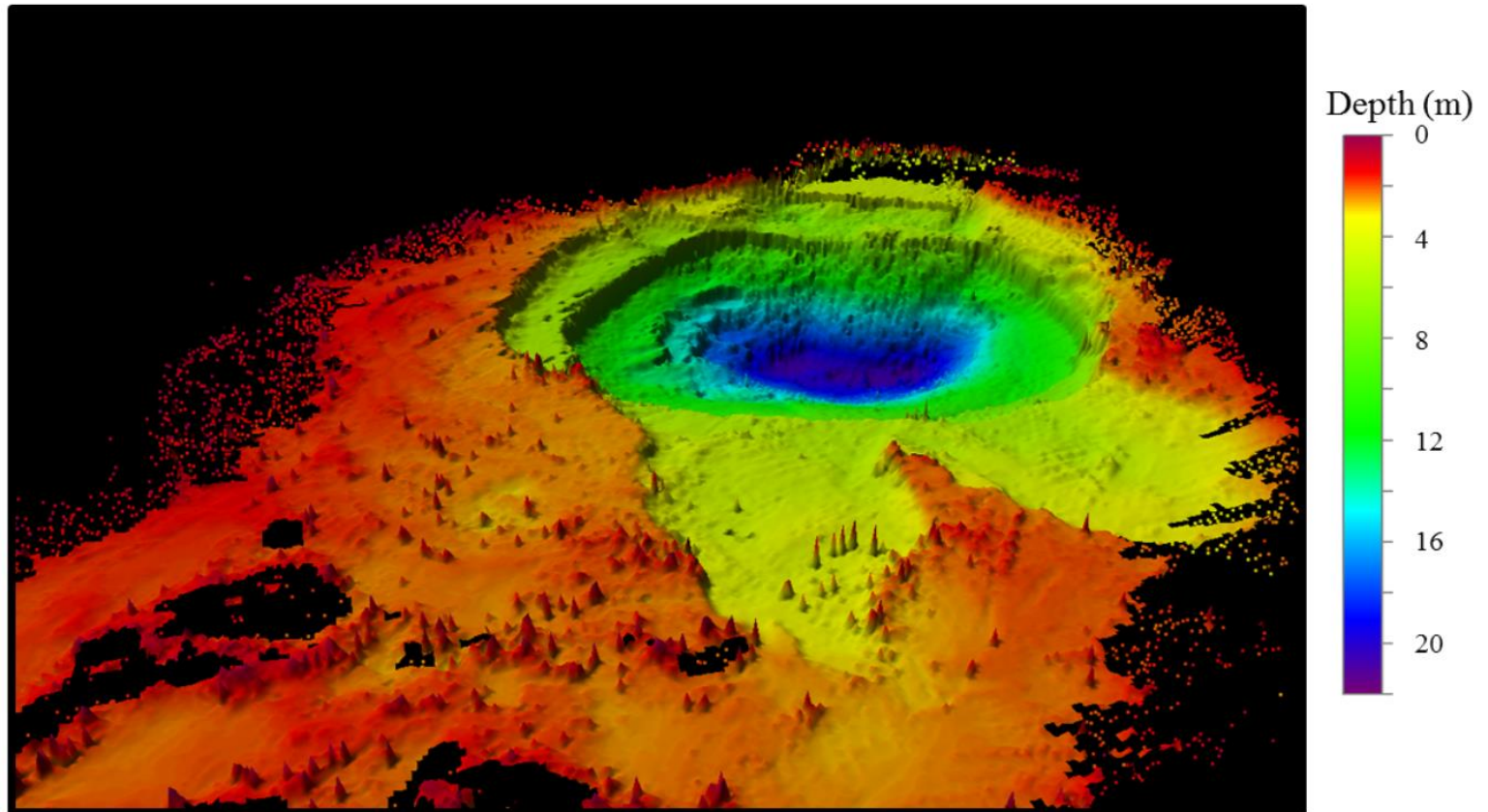


Figure 20. Perspective view of bathymetry of Clifton Court Forebay radial rates area, looking from northwest to southeast. The scour hole near the outflow, nearly 22 m deep, included the highest observed fish densities (not shown). Shallower depths (m) are depicted with hotter colors as indicated in the legend.

Riverbed terrain classes

The riverbed terrain class map (Figure 21) shows the locations and distributions of the five riverbed classes: deep pools, pool margins, channels and runs, channel and bedform margins, and bank edges and steep slopes. Some of these terrain classes were evidently related to spatial distributions of acoustically-detected fish. In particular, more fish were acoustically detected in the deep scour holes found in many of the bends in the river.

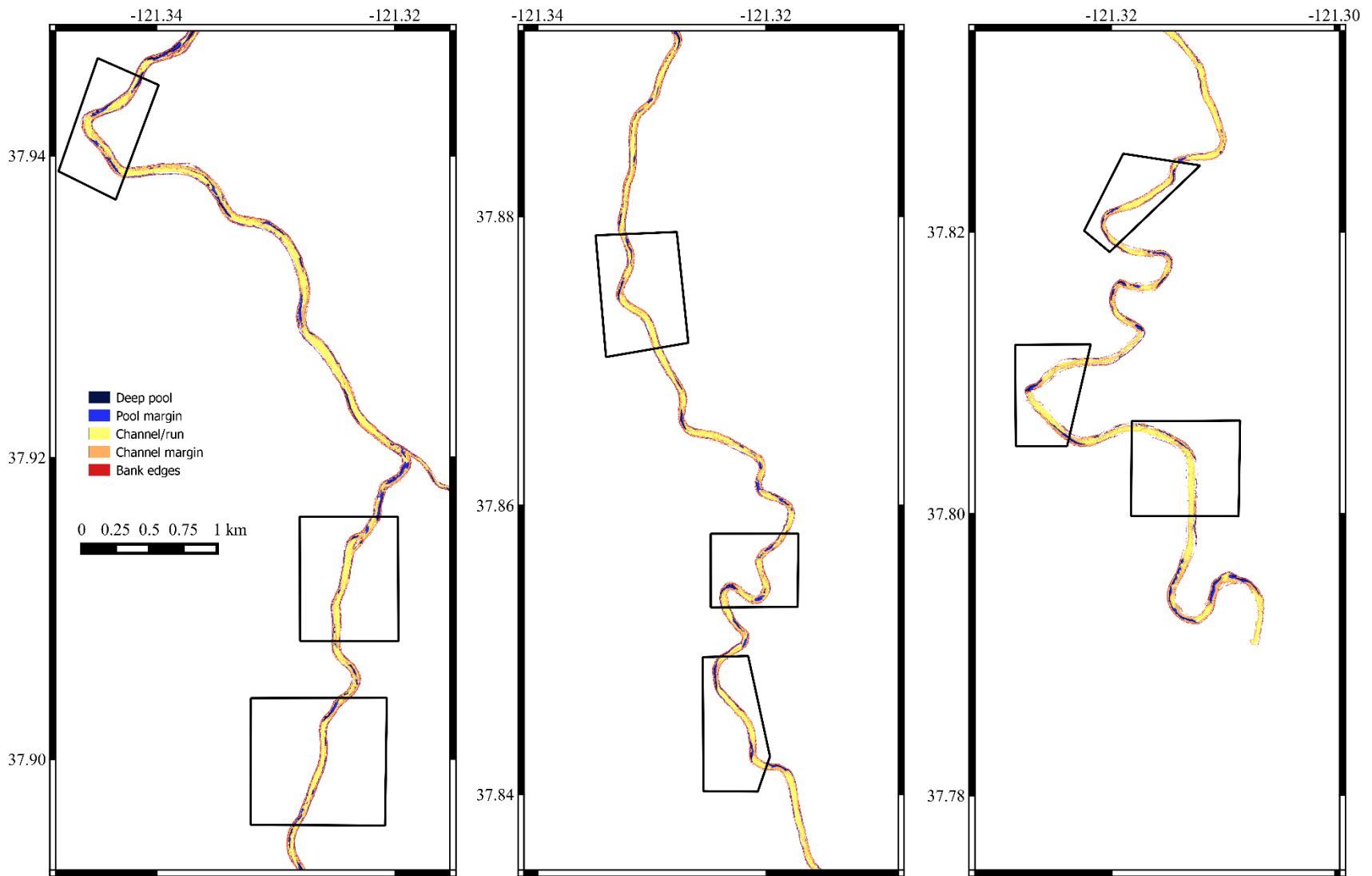


Figure 21. Riverbed terrain class map.

Submerged aquatic vegetation

SAV targets identified from the multibeam sonar data were mapped and delineated, showing a widespread coverage of SAV beds throughout the study area (Figure 22 and Figures A01-A26). SAV was not verified by field sampling. Putative SAV beds covered approximately 50% or more of the river banks in patches from about 20 to > 500 m long.

Although the species of SAV in the study area were not physically identified, the dominant SAV in the Delta, is Brazilian waterweed (*Egeria densa*). Largemouth bass populations increase when this extensive SAV is present (Brown and Michniuk 2007, Nobriga et al. 2003, Conrad et al. 2016). These SAV beds may be important predator habitats in this study area, and mapping them using multibeam sonars with sample verification may be more efficient than other methods.

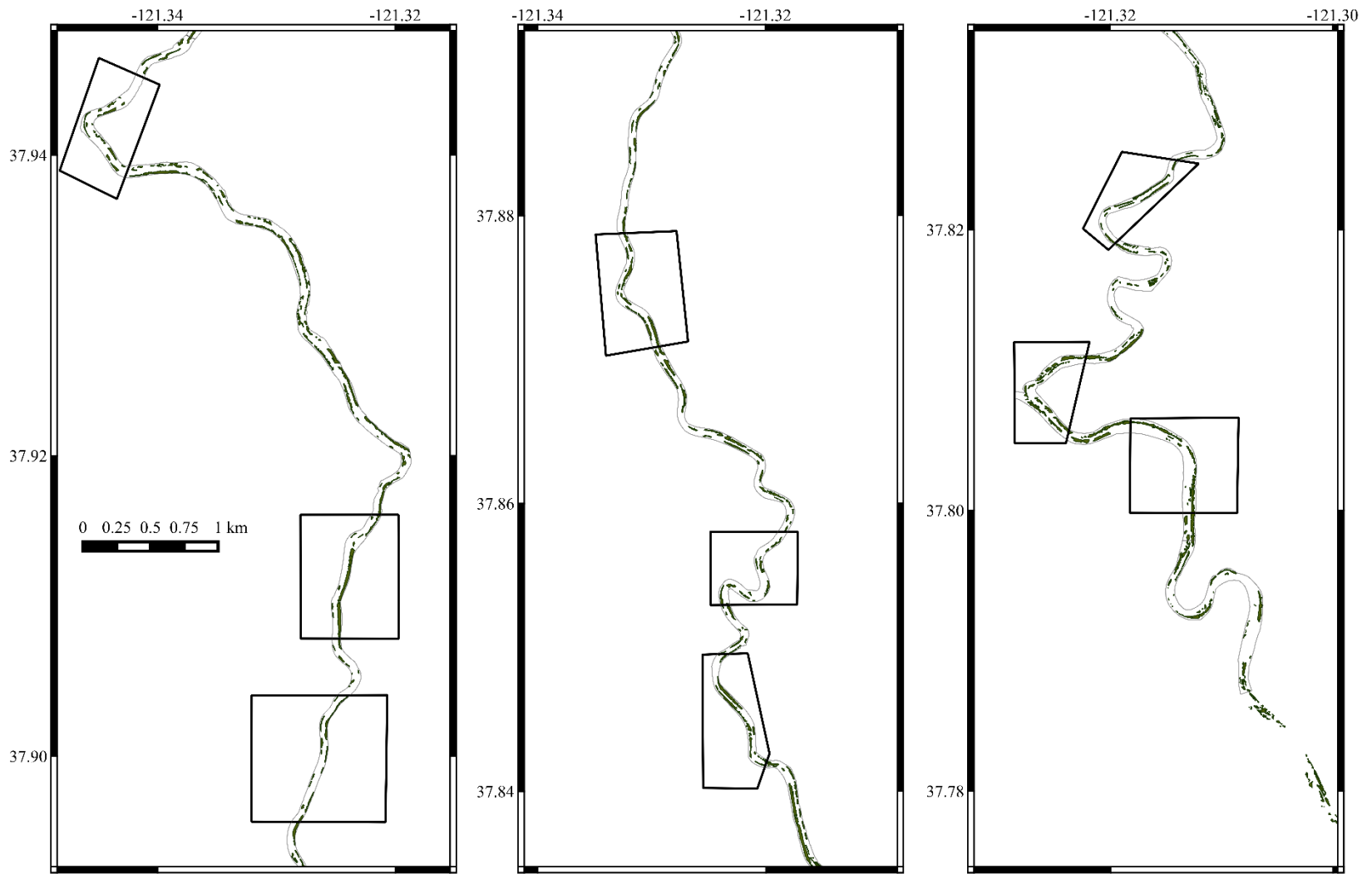


Figure 22. Acoustically-detected locations of submerged aquatic vegetation (SAV) beds (dark-green filled polygons distributed along river edges).

Fish TS modeling

KRM-predicted σ_{bs} was evaluated versus acoustic frequency f and incidence angle. For the sonar frequencies used in these surveys, there are clear differences in $\sigma_{bs}(f)$ for some species such as channel catfish in dorsal incidence (Figure 23). Two species (CHC, WHC) may be differentiated from the others (STB, LMB, BLC) using dorsal incidence $\sigma_{bs}(f)$. STB, LMB, BLC are unlikely to be differentiated by $\sigma_{bs}(f)$ in dorsal incidence, but these species may be differentiated using lateral incidence $\sigma_{bs}(f)$.

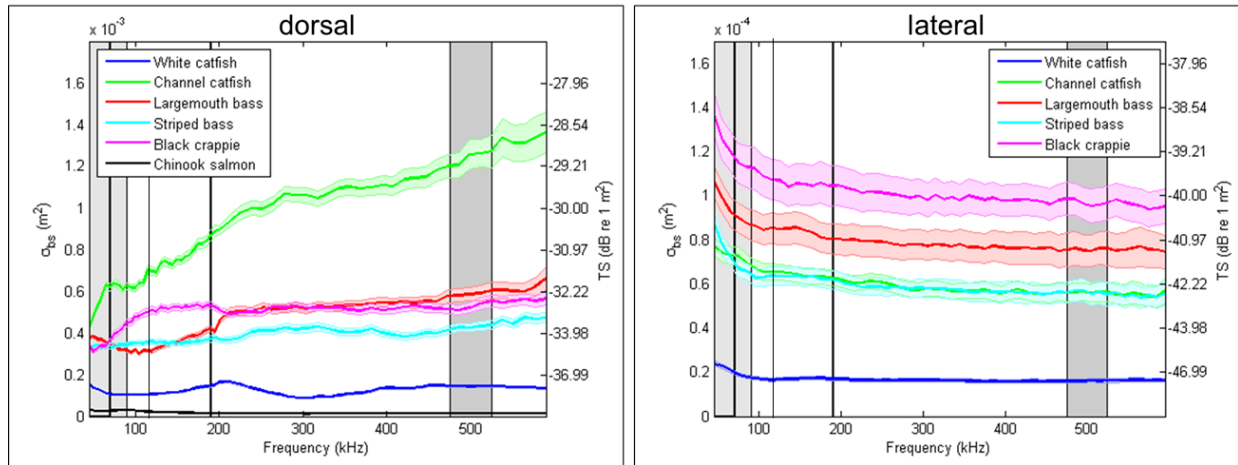


Figure 23. Modeled mean backscattering cross-sectional areas (σ_{bs}) and target strength (TS) for dorsal- (left) and lateral-incidence (right) observations of candidate salmon predators.

KRM-model results indicate that lateral incidence TS of these fish, i.e., in side view, where the beam direction is normal to the long axis of the fish, monotonically increases from -52 to -30 dB for fish with lengths (L) < 10 to > 60 cm, but varies by species (Figure 24). The TS -vs- L curve for LMB is on average approximately 2 dB higher than for STB and the curves for both catfish were about 5 dB lower than STB.

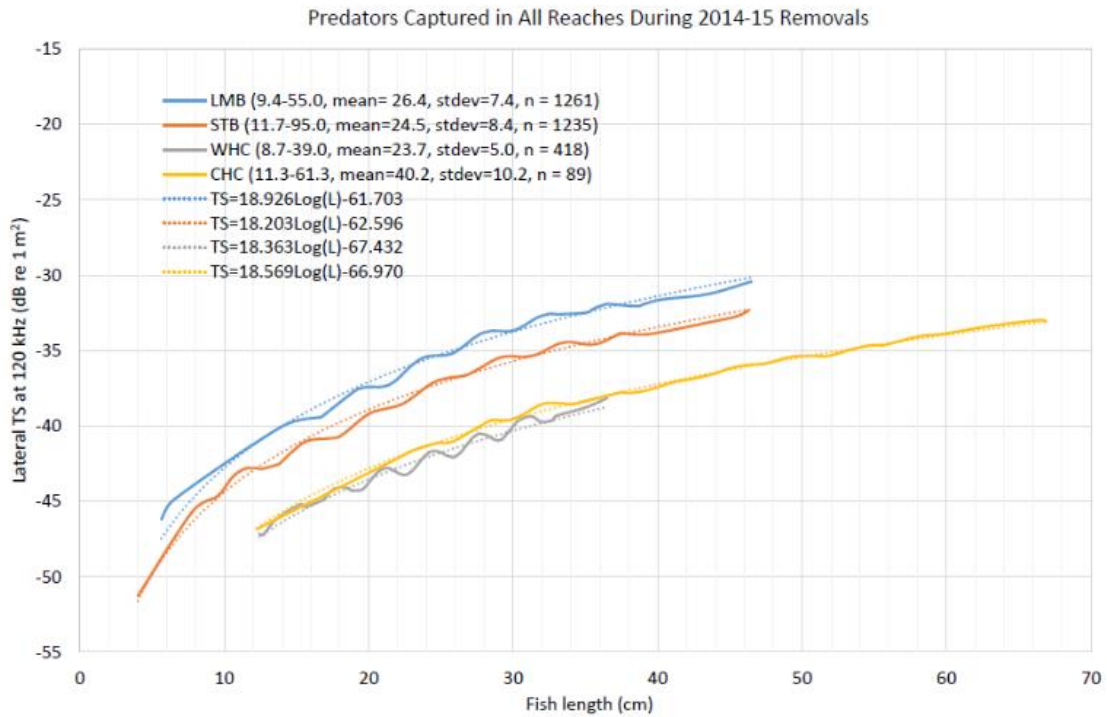


Figure 24. Fish target strength (TS ; dB) vs length for largemouth bass (LMB), striped bass (STB), white catfish (WHC), and channel catfish (CHC) for lateral incidence.

However, for fish that are insonified at non-normal incidence angles, the TS -vs- L relationship is weaker than the TS -vs-incidence-angle relationship. Variation of incidence angles has a much greater effect on TS than size of these fish (Figure 25). Deviations of only 20° from normal (90°) incidence induce a -10 to -15 dB reduction in TS . Inferring fish size from TS in those cases, where it was assumed that TS value indicated the mean of normal incidence target echoes, would erroneously suggest that the fish was perhaps 1/3 to 1/4 of the actual size.

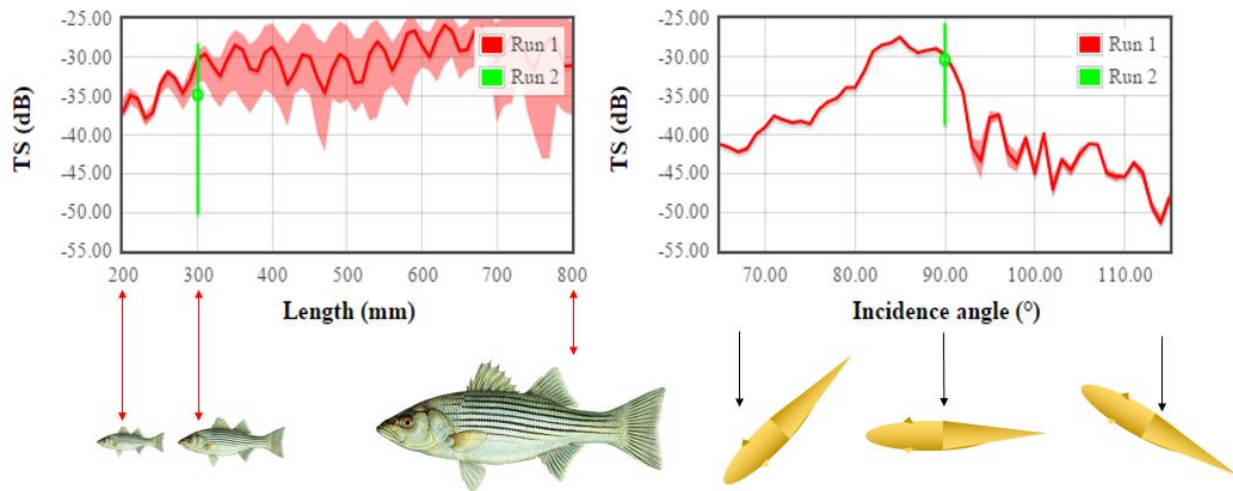


Figure 25. Fish target strength (TS ; dB) vs length and incidence angle.

Single target detections

The mean number of single targets per echo track were 3.6 (SD = 1.3), 5.9 (2.6), and 13.3 (8.0) for the 2015 downward, 2014 side, and 2015 forward sonars, respectively (Table 6). Median values were similar to means. The maximum number of single targets per echo track were 20, 43, and 154, but the high maximum value for the 2015 forward sonar was an outlier and possibly caused by temporarily slowed survey speeds.

Table 6. Target detection statistics: single targets per echo track.

Statistic	2014 side	2015 forward	2015 downward
Mean	5.9	13.3	3.6
Median	5	11	3
Max	43	154	20
Std. Dev.	2.6	8.0	1.3

Echo tracks

Each year, the side and forward sonars detected approximately 50,000 fish echo-tracks over the 19 and 21 survey days of 2014 and 2015, whereas the downward sonar detected approximately 5,000 fish during the 2015 study period (Table 7).

Table 7. Total number of echo tracks detected by each sonar for the main study area.

Sonar	# echo tracks (survey days)
2014 side	49,912 (19)
2015 forward	52,802 (21)
2015 downward	4,829 (21)

The number of fish echo tracks detected per day (Table 8) ranged from 250 to 6,160 (2014 side), 441 to 5,656 (2015 forward), and 37 to 656 (2015 downward). However, the survey coverage distances varied by survey day and these counts of echo tracks should not be interpreted as fish abundance.

Table 8. Number of echo tracks detected by each sonar during each survey day.

2014 side

	March				April				May										
	24	25	27	28	15	16	22	23	6	7	8	9	10	12	13	14	20	21	22
	83	84	86	87	105	106	112	113	126	127	128	129	130	132	133	134	140	141	142
<i>n</i>	3912	5897	3861	1557	2653	6160	3134	2559	762	1299	1444	250	644	2215	2871	2200	3551	2314	2611

2015 forward

	April										May										
	6	8	10	13	14	15	16	20	21	27	28	29	30	4	5	6	12	13	14	19	20
	96	98	100	103	104	105	106	110	111	117	118	119	120	124	125	126	132	133	134	139	140
<i>n</i>	2600	2589	1003	2634	5656	2057	1778	5261	4432	2523	2605	2947	3295	4082	1076	2935	1834	1502	530	441	1022

2015 downward

	April										May										
	6	8	10	13	14	15	16	20	21	27	28	29	30	4	5	6	12	13	14	19	20
	96	98	100	103	104	105	106	110	111	117	118	119	120	124	125	126	132	133	134	139	140
<i>n</i>	115	253	73	143	110	163	174	656	401	226	175	208	184	315	583	401	205	139	37	159	109

Depth distribution of echo tracks

Depth distribution of 2015 echo tracks show that most fish detected by the forward sonar were within 3.5 m of the water surface. In 2015, the majority of fish detected by the downward sonar were found between 1.5 to 6 m below the surface (Figure 26). The forward sonar sampled the shallow parts of the river (mean depth = 4 m) and the downward sonar sampled down to the riverbed, even in the deepest scour holes.

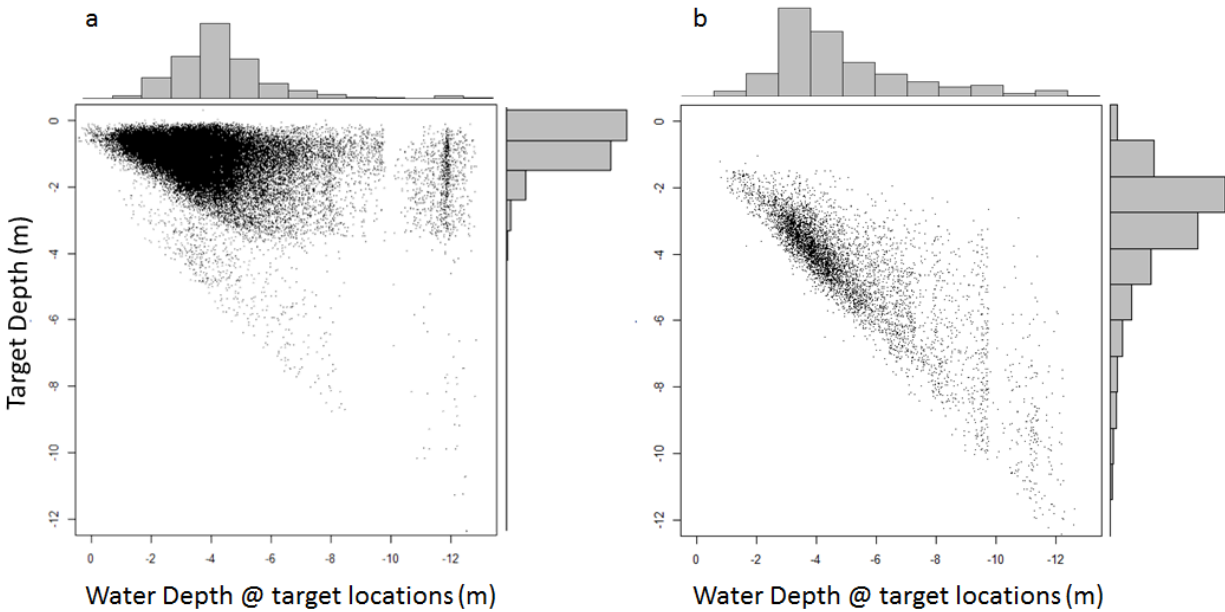


Figure 26. 2015 fish echo track depth distributions versus water depths for forward (a) and downward sonars (b).

Target strengths of echo tracks

Target strength (TS) of fish echo tracks ranged from -60 dB to approximately -10 dB (Figure 27). TS distributions were similar for side (2014) and forward (2015) sonars, with mean TS of approximately -40.5 and -42.5 dB, but TS values from the 2015 downward sonar were lower, with a mean of -48 dB (Table 9).

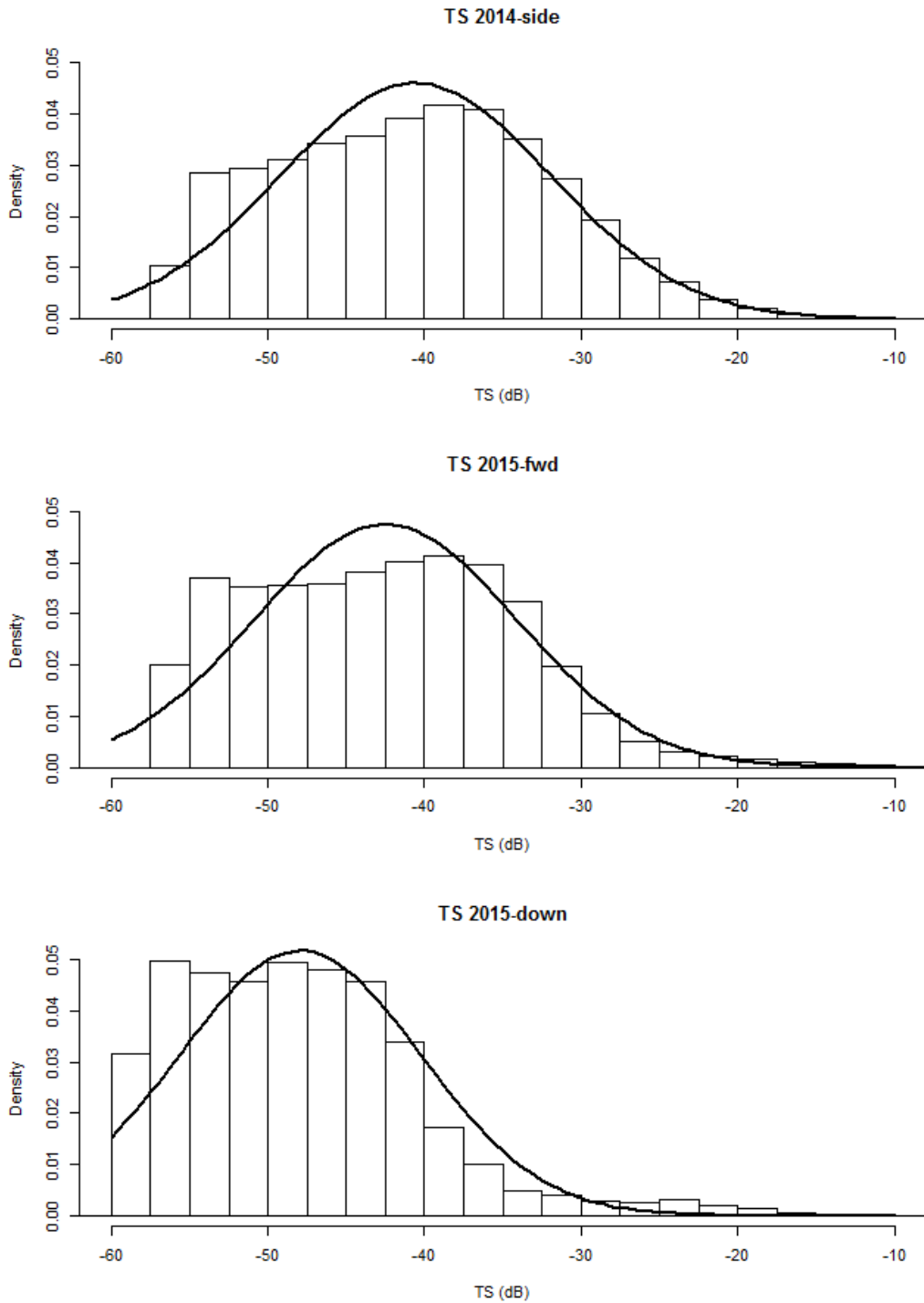


Figure 27. Target strength (TS) distributions for all fish, from echo tracks data for side (2014; top), forward (2015; middle), and downward (2015; bottom) sonars.

Table 9. Fish echo track *TS* (dB) distribution statistics.

Sonar	<i>mean TS</i>	<i>med TS</i>	<i>st. dev. TS</i>
2014 side	-40.58	-40.51	8.67
2015 forward	-42.50	-42.60	8.41
2015 downward	-47.95	-48.67	7.71

Fish density and abundance estimates

Fish density estimates

Counts of echo tracks were compensated for sampled volumes and probabilities of detection, and converted to densities per unit of sampled volume. This was done so that observations from the variously-oriented sonar beams acquired from different parts of the river were comparable.

Mean densities of fish were estimated for each 10-m river segment (Figures 28-31), for each study reach (Tables 10-12); and for the entire 26-km length of river, for all survey days, during 2014 and 2015.

Fish densities estimated from the 2014 and 2015 side and forward sonars show strong temporal and spatial variability (Figures 28, left and center panels, 29 and 30). Particularly during 2014, periods of very high densities early in the season were followed by a period of low densities throughout the river. Later in the 2014 season, high densities recurred in the northern 2/3 of the study area while densities in most of the southern section remained lower. During 2015, densities from the forward sonar were less variable over time than 2014 when considered on a whole-river basis, but were highly variable over time for some small regions.

Many of the density estimates from the downward sonar were zero fish per 10-m river segment (Figures 28, right panel, and Figure 31). The downward sonar found consistently high densities in some small areas (e.g. between northings 4,190,000 and 4,192,000), and the highest densities encountered were detected on multiple days during 2015 throughout the southern stretches (between 4,185,000 and 4,189,000 N).

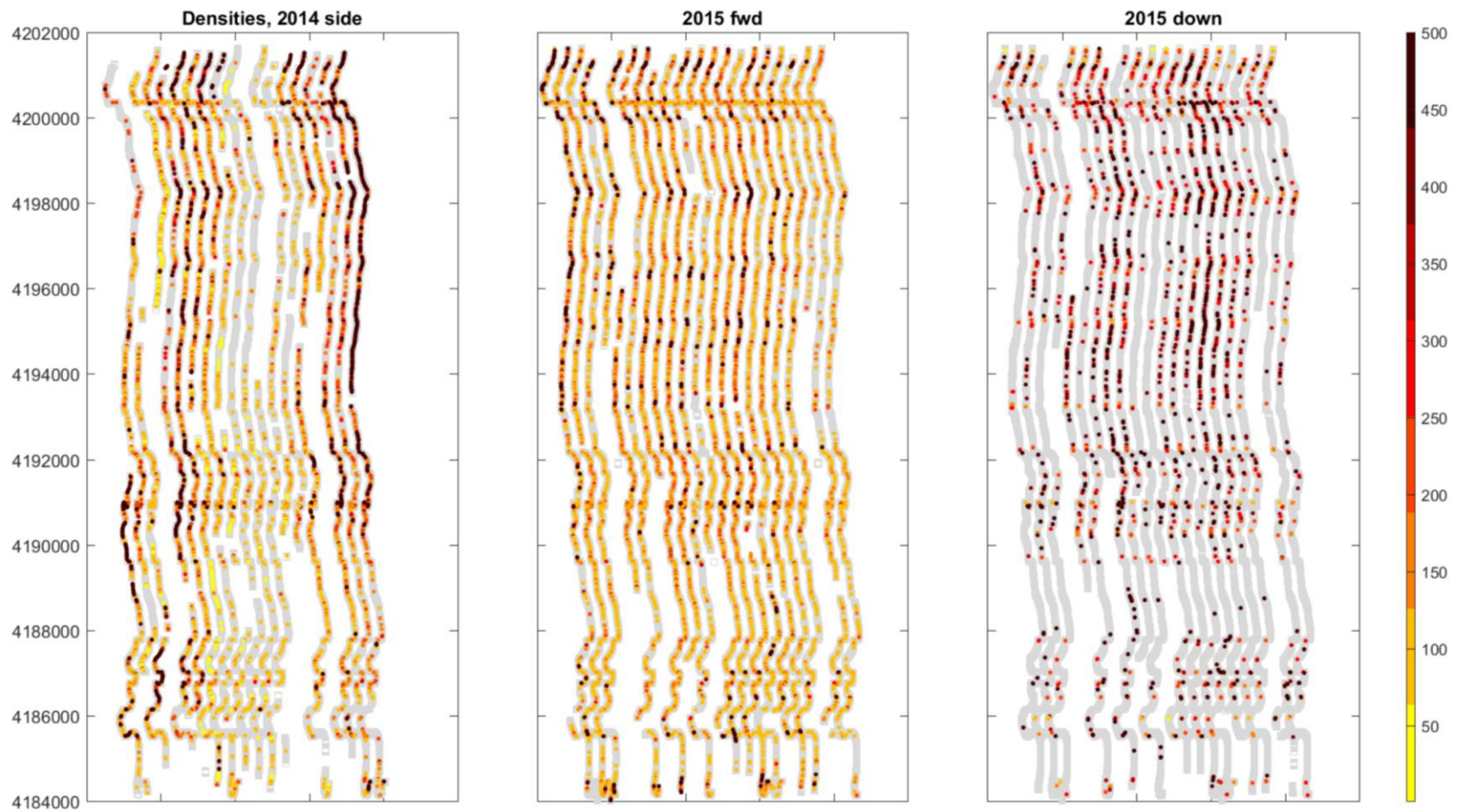
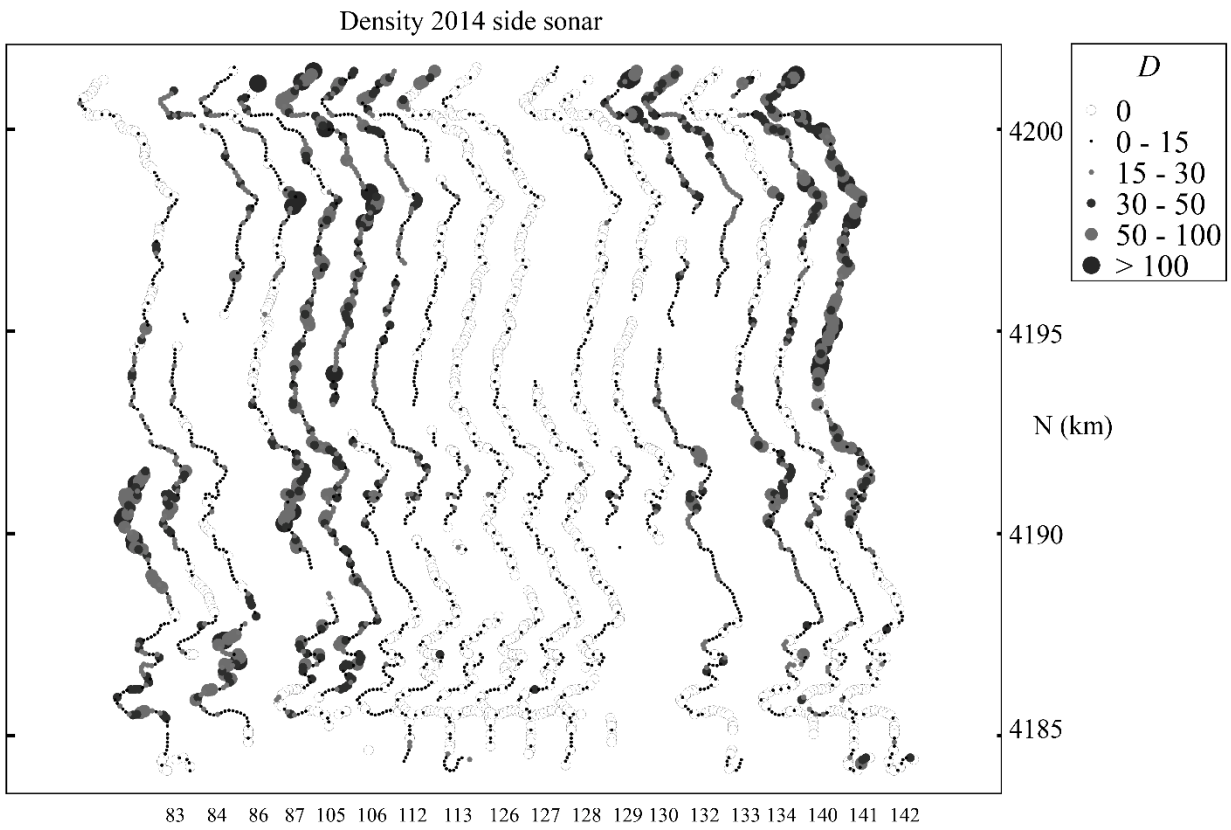
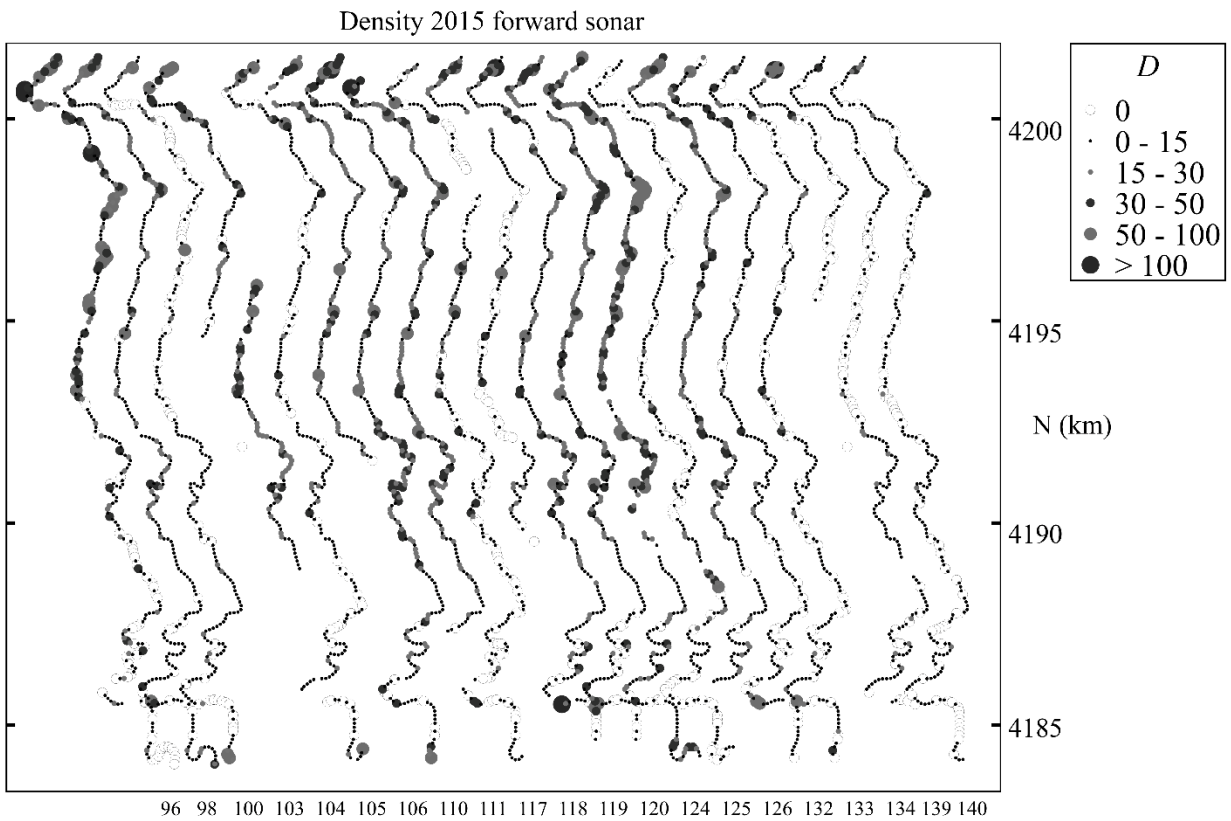


Figure 28. Fish mean density estimates from acoustic surveys, summarized by 10-m river segments and survey day, for the SJR from Port of Stockton to Lathrop. Transducers (left to right): 2014 120 kHz, 2015 120 kHz, 2015 200 kHz.



*Figure 29. Fish mean density estimates from the 2014 acoustic surveys using the side sonar, summarized by 10-m river segments and survey day, for the SJR from Port of Stockton to Lathrop. Community sampling date (from e-fishing efforts) denoted with an * below the Julian day.*



*Figure 30. Fish mean density estimates from the 2015 acoustic surveys using the forward sonar, summarized by 10-m river segments and survey day, for the SJR from Port of Stockton to Lathrop. Community sampling dates (from e-fishing efforts) denoted with an * below the Julian day.*

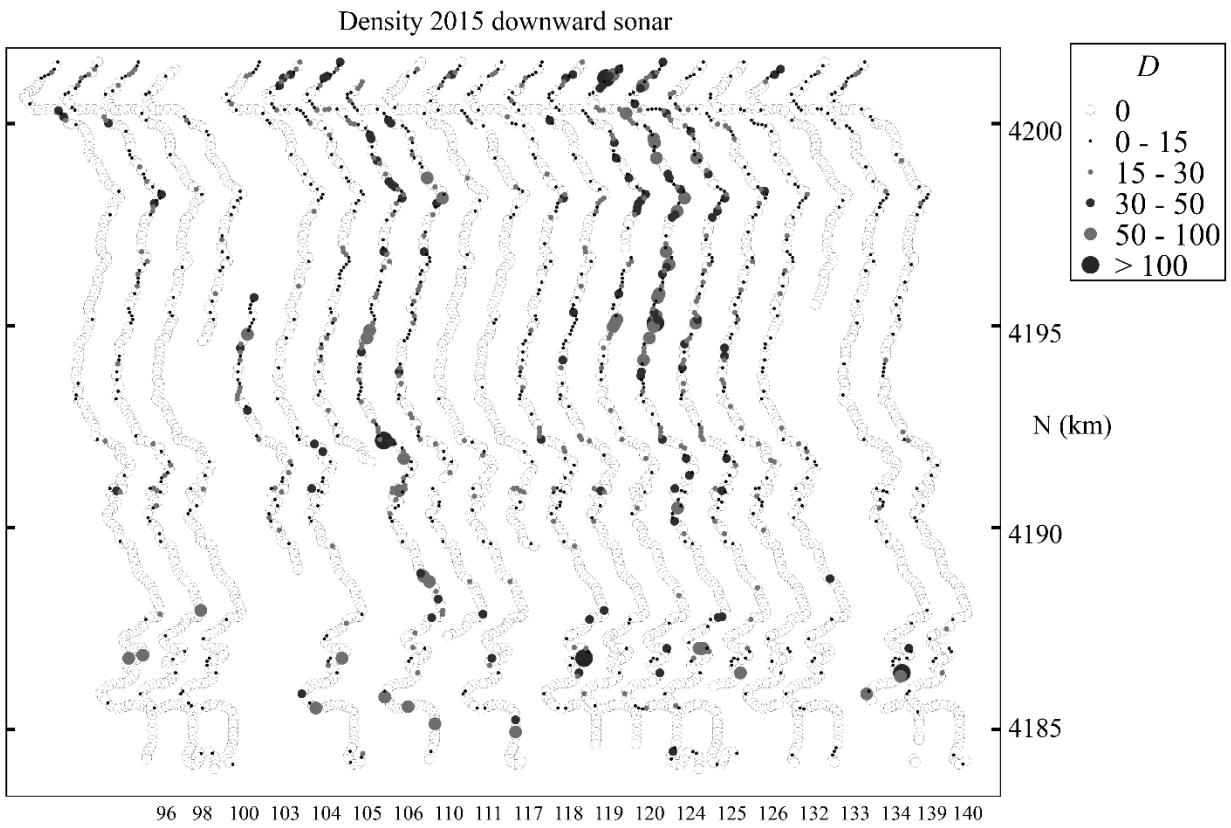


*Figure 31. Fish mean density estimates from the 2015 acoustic surveys using the downward sonar, summarized by 10-m river segments and survey day, for the SJR from Port of Stockton to Lathrop. Community sampling dates (from e-fishing efforts) denoted with an * below the Julian day.*

Density by study reach

Mean densities by study reach (Figure 2) ranged from 0 to 178 fish 1000 m⁻³ for 2014 (Table 10). In 2015, mean densities per reach ranged from 0 to 75 fish 1000 m⁻³ for the forward sonar (Table 11), and 0 to 40 fish 1000 m⁻³ for the downward sonar (Table 12). All of those highest density values occurring near the Port of Stockton deep-water shipping channel, north of study reach A3.

The zero density values tended to be in the interim sections that covered short distances (1.1, 4.1, 7.1) and in reaches with very shallow water for the downward sonar.

Table 10. Daily mean fish densities (fish 1000 m⁻³) by study reach for 2014, from the side 120-kHz sonar. “NA” indicates no data.

Reach	March			April					May										
	24	25	27	28	15	16	22	23	6	7	8	9	10	12	13	14	20	21	22
	83	84	86	87	105	106	112	113	126	127	128	129	130	132	133	134	140	141	142
0.1	3.4	NA	0.0	NA	NA	0.0	11.9	5.2	2.5	0.4	3.2	0.0	NA	NA	2.9	NA	NA	13.0	6.2
C1	18.0	NA	3.5	NA	2.0	NA	2.2	1.5	1.7	0.8	1.9	0.3	NA	NA	0.0	NA	0.0	1.3	0.5
1.1	48.9	NA	9.4	NA	11.5	0.8	6.1	1.0	0.6	0.3	0.0	0.0	NA	NA	1.0	NA	3.1	6.4	2.2
R1	16.8	NA	30.6	NA	7.9	6.9	2.2	1.0	2.5	1.6	1.4	0.6	NA	NA	1.5	NA	2.9	11.8	5.2
2.3	22.1	1.1	42.9	NA	20.7	28.5	5.1	3.3	2.6	2.4	3.5	1.6	NA	NA	9.9	NA	11.8	4.6	4.2
A1	15.8	7.0	61.3	NA	25.8	26.3	2.3	1.9	1.6	0.5	1.2	1.1	NA	NA	7.7	NA	10.5	2.6	5.0
3.5	29.8	4.0	9.8	NA	11.5	20.4	2.3	1.6	2.8	0.5	1.3	1.3	0.0	NA	8.7	NA	11.1	4.3	4.0
C2	82.5	22.7	1.7	NA	49.6	26.1	11.6	5.4	3.2	0.6	1.8	1.2	8.0	2.6	15.4	NA	19.5	7.5	14.2
4.1	54.8	44.1	9.9	NA	86.0	27.4	10.6	5.8	8.1	2.8	1.8	0.6	11.7	14.0	36.7	NA	22.3	23.0	23.3
R2	66.3	29.2	5.6	NA	62.0	32.3	24.1	14.1	8.6	4.3	4.1	1.8	10.1	3.0	21.3	NA	44.0	10.0	35.3
5.5	49.4	18.1	7.6	NA	25.7	37.5	9.7	16.4	5.4	1.9	2.1	2.4	6.6	3.0	23.9	NA	26.9	9.2	38.1
A2	NA	13.3	6.3	NA	9.1	30.4	21.8	8.4	6.9	0.6	2.3	0.9	3.0	3.9	17.3	NA	25.4	6.2	43.0
6.5	NA	17.1	8.7	0.0	3.4	34.3	29.9	19.0	3.7	0.2	0.7	4.9	3.3	0.6	7.5	NA	10.5	13.4	91.8
C3	NA	1.9	NA	15.0	3.9	25.5	35.5	16.8	3.4	0.5	0.7	NA	1.5	1.3	14.5	12.4	3.9	6.4	60.5
7.1	NA	4.6	NA	8.7	10.0	37.0	21.6	14.8	2.5	2.3	0.7	NA	1.1	1.8	13.5	9.4	5.3	12.3	48.7
R3	NA	9.5	NA	10.7	6.7	24.5	41.4	13.5	2.5	0.5	0.4	NA	3.4	1.5	0.0	14.4	2.3	21.6	61.3
8.5	NA	2.5	NA	17.7	23.6	16.3	36.8	20.2	8.7	1.6	3.2	NA	5.2	1.7	24.4	23.4	12.9	38.4	65.4
A3	NA	3.6	NA	23.6	18.0	21.1	51.7	20.7	38.4	11.3	0.7	NA	0.8	0.5	17.5	31.6	5.1	12.9	43.8
9.1	NA	0.0	NA	NA	6.9	178.1	79.0	32.6	30.4	39.8	0.5	NA	2.0	1.8	96.4	66.3	2.2	28.9	93.4

Table 11. Daily mean fish densities (fish 1000 m⁻³) by study reach for 2015, from the forward 120-kHz sonar. “NA” indicates no data.

Reach	April											May									
	6	8	10	13	14	15	16	20	21	27	28	29	30	4	5	6	12	13	14	19	20
	96	98	100	103	104	105	106	110	111	117	118	119	120	124	125	126	132	133	134	139	140
0.1	2.8	9.8	23.6	NA	NA	9.2	NA	22.2	NA	5.6	NA	1.2	3.0	19.9	2.4	NA	5.9	9.5	NA	NA	3.0
C1	1.7	2.6	1.2	NA	NA	2.5	NA	3.6	NA	2.3	NA	11.0	1.6	1.9	0.9	NA	2.4	2.1	NA	0.0	0.3
1.1	4.8	3.9	6.0	NA	NA	0.7	NA	4.6	NA	3.0	NA	32.7	7.0	4.7	2.3	NA	4.1	4.7	NA	1.0	2.6
R1	9.9	15.1	3.0	NA	NA	6.3	NA	12.0	NA	12.6	NA	3.3	19.0	12.4	0.9	12.5	18.3	12.5	NA	3.8	3.8
2.3	7.4	5.0	6.3	NA	NA	6.3	NA	11.0	NA	3.8	NA	12.6	6.7	12.3	5.6	11.5	4.6	5.2	NA	7.8	4.9
A1	10.1	3.6	7.9	NA	NA	3.6	NA	10.7	6.8	2.9	NA	8.0	3.3	8.4	24.8	7.9	5.5	2.5	NA	5.2	1.7
3.5	5.2	6.8	5.7	NA	8.5	2.6	NA	13.4	10.9	2.3	0.0	10.7	6.1	8.6	16.6	6.2	4.6	3.1	NA	4.3	2.8
C2	11.3	14.0	4.7	NA	13.6	8.5	NA	20.5	15.3	8.7	5.9	15.8	16.1	23.3	7.6	13.4	6.3	4.6	NA	6.4	4.2
4.1	8.5	18.5	7.4	NA	19.9	10.5	NA	22.9	22.1	11.7	9.1	17.6	14.7	18.3	3.0	15.7	7.2	6.1	NA	4.2	3.7
R2	9.2	18.1	6.9	NA	20.6	12.0	NA	29.1	25.9	3.9	9.1	23.1	28.8	33.2	4.7	22.4	8.3	6.2	NA	9.8	6.4
5.5	9.7	13.1	3.5	0.0	20.3	4.1	11.6	24.9	21.5	4.8	2.4	18.0	16.2	32.5	3.5	18.4	6.8	6.8	0.0	5.0	3.7
A2	23.6	12.3	3.1	NA	22.9	4.8	12.6	18.6	20.4	10.0	3.8	13.6	18.3	26.2	9.6	14.1	8.0	8.4	NA	3.9	2.9
6.5	31.1	12.6	4.5	6.1	23.7	4.9	22.0	17.3	20.0	14.2	6.1	14.1	25.0	31.2	6.6	16.9	8.1	6.6	14.5	1.7	3.9
C3	21.6	8.5	4.2	12.9	31.0	8.4	18.4	8.5	16.7	17.1	9.9	10.2	15.7	34.3	7.1	17.6	7.3	5.8	1.4	1.0	2.9
7.1	56.3	14.8	10.7	18.9	NA	3.3	15.1	18.9	20.0	6.0	6.3	13.2	22.2	37.6	2.2	18.4	9.3	4.1	0.5	1.1	3.0
R3	18.3	9.3	1.0	7.5	NA	2.7	8.6	6.6	14.3	4.9	3.0	9.0	13.2	21.9	3.9	14.4	7.6	5.7	1.4	1.1	1.7
8.5	26.8	18.3	3.0	14.2	NA	10.9	17.7	16.0	23.2	5.6	6.0	14.1	21.0	34.1	3.5	22.3	12.7	6.4	4.5	5.7	5.5
A3	44.5	13.1	2.6	22.3	NA	8.7	20.6	23.3	25.8	11.7	15.8	12.1	22.5	31.7	6.6	16.4	19.0	12.7	8.4	5.1	5.2
9.1	75.1	40.7	21.1	39.0	NA	36.8	31.6	54.9	NA	11.6	40.4	41.1	33.3	34.2	2.9	44.4	17.8	12.7	67.3	11.1	18.4

Table 12. Daily mean fish densities (fish 1000 m⁻³) by study reach for 2015, from the downward 200-kHz sonar. “NA” indicates no data.

Reach	April										May										
	6	8	10	13	14	15	16	20	21	27	28	29	30	4	5	6	12	13	14	19	20
	96	98	100	103	104	105	106	110	111	117	118	119	120	124	125	126	132	133	134	139	140
0.1	0.0	0.3	0.5	NA	NA	3.3	NA	2.1	NA	0.0	NA	0.0	0.0	3.5	0.6	NA	0.6	2.6	NA	0.0	1.0
C1	0.0	0.0	0.0	NA	NA	0.0	NA	5.9	NA	10.1	NA	0.0	0.0	0.0	0.0	NA	0.0	0.0	NA	1.2	0.0
1.1	0.0	0.0	2.5	NA	NA	8.4	NA	15.3	NA	2.5	NA	3.0	0.0	4.8	0.0	NA	0.0	0.6	NA	0.0	0.0
R1	1.2	1.1	2.9	NA	NA	7.6	NA	10.9	NA	2.5	NA	0.8	2.3	2.8	3.1	0.0	0.3	1.0	NA	7.7	0.8
2.3	6.6	1.3	1.4	NA	NA	6.8	NA	2.7	NA	3.9	NA	11.5	1.0	5.7	9.5	6.2	1.3	0.8	NA	15.8	3.3
A1	0.0	1.0	0.6	NA	NA	3.2	NA	2.9	0.0	0.0	NA	1.6	0.7	0.7	2.0	0.0	0.5	1.2	NA	0.7	3.1
3.5	1.6	2.3	0.2	NA	0.6	1.2	NA	18.7	2.5	1.4	2.8	3.3	0.3	1.0	4.1	1.4	0.0	2.0	NA	0.6	0.3
C2	0.6	3.5	0.5	NA	5.2	2.7	NA	4.2	2.3	0.9	0.0	3.4	3.1	1.1	7.9	7.0	1.9	0.4	NA	1.7	0.7
4.1	0.0	5.5	4.7	NA	4.4	2.1	NA	7.5	1.9	6.1	4.2	5.3	0.8	2.5	14.4	4.0	7.1	2.4	NA	6.6	0.9
R2	6.9	10.2	2.9	NA	6.6	4.9	NA	18.5	4.3	1.1	9.0	6.9	6.5	0.4	11.2	7.1	4.0	1.0	NA	1.7	1.1
5.5	1.6	3.0	0.2	NA	3.1	4.9	0.9	19.4	7.3	3.3	0.7	8.0	3.3	3.3	9.3	9.2	4.3	4.5	NA	0.3	3.3
A2	2.0	1.1	0.0	NA	14.1	0.7	3.4	6.5	6.7	1.0	1.0	5.6	4.0	2.1	5.9	4.8	5.7	1.4	NA	0.4	0.0
6.5	0.5	5.0	0.9	2.2	12.7	1.1	8.3	17.0	9.4	0.0	0.6	5.6	9.5	18.0	35.1	19.3	10.3	3.1	0.0	0.8	3.6
C3	0.0	7.5	1.2	3.1	34.8	1.6	5.1	9.4	8.9	0.6	0.0	3.5	3.6	11.1	30.3	11.3	5.1	6.9	0.0	0.9	1.5
7.1	0.0	9.1	1.9	3.8	NA	1.1	14.0	15.2	14.6	1.7	0.0	2.0	5.0	17.1	27.0	9.2	4.3	4.9	0.0	2.9	2.3
R3	0.7	1.6	0.0	4.3	NA	0.0	1.6	6.6	4.7	0.0	2.1	3.6	2.5	3.9	13.5	6.2	2.8	3.3	0.0	0.9	1.4
8.5	3.4	8.3	1.1	2.1	NA	2.3	4.8	17.1	10.8	0.8	3.0	5.8	5.1	13.1	23.1	13.8	7.7	3.7	0.4	3.7	3.0
A3	0.5	6.0	4.1	0.9	NA	3.6	9.3	6.1	10.3	0.3	4.2	4.0	6.0	9.1	14.9	17.2	8.7	1.8	0.7	4.3	4.6
9.1	9.5	13.1	11.1	0.4	NA	8.5	20.7	21.5	34.0	5.7	14.3	8.1	9.3	15.3	40.0	21.9	3.7	0.6	18.8	6.8	10.3

The spatial distribution of mean fish densities (collapsed over all survey days) had similar patterns between 2014 and 2015 (side and forward sonars) except for shifts in locations of the spikes of high density (Figure 32).

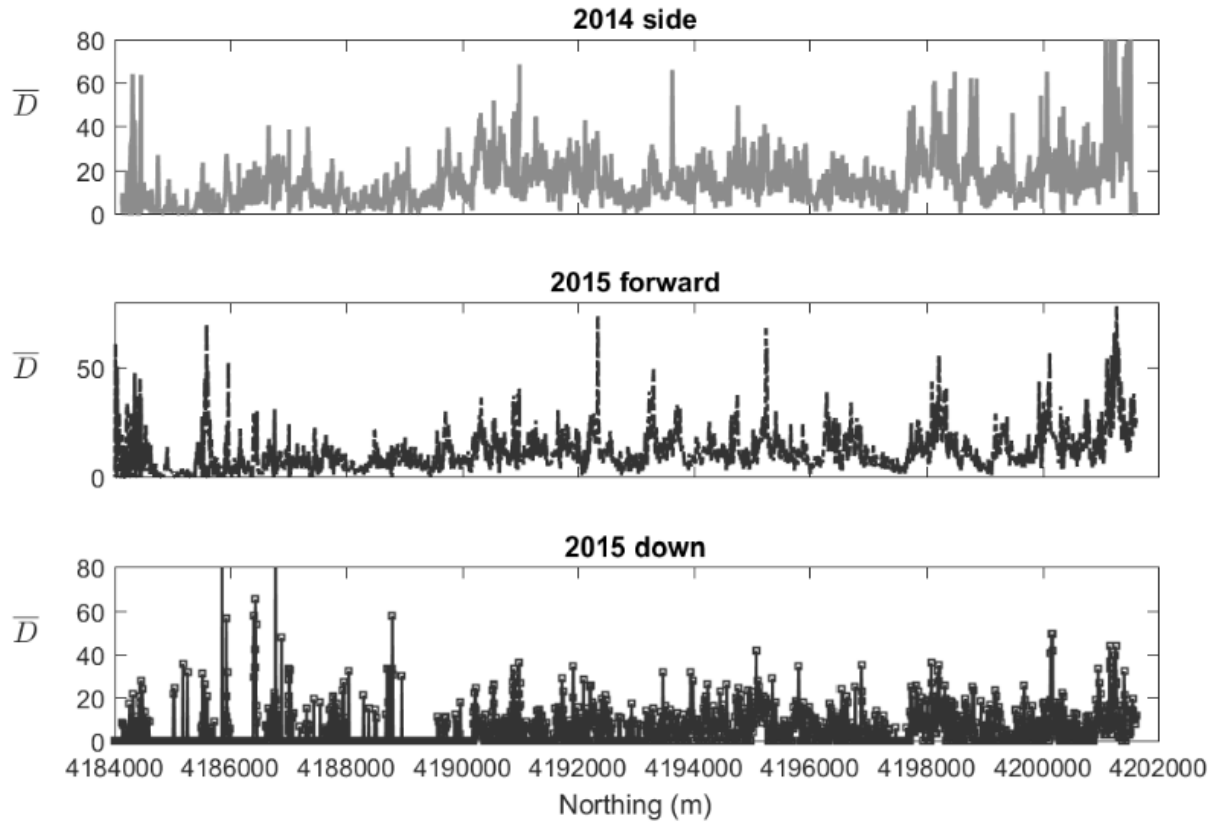


Figure 32. Mean fish density averaged over all days per 10-m river segment by year.

Density by time

Fish density distributions from 10-m river segments were skewed by many zeros such that median density, considering the entire north-south survey coverage on any day, was zero for 13 survey days of 2014 and 14 days of 2015 forward sonars. Upper quartile density values were variable and ranged to about 50 fish 1000 m^{-3} for the 2014 side sonar and 30 fish 1000 m^{-3} for the 2015 forward sonar. For the 2015 downward sonar, all survey days had a median and upper quartile density of zero (Figures 33, and A27-A30).

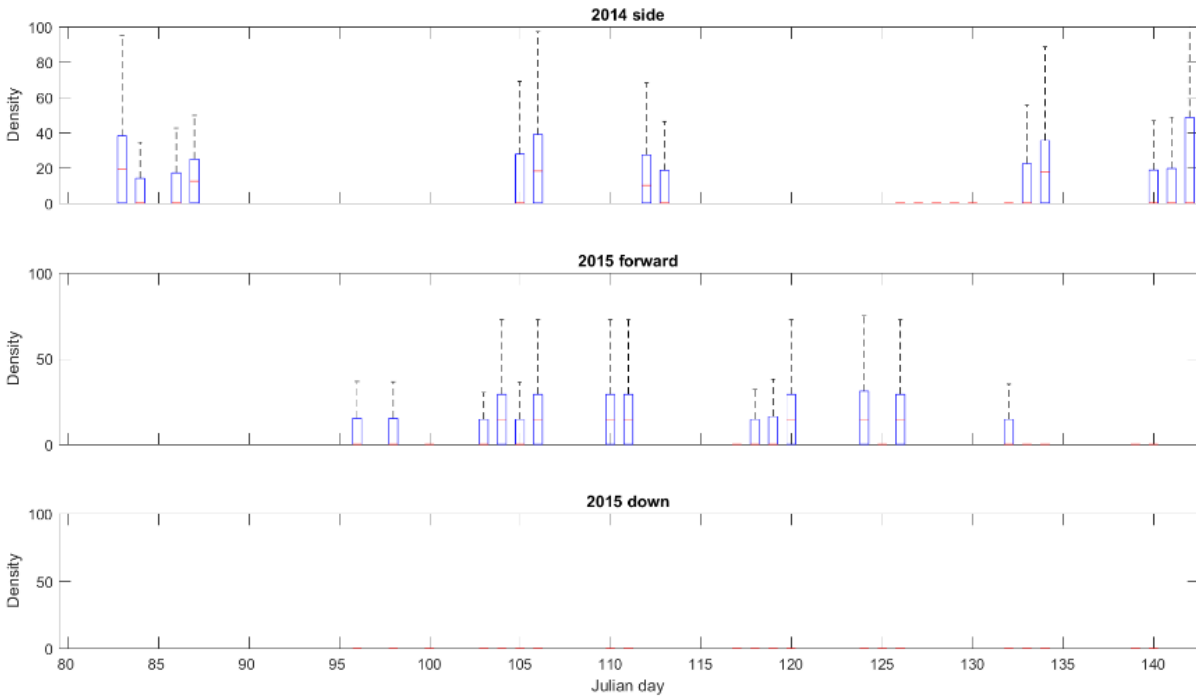


Figure 33. Distribution of fish densities (# fish 1000 m^{-3}), including zeros, per 10-m segment, for each survey date (Julian Day) and by transducer type, represented by box-whisker plots.

With zeros excluded from the full-survey, per-day density distributions, median fish densities (from 10-m river segments) ranged from about 20 to 65 fish 1000 m⁻³ from the 2014 side sonar, 15 to 30 fish 1000 m⁻³ from the 2015 forward sonar, and 40 to 75 fish 1000 m⁻³ from the 2015 downward sonar (Figure 34).

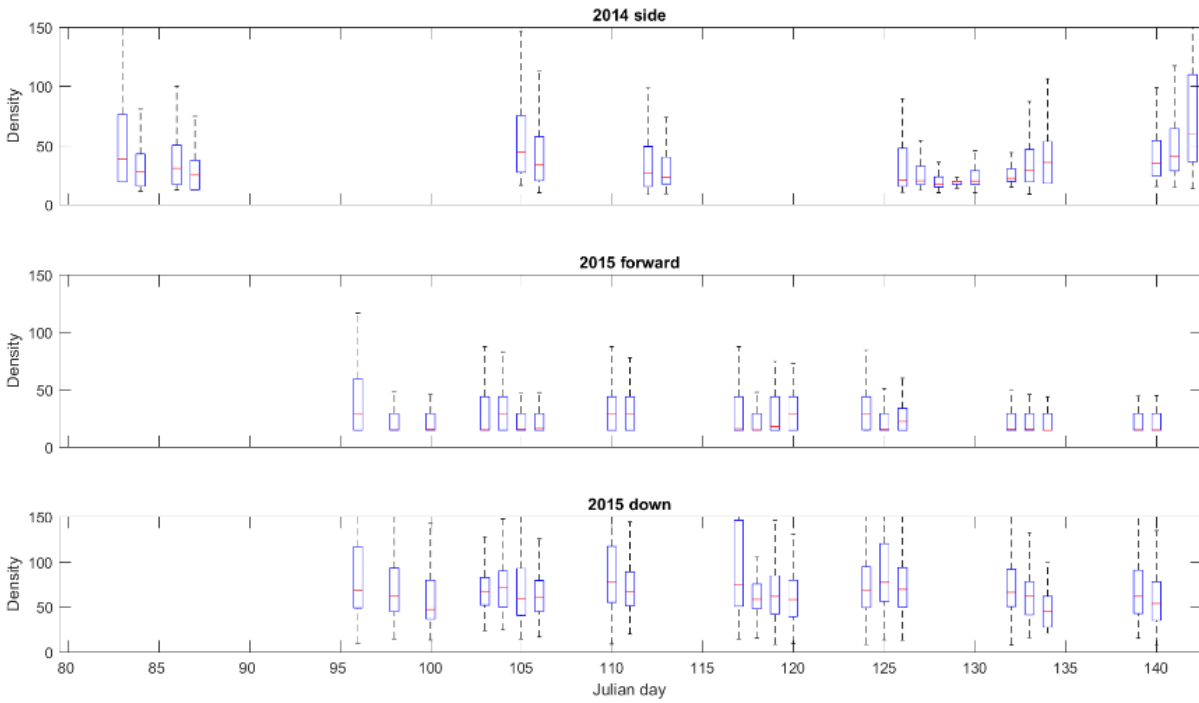


Figure 34. Distribution of fish densities (# fish 1000 m⁻³), excluding zeros, per 10-m segment, for each survey date (Julian Day) and by transducer type, represented by box-whisker plots.

Fish abundance estimates

Preliminary estimates of fish abundance, summed by 10-m river segment, are presented for the entire surveyed river (Figures 35-38) and for each study reach (Tables 13-15). Spatial and temporal patterns of abundance are similar to those of density.

Fish abundance estimates from the 2014 and 2015 side and forward sonars show strong temporal and spatial variability (Figure 35 left and center panels, Figures 36 and 37). The northern portion of the study area had very high values throughout the 2014 season, while the rest of the river varied between periods of high (early and late) and low (middle) abundances.

During 2015, abundances from the downward sonar appeared less variable overall but values fluctuated quickly from high to low (and low to high) in small regions (Figure 35, right panel, and Figure 38).

Some localized areas had consistently high abundances (orange and red points) such as near northing 4,200,250 on nearly all survey days in both years.

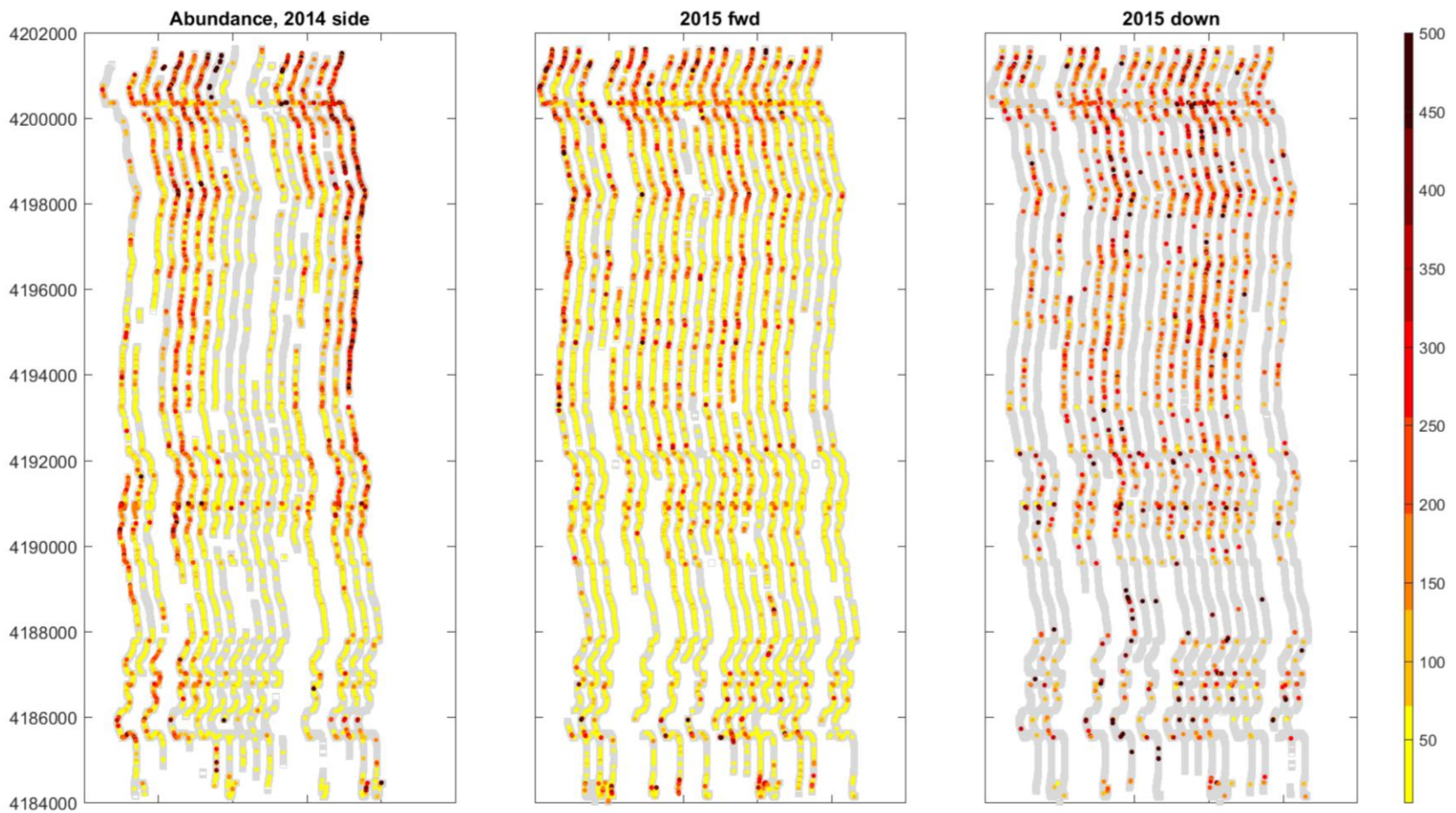


Figure 35. Maps of fish abundance estimates from acoustic surveys, summarized by 10-m river segments and survey day (Julian Day along the horizontal axis) for the SJR from Port of Stockton to Lathrop. Sonars (left to right): 2014 120 kHz, 2015 120 kHz, 2015 200 kHz.

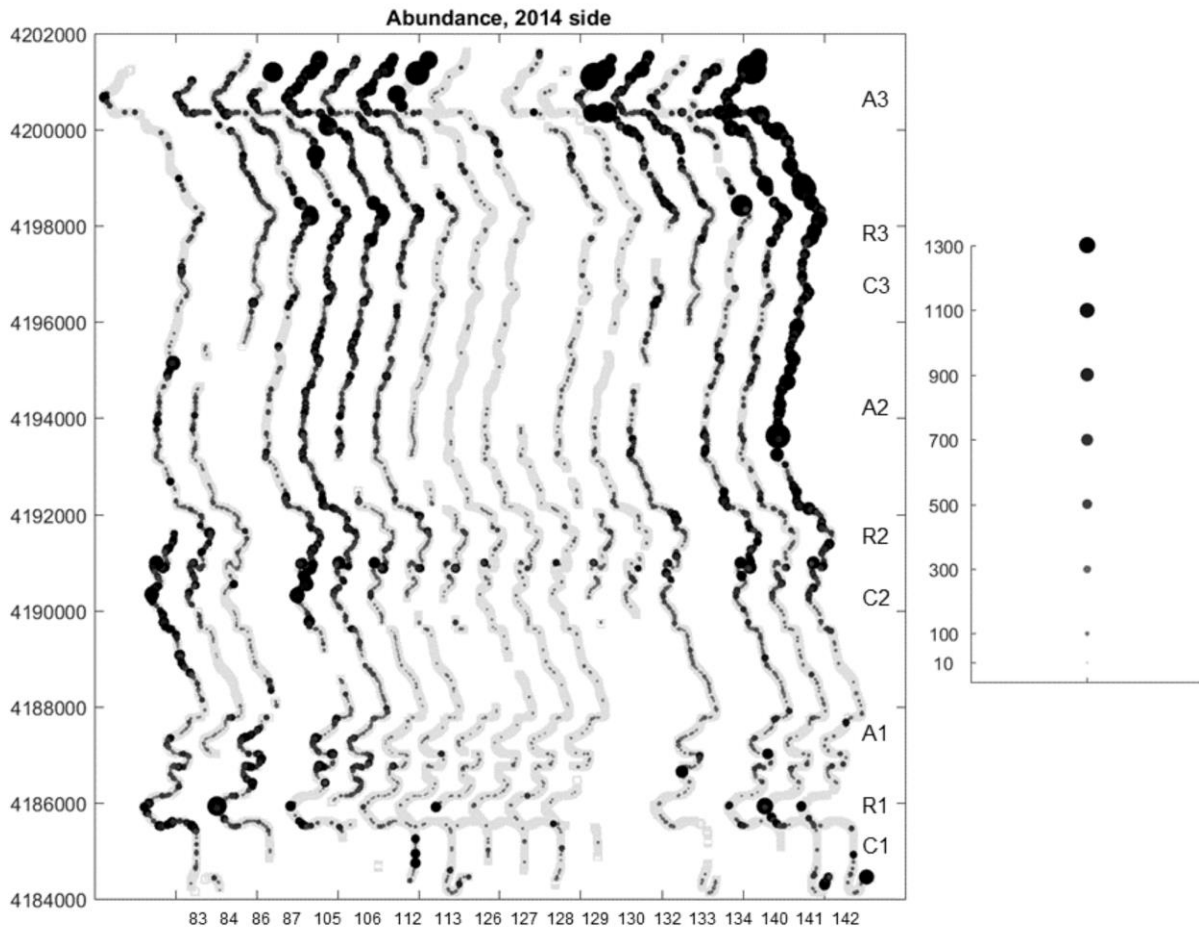


Figure 36. Maps of fish abundance estimates from the 2014 acoustic surveys using the side sonar, as sum of abundance within 10-m river segments and by survey day, for the SJR from Port of Stockton to Lathrop.

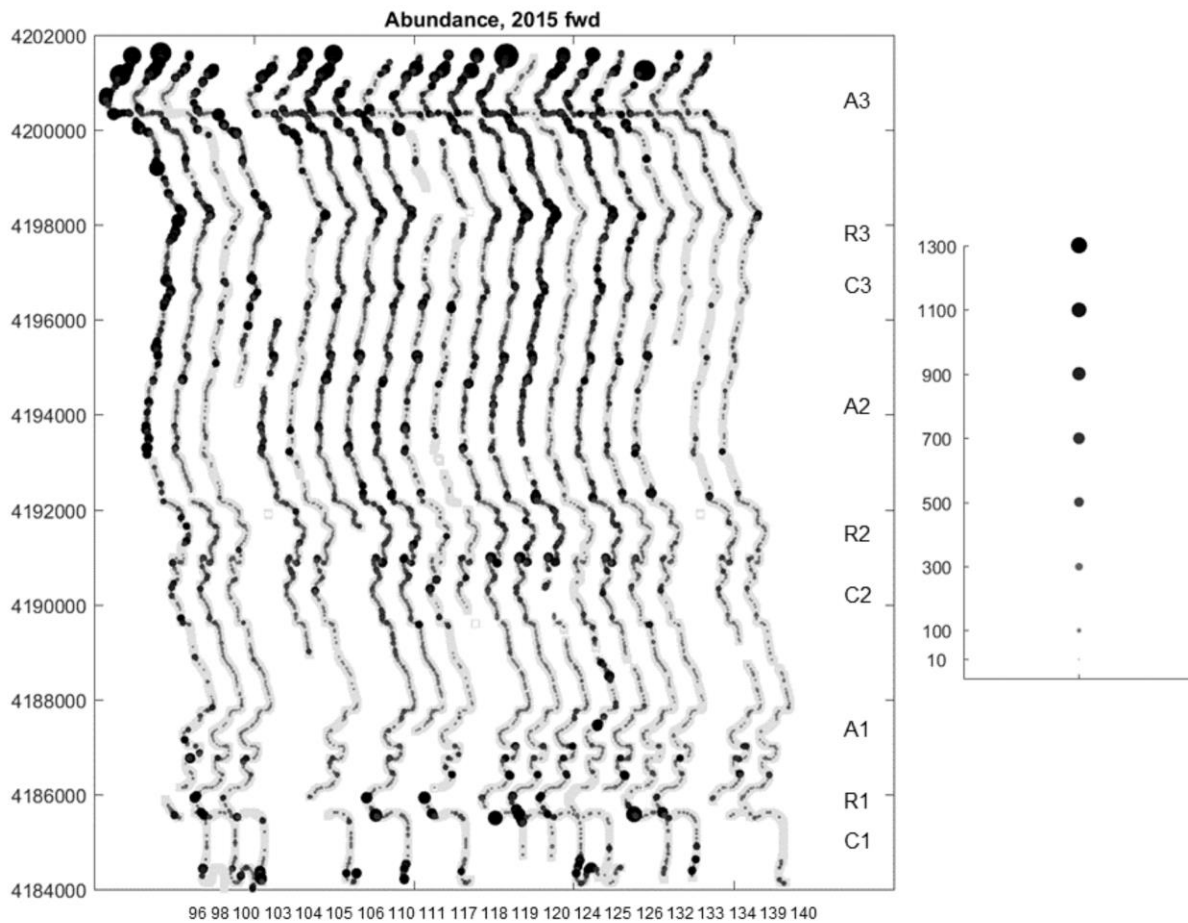


Figure 37. Maps of fish abundance estimates from the 2015 acoustic surveys using the forward sonar, as sum of abundance within 10-m river segments and by survey day, for the SJR from Port of Stockton to Lathrop.

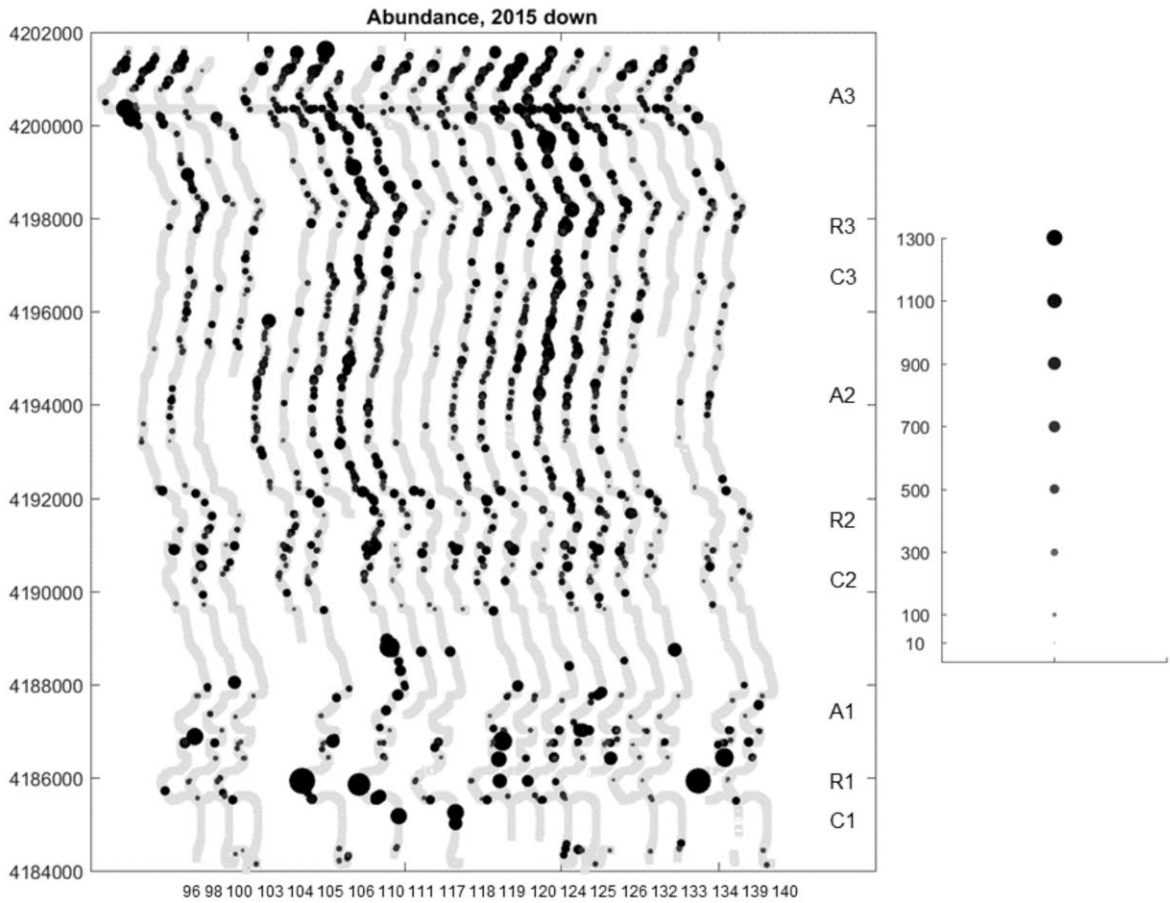


Figure 38. Maps of fish abundance estimates from the 2015 acoustic surveys using the down sonar, as sum of abundance within 10-m river segments and by survey day, for the SJR from Port of Stockton to Lathrop.

Abundance by study reach

For the 2014 side sonar, daily summed fish abundance ranged from 0 to 16,300 fish per 1-km study reach ('C#', 'R#', 'A#' in Tables 13-15). In the interim-sections (numbered reach labels in the tables) (Table 13), fish abundance ranged from 0 to 40,000 with one outlier of > 70,000 on 22 May 2014 in section 8.5. Section 8.5 covered nearly 4 km.

During 2015, fish abundance by reach ranged from 0 to 38,000 for the forward sonar (Table 14), and from 0 to nearly 27,000 for the downward sonar (Table 15), including section 8.5.

The zeros tended to be in the interim sections that covered short distances (1.1, 4.1, 7.1). The highest abundances of 2014 and 2015 for all three sonars occurred in river section 8.5, in the northern part of the study area downstream of R3 and upstream of A3. Section 8.5 was a long interim stretch (Figure 2), and these estimates should be considered relative to the river distance by reach.

Table 13. Daily summed fish abundance by study reach for 2014 side sonar. "NA" indicates no data.

Reach	March				April				May										
	24	25	27	28	15	16	22	23	6	7	8	9	10	12	13	14	20	21	22
	83	84	86	87	105	106	112	113	126	127	128	129	130	132	133	134	140	141	142
0.1	989	NA	0	NA	NA	0	1849	2135	126	37	559	0	NA	NA	669	NA	NA	5131	3122
C1	4575	NA	1004	NA	448	NA	570	409	315	188	574	48	NA	NA	0	NA	0	384	141
1.1	5840	NA	1440	NA	1906	33	924	142	77	52	0	0	NA	NA	169	NA	500	986	362
R1	4179	NA	8140	NA	2645	315	577	183	754	331	271	133	NA	NA	426	NA	1204	4566	2075
2.3	7098	38	14795	NA	8539	9783	2042	1240	766	690	1096	394	NA	NA	3567	NA	4393	1625	1386
A1	2619	1136	9578	NA	4487	4458	366	312	281	79	192	202	NA	NA	1317	NA	1842	454	805
3.5	11042	1622	2979	NA	3394	8020	873	620	322	178	585	538	0	NA	3641	NA	4631	1859	1733
C2	16197	3971	329	NA	10196	4428	2030	511	274	126	348	230	392	365	2984	NA	4006	1566	2866
4.1	4881	3551	1097	NA	8578	2032	1124	556	690	306	187	78	910	1364	3213	NA	2619	2679	2537
R2	14921	5902	1281	NA	14931	7680	5966	3446	2267	1143	872	440	2584	531	4148	NA	10280	2558	8484
5.5	2618	6191	3010	NA	10263	14524	3105	6499	1578	788	844	909	1892	1284	9409	NA	10847	3602	15329
A2	NA	2339	1296	NA	1977	6421	2414	1817	714	124	427	186	556	830	3630	NA	5382	1367	6632
6.5	NA	7328	2423	0	1488	15220	11155	7326	1655	103	269	154	1408	237	2302	NA	4494	5977	39886
C3	NA	429	NA	3379	924	5718	7870	3199	772	104	148	NA	263	170	2782	1642	830	1358	13302
7.1	NA	554	NA	1075	1226	4434	2579	789	311	277	73	NA	138	245	1480	1099	608	1513	5885
R3	NA	2244	NA	2626	1687	5967	10270	3256	588	146	118	NA	722	355	0	3532	576	5400	15040
8.5	NA	2493	NA	17458	25530	17548	38993	22050	7929	1786	3646	NA	5216	1689	24872	25346	12584	41081	71686
A3	NA	1234	NA	7493	5603	5860	16301	6550	11950	3796	227	NA	244	128	5622	9568	1650	2000	13716
9.1	NA	0	NA	NA	1870	9463	19489	7516	7209	8405	133	NA	799	69	20139	15775	480	5686	23242

Table 14. Daily summed fish abundance by study reach for 2015 forward sonar. "NA" indicates no data.

Reach	April											May									
	6	8	10	13	14	15	16	20	21	27	28	29	30	4	5	6	12	13	14	19	20
	96	98	100	103	104	105	106	110	111	117	118	119	120	124	125	126	132	133	134	139	140
0.1	1380	4937	5473	NA	NA	2605	NA	4436	NA	1613	NA	85	256	10228	1072	NA	1178	1853	NA	NA	742
C1	450	706	360	NA	NA	745	NA	961	NA	684	NA	3312	313	547	230	NA	532	593	NA	0	82
1.1	264	631	750	NA	NA	45	NA	674	NA	389	NA	4267	1092	760	310	NA	633	800	NA	84	372
R1	1572	4778	871	NA	NA	464	NA	4177	NA	2814	NA	842	5845	3305	257	344	4947	3521	NA	528	859
2.3	2615	1874	2351	NA	NA	2247	NA	3802	NA	1338	NA	5064	2578	4612	1840	4369	1459	1720	NA	3144	1699
A1	1681	617	1310	NA	NA	637	NA	1884	815	502	NA	1343	584	1483	3857	1275	985	426	NA	902	303
3.5	2136	2753	2366	NA	1240	1061	NA	5665	4396	973	0	4169	2618	3216	6408	2291	2024	1330	NA	1416	1094
C2	2280	2729	920	NA	2479	1508	NA	3944	3001	1800	829	2618	3177	1456	1426	2639	1377	1015	NA	1258	893
4.1	879	1748	806	NA	2206	1101	NA	2618	2420	1138	980	1896	1571	710	323	1445	762	706	NA	476	416
R2	2045	4401	1621	NA	4601	2765	NA	6885	5713	858	2285	5970	7075	8035	1038	5477	1928	1461	NA	2351	1460
5.5	3735	4751	1414	0	8199	1460	4190	10035	8495	1904	810	7211	6617	11816	1464	7494	2707	2652	0	2070	1461
A2	4595	2594	653	NA	4928	948	2614	3979	4297	2207	492	2467	2898	3432	1970	3003	1656	1840	NA	836	630
6.5	13179	5788	1852	1077	8968	2121	9864	7601	8952	6537	2562	6093	11303	13854	2902	7540	3683	3008	152	746	1713
C3	4988	1884	949	2724	2971	1850	4118	1924	3734	3945	2118	2298	3480	7787	1604	3946	1682	1281	345	228	650
7.1	6853	1785	1270	2401	NA	411	1820	2285	2417	752	768	1623	2647	4580	273	2251	1119	491	67	136	372
R3	4694	2317	235	1887	NA	771	2113	1574	3461	891	762	2278	3279	5377	963	3550	1811	1513	359	267	426
8.5	29184	19480	3595	15730	NA	12237	20221	17689	25982	4684	4749	16222	20865	37920	4074	25575	14564	7251	5207	6477	6269
A3	14089	4063	796	5820	NA	2694	3302	7320	7016	3629	4928	3784	7134	9834	1709	5165	5939	3939	2472	1699	1577
9.1	23685	13067	6472	7011	NA	8721	9379	18221	NA	2396	10664	12389	11446	13145	649	14258	5782	3869	11882	3480	5240

Table 15. Daily summed fish abundance by study reach for 2015 downward sonar. "NA" indicates no data.

Reach	April												May								
	6	8	10	13	14	15	16	20	21	27	28	29	30	4	5	6	12	13	14	19	20
	96	98	100	103	104	105	106	110	111	117	118	119	120	124	125	126	132	133	134	139	140
0.1	0	166	117	NA	NA	1074	NA	307	NA	0	NA	0	0	1923	303	NA	117	506	NA	0	267
C1	0	0	0	NA	NA	0	NA	1241	NA	2707	NA	0	0	0	0	NA	0	0	NA	292	0
1.1	0	0	363	NA	NA	1298	NA	1927	NA	346	NA	450	0	756	0	NA	0	116	NA	0	0
R1	353	467	1157	NA	NA	4054	NA	3443	NA	593	NA	398	1589	1221	1167	0	66	353	NA	3833	163
2.3	2425	669	599	NA	NA	2182	NA	948	NA	1585	NA	4451	440	2388	3508	3109	509	403	NA	6807	1498
A1	0	158	98	NA	NA	568	NA	421	0	0	NA	291	129	131	378	0	88	209	NA	118	503
3.5	646	719	88	NA	80	473	NA	7822	859	633	89	1328	149	401	1735	534	0	872	NA	221	133
C2	113	661	135	NA	1086	517	NA	890	346	201	0	595	519	158	1519	1273	391	94	NA	337	128
4.1	0	620	433	NA	550	246	NA	806	223	610	384	609	103	218	1553	404	811	301	NA	720	110
R2	1477	2424	697	NA	1672	1477	NA	4307	449	295	1694	2029	1824	92	3125	1884	907	269	NA	523	274
5.5	592	1237	87	NA	1291	1849	318	6146	2986	1237	294	3298	1286	1176	3842	3787	1728	1838	NA	126	1242
A2	407	223	0	NA	2975	142	698	1514	1437	215	202	1101	884	299	1229	1006	1208	315	NA	80	0
6.5	232	2204	371	453	5316	507	3809	7627	4095	0	278	2387	3810	7593	15414	8628	4459	1371	0	336	1590
C3	0	1554	236	700	2051	351	1137	1849	1797	149	0	805	798	2484	6847	2523	1162	1559	0	221	341
7.1	0	1160	234	482	NA	163	1717	1887	1774	205	0	280	588	1328	3314	1122	534	597	0	359	278
R3	210	376	0	1039	NA	0	382	1769	1093	0	504	867	564	893	3503	1488	778	744	0	213	368
8.5	4674	8811	1187	2510	NA	2451	5336	19515	12305	854	2855	6444	5687	14183	26778	16063	8623	3904	348	4101	3367
A3	182	1826	1235	223	NA	1179	2904	1852	3276	100	1365	1180	1961	2830	4428	5382	2710	585	234	1346	1424
9.1	2723	3536	3500	70	NA	3065	7512	8796	936	1441	3893	2546	3526	5408	10243	8165	1437	211	3502	2090	3722

Patterns of spatial distribution of mean fish abundance, over all survey days for each location (10-m river segment), were similar between 2014 and 2015 for all three transducer orientations, including occasional spikes of high abundances (seen more readily in 2014 side and 2015 forward sonars; Figure 39). During each year, several small stretches had much higher abundance than their neighboring areas.

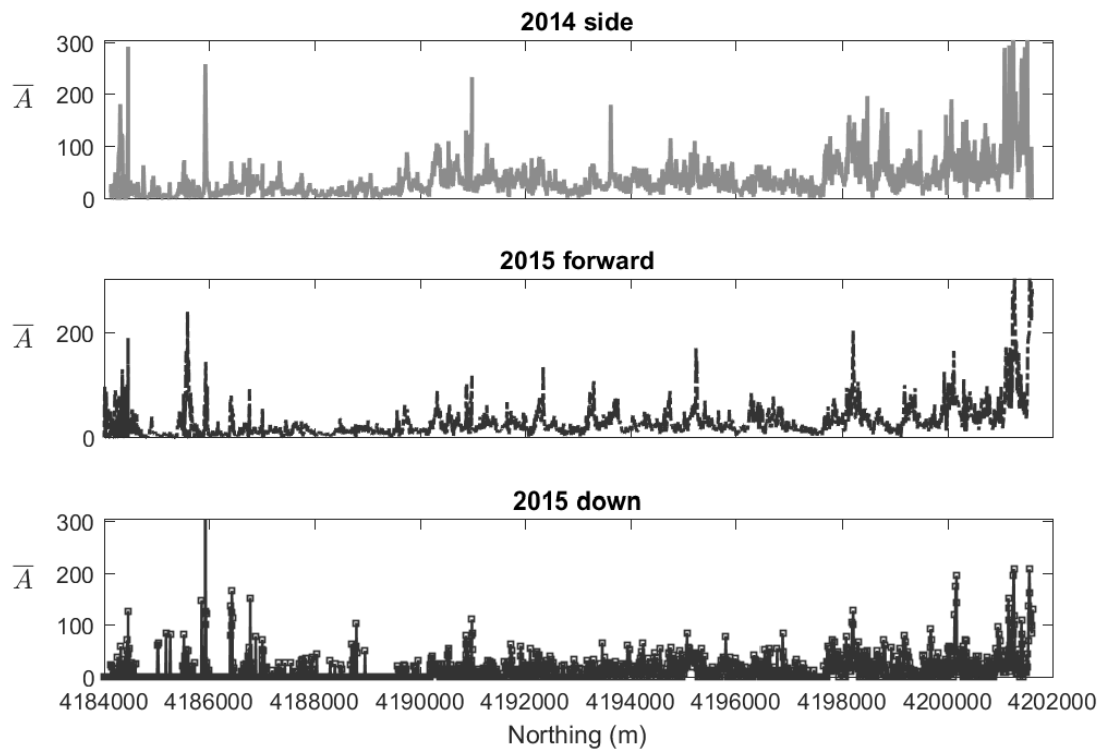


Figure 39. Mean fish abundance averaged over all days per 10-m river segment.

Fish abundance distributions from 10-m segments, like density distributions, were skewed by many zeros (Figure 40). Daily median abundance was 0 for 14 survey days of 2014 and 12 survey days of 2015 forward sonars. Upper quartile abundance values were variable and ranged from 0 to just over 100 for the 2014 side sonar and 80 for the 2015 forward sonar. For the 2015 downward sonar, all survey days had a median and upper quartile abundance of zero using this 10-m segment integration scale.

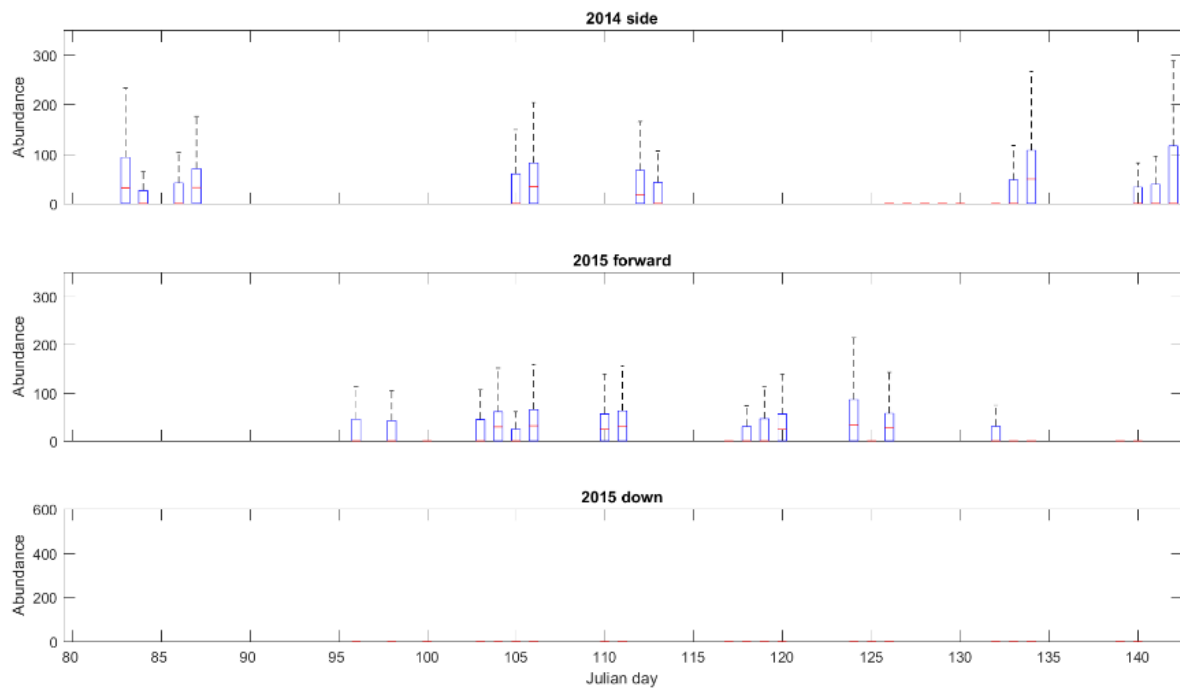


Figure 40. Distribution of fish abundance, including zeros, per 10-m segment by time (Julian days) are represented by box-whisker plots for 2014 side (top), 2015 forward (middle) and 2015 downward (bottom).

With zeros excluded, daily median fish abundance ranged from about 30 to 150 fish per 10-m segment from the 2014 side sonar, 30 to 50 from the 2015 forward sonar, and 150 to 200 from the 2015 downward sonar (Figure 41).

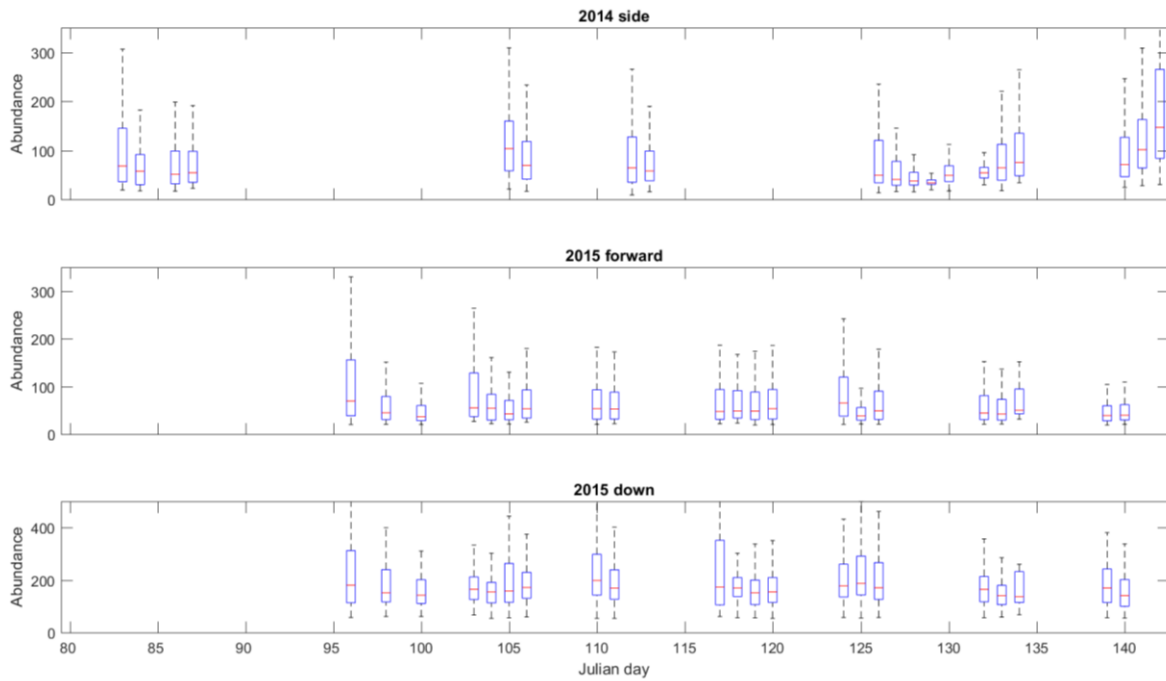


Figure 41. Distribution of fish abundance, excluding zeros, per 10-m segment by time (Julian days), represented by box-whisker plots for 2014 side (top), 2015 forward (middle), and 2015 downward (bottom).

All survey efforts were meant to cover at least one 3-reach block where tethering experiments were being conducted on that day; most surveys covered the entire 26-km stretch including all three blocks. Survey coverage area ranged from 7 to 24.2 km in 2014 and from 7.7 to 24.7 km in 2015 (Figure 42).

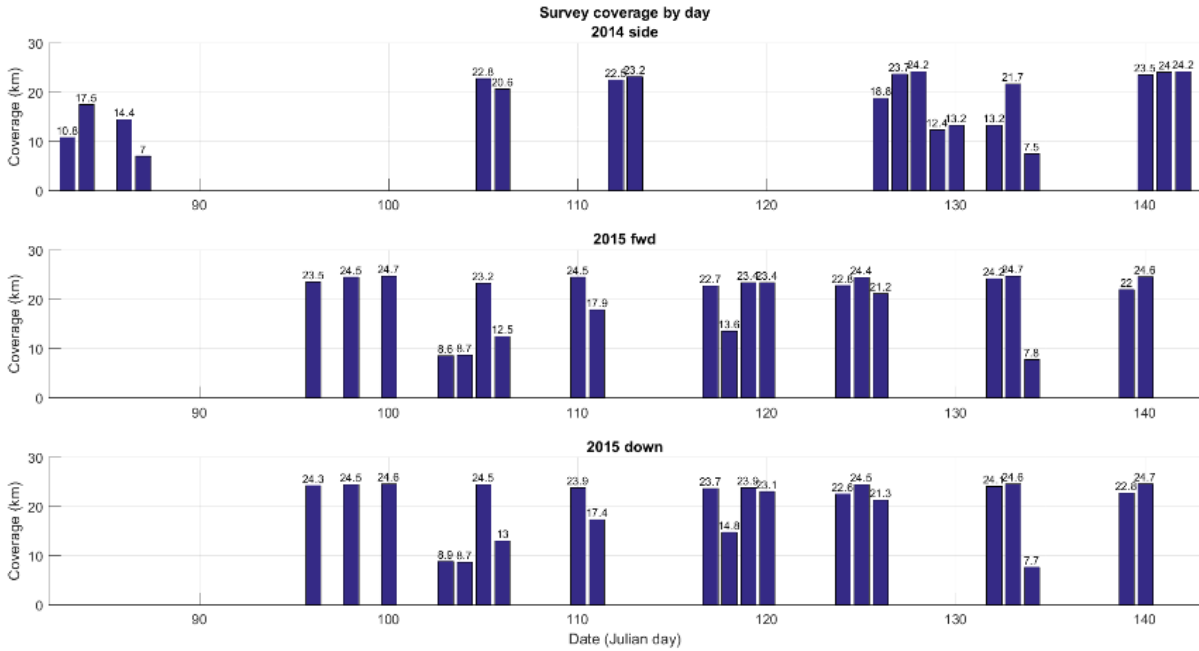


Figure 42. Survey coverage per day (Julian days) for the full river for 2014 side (top), 2015 forward (middle), and 2015 downward (bottom).

For days when > 80% of the river was covered by the acoustic survey, total fish abundance estimates ranged from 10,000 to 128,000 fish, and one outlier abundance of 228,000 fish on JD 142, for the 2014 side sonar. During 2015, total fish abundance ranged from 25,000 to 127,000 for the forward sonar, and 10,000 to 89,000 for the downward sonar (Figure 43).

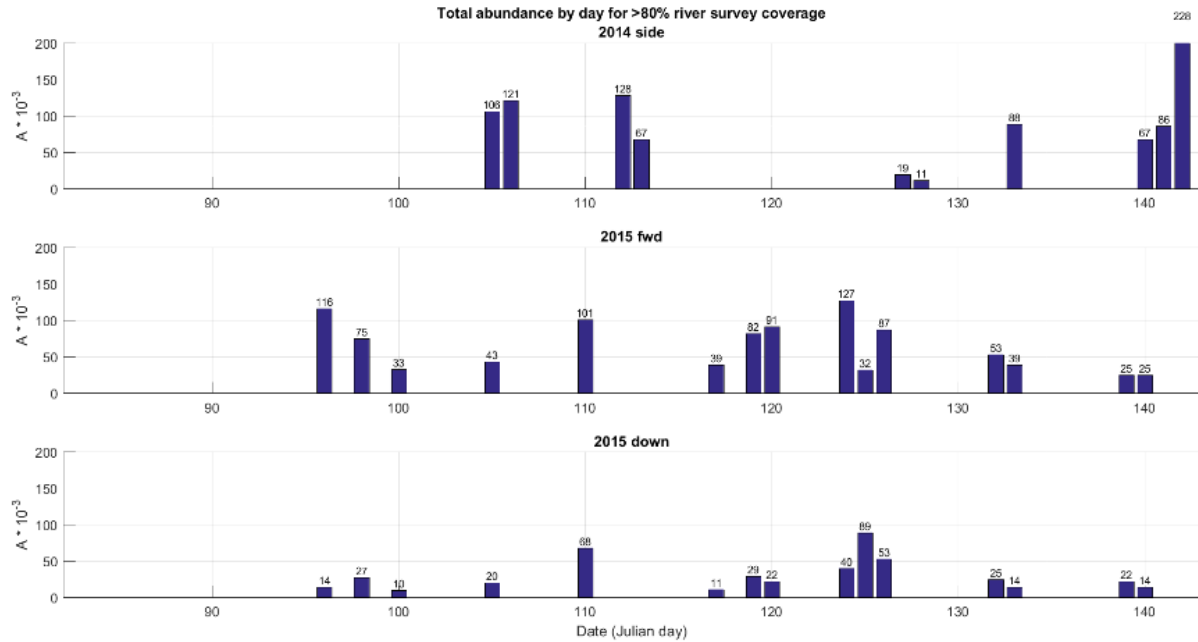


Figure 43. Total fish abundance per day (Julian days) for the full river (survey coverage > 80%) for 2014 side (top), 2015 forward (middle), and 2015 downward (bottom).

Including all days, regardless of survey coverage, fish abundance per 1-km distance of river ranged from 200 to 9,400 fish km^{-1} for the 2014 downward sonar, from 1000 to 5600 for the 2015 forward sonar, and from 500 to 3600 for the 2015 downward sonar (Figure 44).

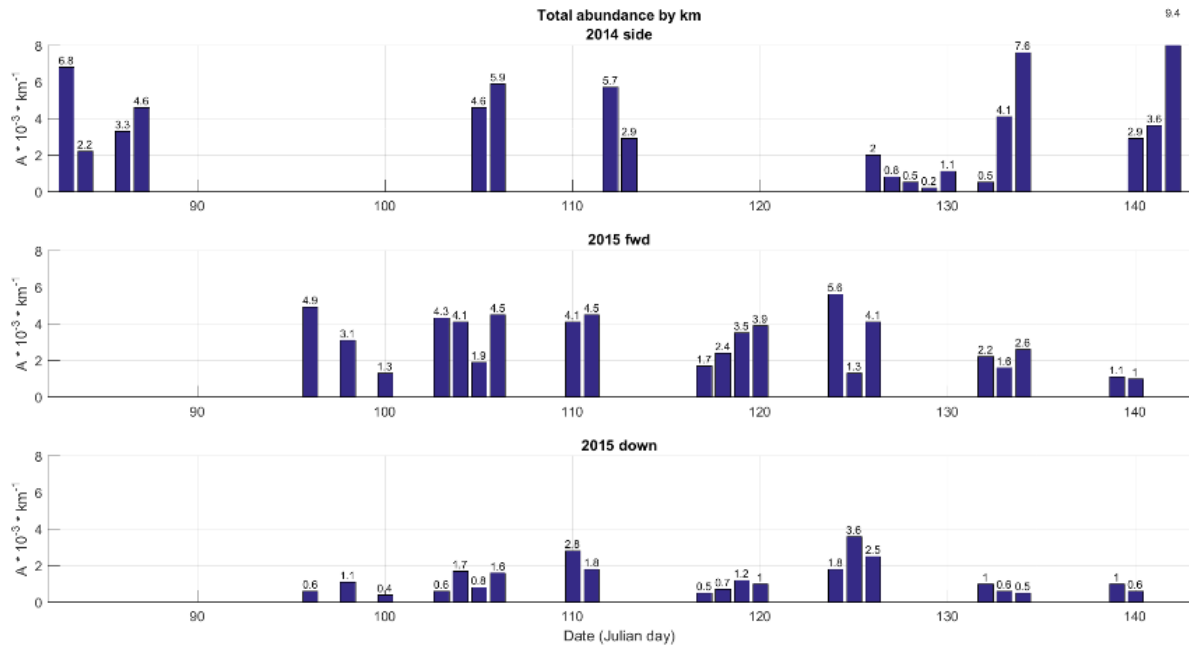


Figure 44. Fish abundance per km by day (Julian days) for all survey days: 2014 side (top), 2015 forward (middle), and 2015 downward (bottom).

Abundance estimates were derived from density estimates scaled to the full river volume within each 10-m river segment. These estimates may be biased high because the scaling to full volume considered all parts of the river within each segment to have the same probability of fish occurrence. Future work is planned to better resolve fish-habitat associations which will reduce error of abundance estimates.

Areas with persistent high densities

Areas with persistent high densities of fish were defined as the proportion of time $p_{days, D_{high}}$ when the density of fish exceeded the overall median density ($29 \text{ fish } 1000 \text{ m}^{-3}$). Figures 45 and 46 show the distributions and maps of the proportion of time that high density $D > D_{med}$ occurred within each 10-m river segment, by year and sonar. Persistence of high densities $p_{days, D_{high}} > 20\%$ occurred commonly, and $p_{days, D_{high}} > 40\%$ or 50% occurred rarely (Figure 45). Locations where densities were high for more than half of the survey period ($p_{days, D_{high}} > 50\%$) (March - May 2014, and April - May 2015) are considered 'hotspots.'

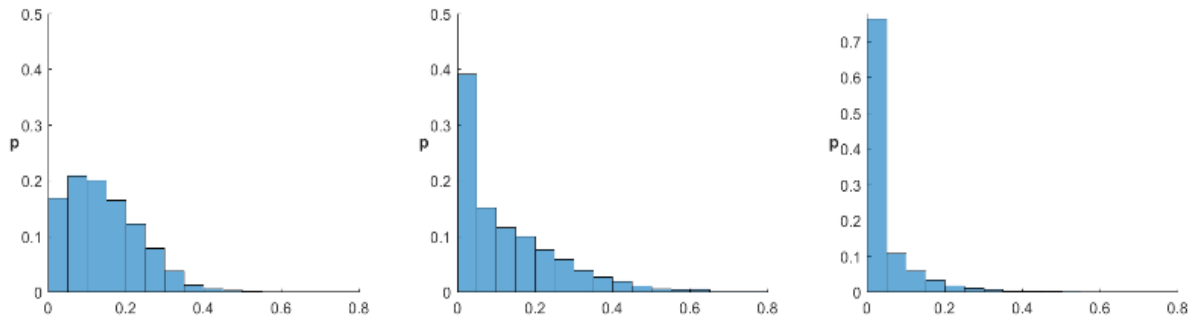


Figure 45. Histograms of the proportion of time that fish density exceeded median fish density ($D > D_{med}$) for 2014 side, 2015 forward, and 2015 downward (from left to right).

Hotspots were identified during 2014 and 2015 in both shallow and deep water. Areas with persistent high density are evident just south of Port of Stockton ($4,200,000 < N < 4,202,000$), in the vicinity of the confluence of French Camp Slough and the San Joaquin River ($N \sim 4,198,000$), and in a highly meandering section of river $4,190,000 < N < 4,192,000$ (Figure 46).

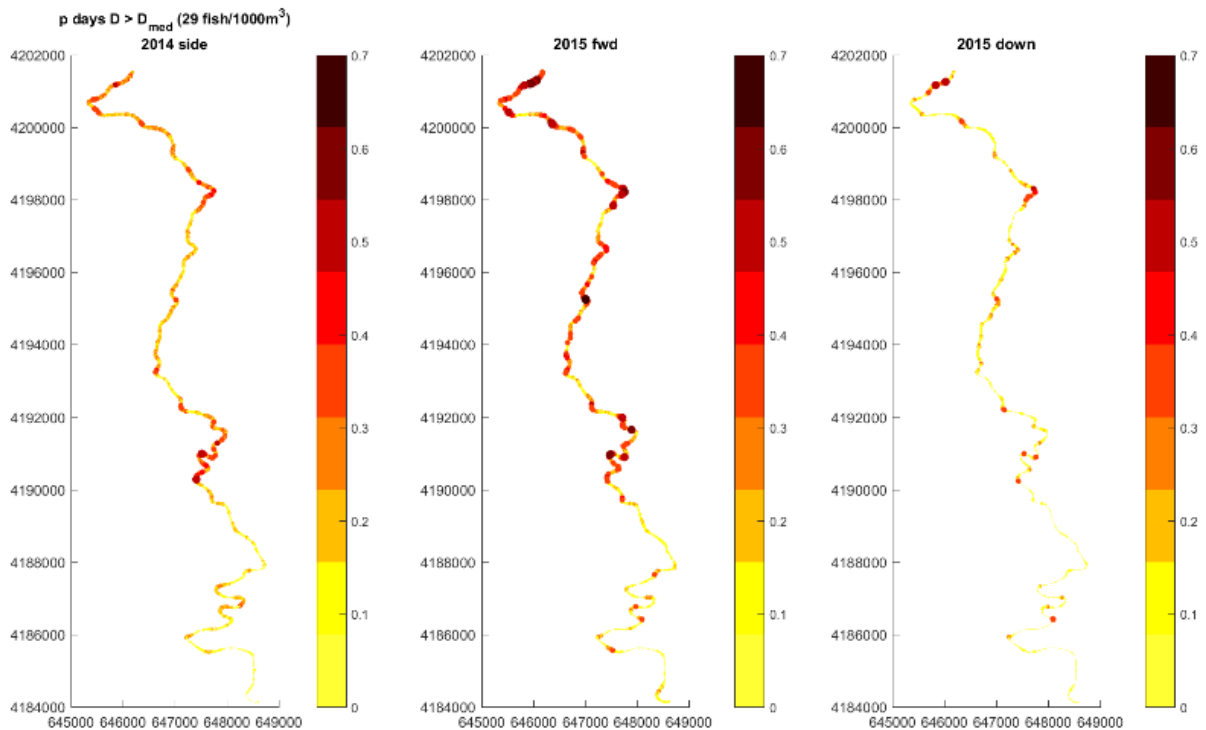


Figure 46. Proportion of time that fish density exceeded median fish density ($p_{days, D_{high}}$ where $D > D_{med}$).

For the 2014 side, 2015 forward, and 2015 downward sonars, respectively, 83, 81, and 44% of the river had daily fish densities which exceeded the median density for the entire study period ($D > D_{med}$). This indicates that high densities were common in all except the southern part of the study area ($< N$ 4,189,000) for the shallow and near-surface waters sampled by the 2014 side and 2015 forward sonars. Low densities were common for the southern half of the study area in the shallower waters sampled by the 2015 downward sonar, but high densities were common in the deep pools near river bends (Figure 47).

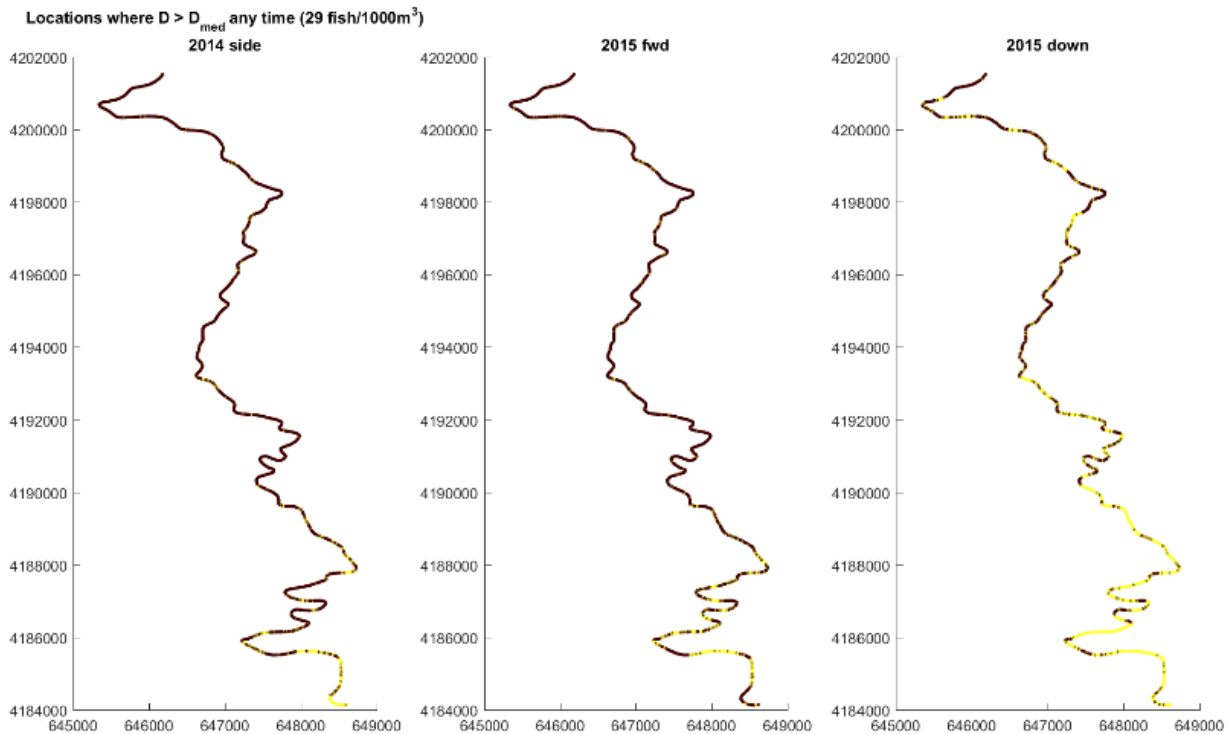


Figure 47. Locations where fish density exceeded median fish density ($D > D_{med}$) at any time, for 2014 side, 2015 forward, and 2015 downward (from left to right). Dark brown indicates presence and yellow indicates absence.

Fish density comparisons

Density comparisons by space

Multiple-comparison tests (Kruskal-Wallis statistic) of mean densities for each reach show significant differences of fish densities between the southern and northern reaches (evident as non-overlapping bounding bars). Densities in C1, R1, and A1 were lower than densities in C2, R2, A2, C3, R3, and A3 for the 2014 side and 2015 forward sonars (Figure 48, left and center panels). C1 densities were consistently lower than all other densities for 2015 side and 2015 forward sonars. A3 and R2 had the highest densities in 2015, while R2 was highest in both years (see Figure 2 for reach locations).

Densities of fish estimated from the 2015 downward sonar (Figure 48, right panel) were more commonly lower in the south (reaches 0.1 through C2) and higher in the north, with a few notable exceptions: densities in reaches A2 and R3 were as low as A1, R1, and C2. Highest densities occurred between reaches A2 and C3, in reach A3, and just to the north of A3. Densities in C1 were still lowest, but not significantly different from those in the river just south, upstream, of C1 or those in the segment between reaches A1 and C2.

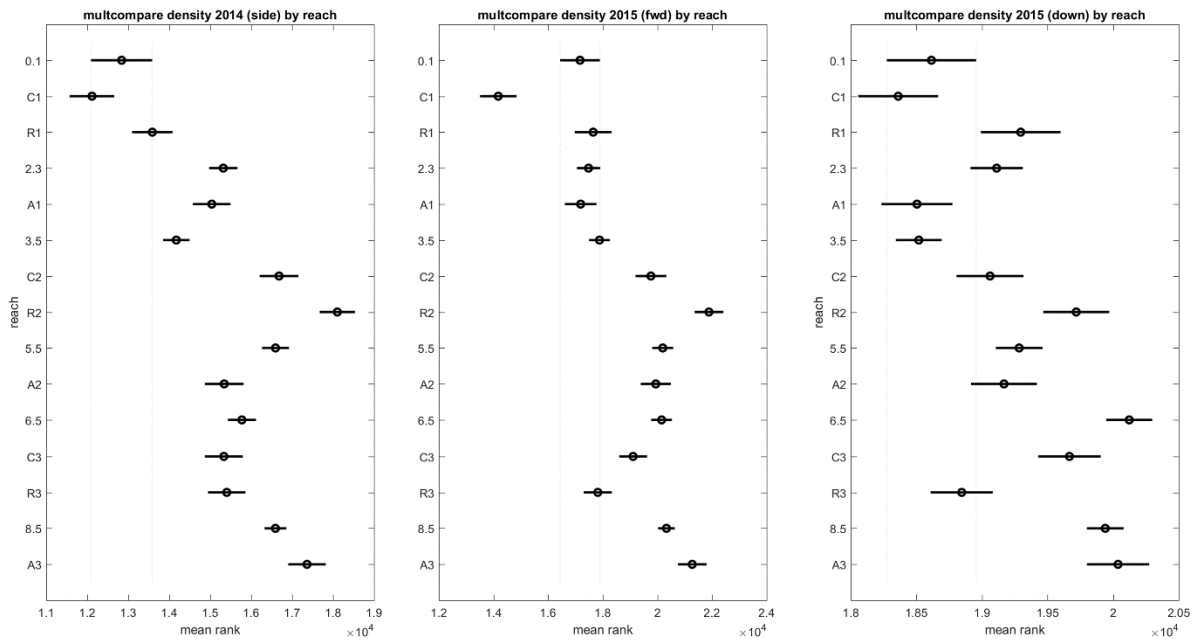


Figure 48. Multiple comparison test of mean annual fish densities by study reach for 2014 and 2015, ordered from south/upstream (top) to north/downstream (bottom).

Density comparisons by time

Multiple-comparison tests also indicate that fish densities varied by date. During 2014, densities of fish from the forward sonar were high in the beginning of the season, decreased to lowest in the middle of the season (JD 2014 127-128) and increased again

later in the season (Figure 49, left panel). In contrast, densities from the 2015 forward and downward sonars were highest in the middle of the season (Figure 49, center panel).

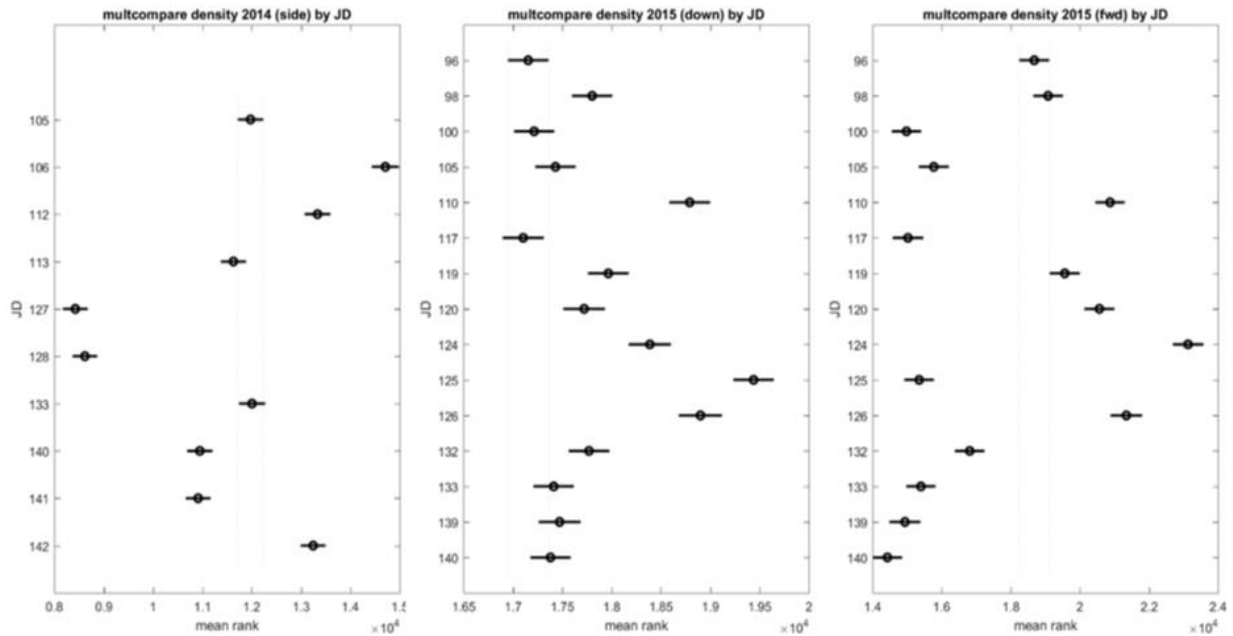


Figure 49. Whole-river mean fish density differences over time. Multiple comparison test of fish densities by Julian day (JD) for 2014 and 2015.

Multiple-comparison tests of densities in each reach show differences between dates (Figures 50 - 58). There were six predator removal and addition dates in 2014 and three in 2015: May 6 -7, 2014 and April 29, 2015 in R1/A1; May 8-9, 2014 and April 28, 2015 in R2/A2; and May 12-13, 2014 and April 27, 2015 in R3/A3, and these are indicated on the figures. Often, densities measured on the same day and just prior to removal and addition events were not significantly different from those measured the following day.

In removal ("R") reaches, no significant decreases were detected on the day after removals. In four instances density increased significantly on the day after removals in "R" reaches. In addition ("A") reaches on one instance density increased significantly on the day after additions, and in three instances density decreased significantly on the day after additions. In control ("C") reaches examined the day after removal or addition efforts were made in the same block (e.g., C1, R1, A1), no significant increases were detected the day after efforts and in two instances density decreased significantly on the day after efforts. (Table 16).

Table 16. Summary of density changes in R and A reaches the day after fish removals and additions for predator-density manipulation experiments. Numbers in parentheses indicate number of days with a significant change, date of significant changes noted.

Manipulation	Reach	Decrease	Date	Increase	Date
Removal	R1	1 (0)		3 (1)	JD2015-120
Removal	R2	1 (0)		3 (2)	JD2014-130 JD2015-119
Removal	R3	2 (0)		2 (1)	JD2014-134
Addition	A1	3 (1)	JD2015-120	1 (0)	
Addition	A2	1 (0)		3 (1)	JD2015-119
Addition	A3	2 (2)	JD2014-133 JD2014-134	2 (0)	
Control	C1	2 (0)		2 (0)	
Control	C2	1 (0)		3 (1)	JD2015-119
Control	C3	2 (0)		2 (1)	JD2014-133

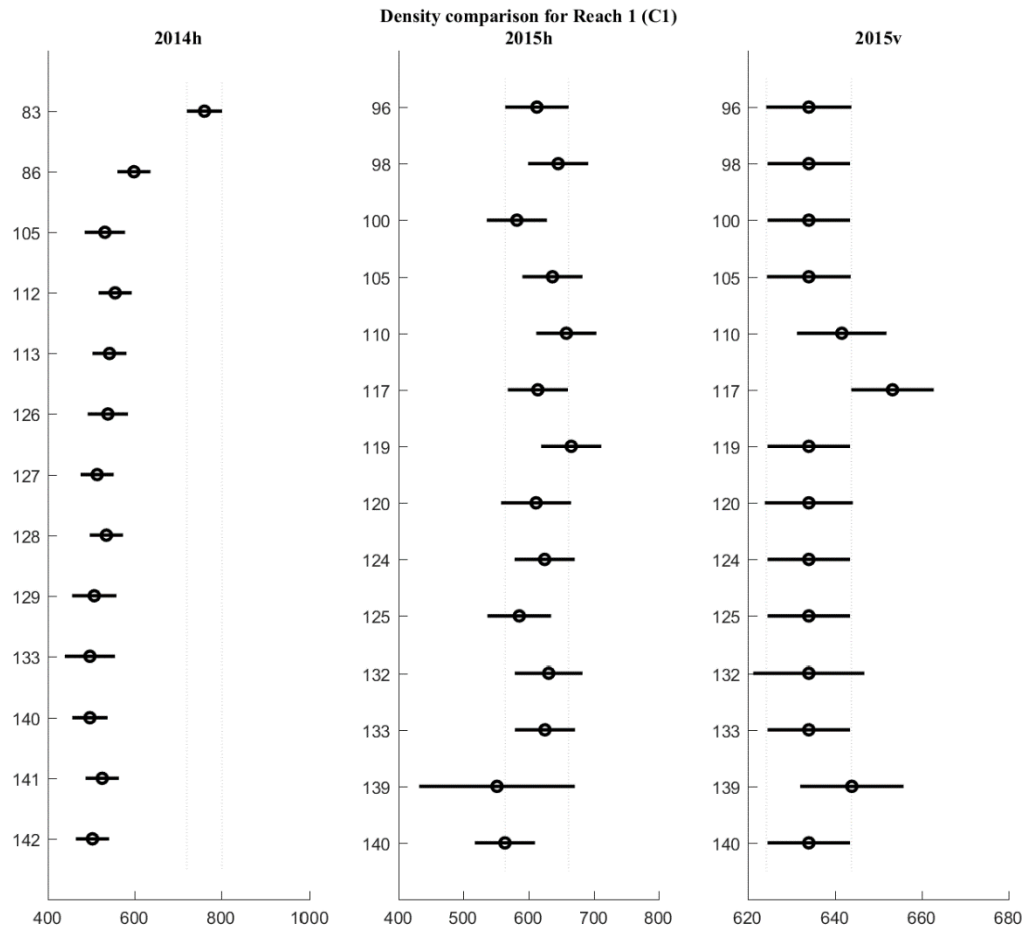


Figure 50. Multiple comparison test of fish densities by time (Julian day) for reach C1 in 2014 and 2015.

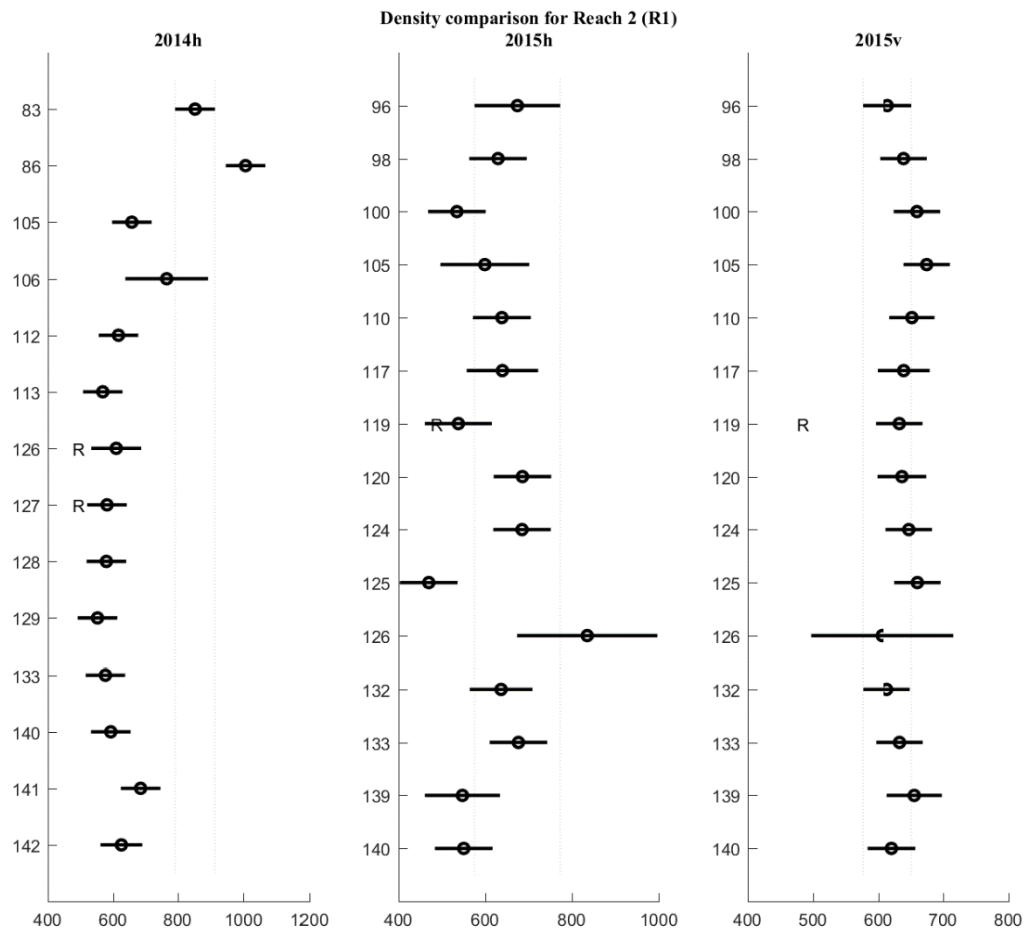


Figure 51. Multiple comparison test of fish densities by time (Julian day) for reach R1 for 2014 and 2015. Predator removals are indicated by "R."

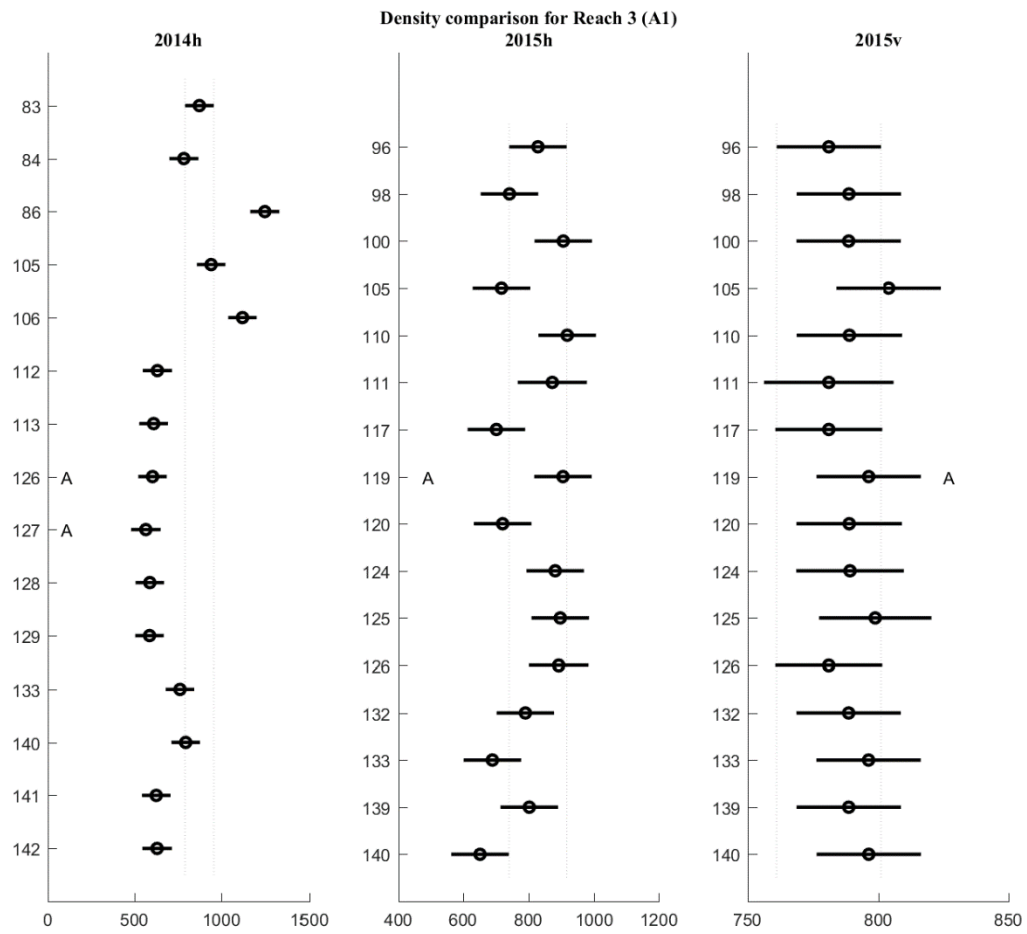


Figure 52. Multiple comparison test of fish densities by time (Julian day) for reach A1 in 2014 and 2015. Predator additions are indicated by "A."

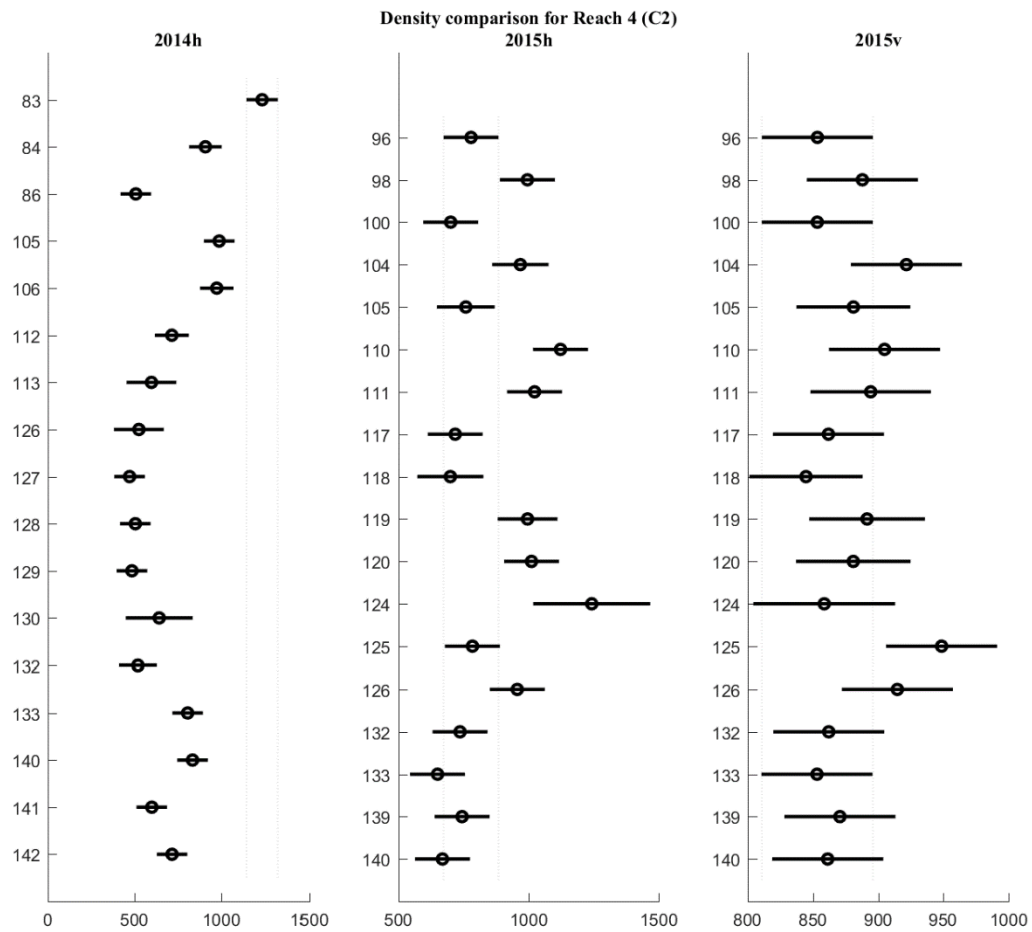


Figure 53. Multiple comparison test of fish densities by time (Julian day) for reach C2 in 2014 and 2015.

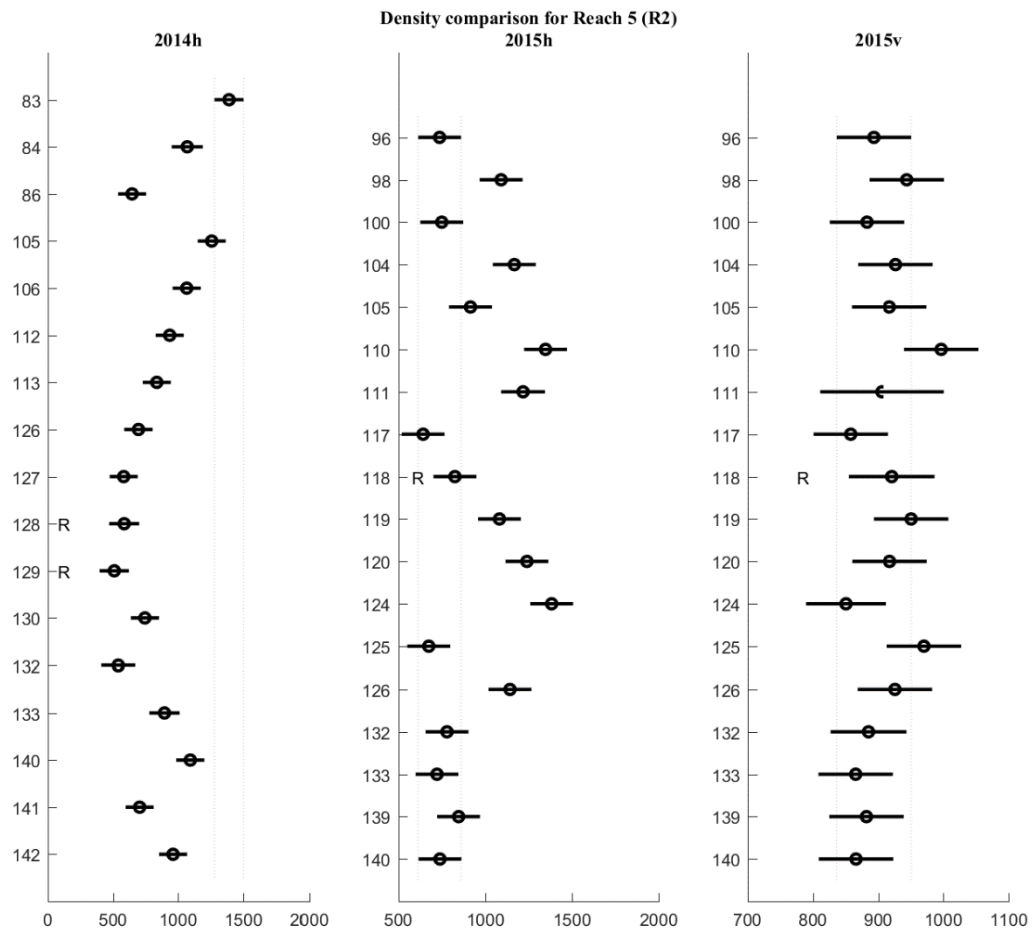


Figure 54. Multiple comparison test of fish densities by time (Julian day) for reach R2 in 2014 and 2015. Predator removals are indicated by "R."

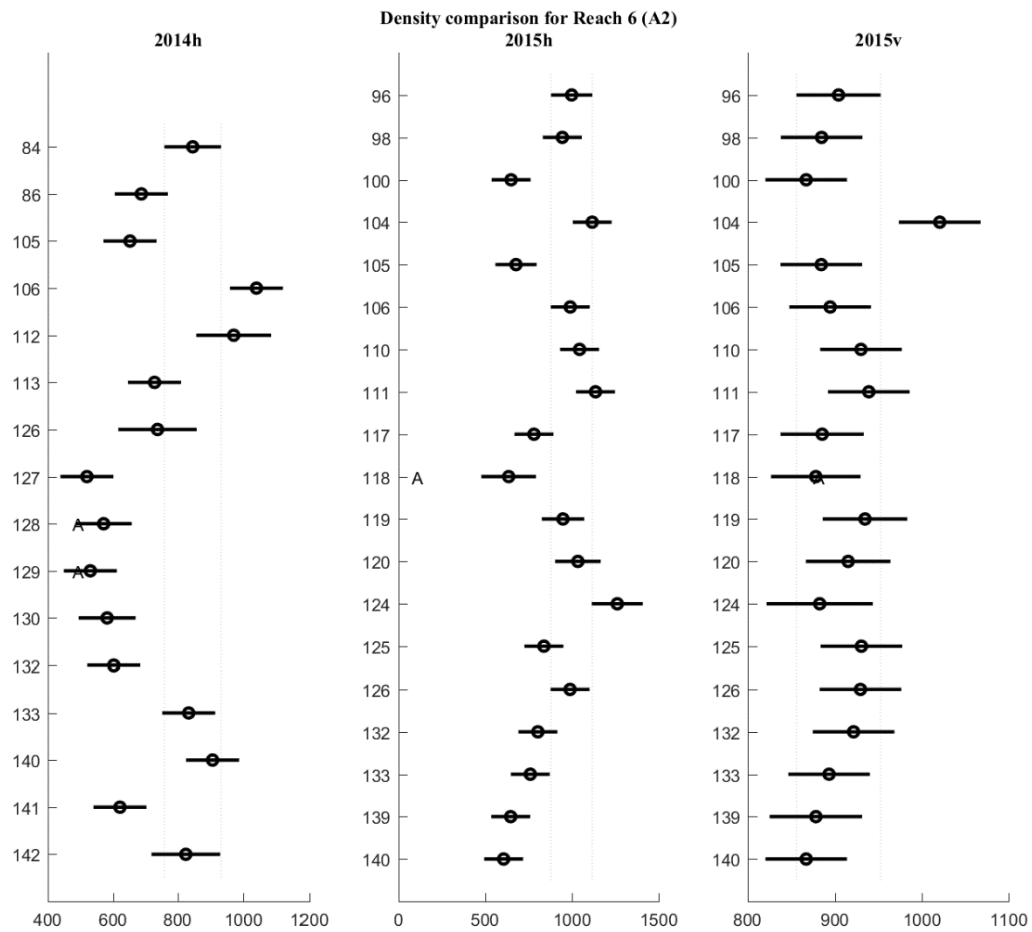


Figure 55. Multiple comparison test of fish densities by time (Julian day) for reach A2 in 2014 and 2015. Predator additions are indicated by "A."

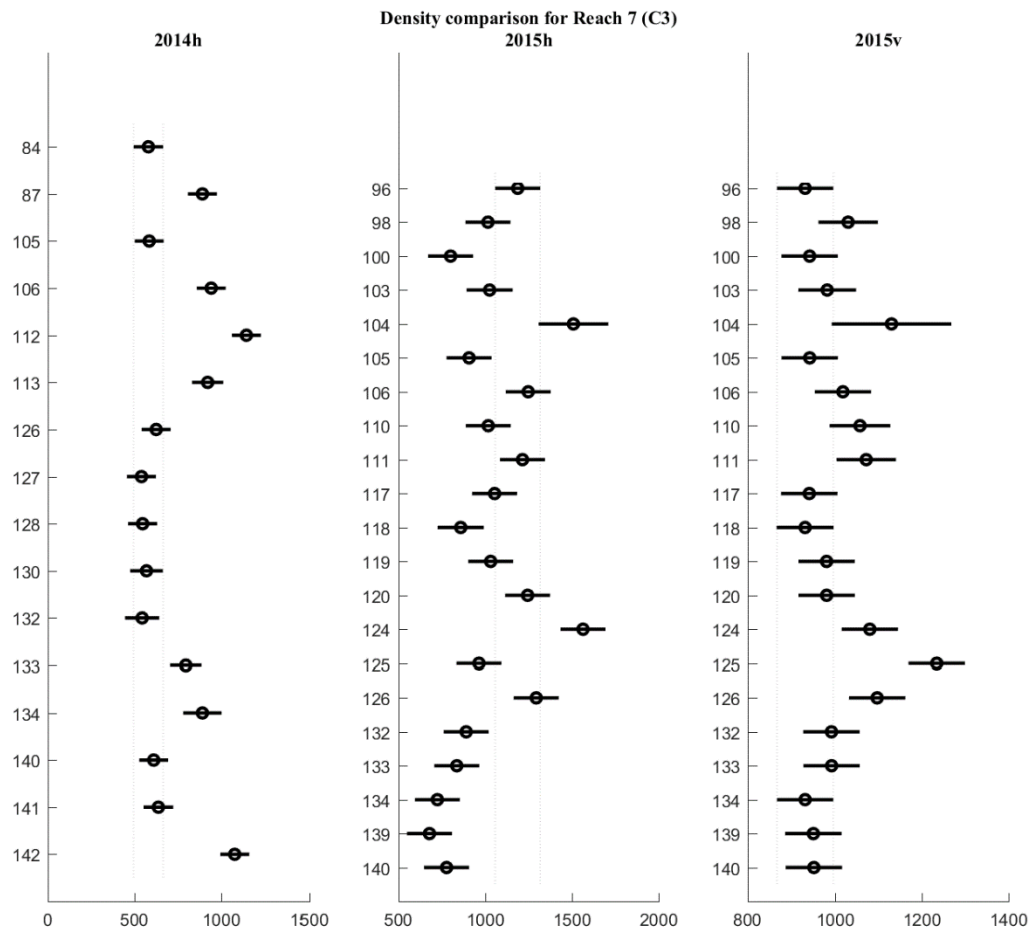


Figure 56. Multiple comparison test of fish densities by time (Julian day) for reach C3 in 2014 and 2015.

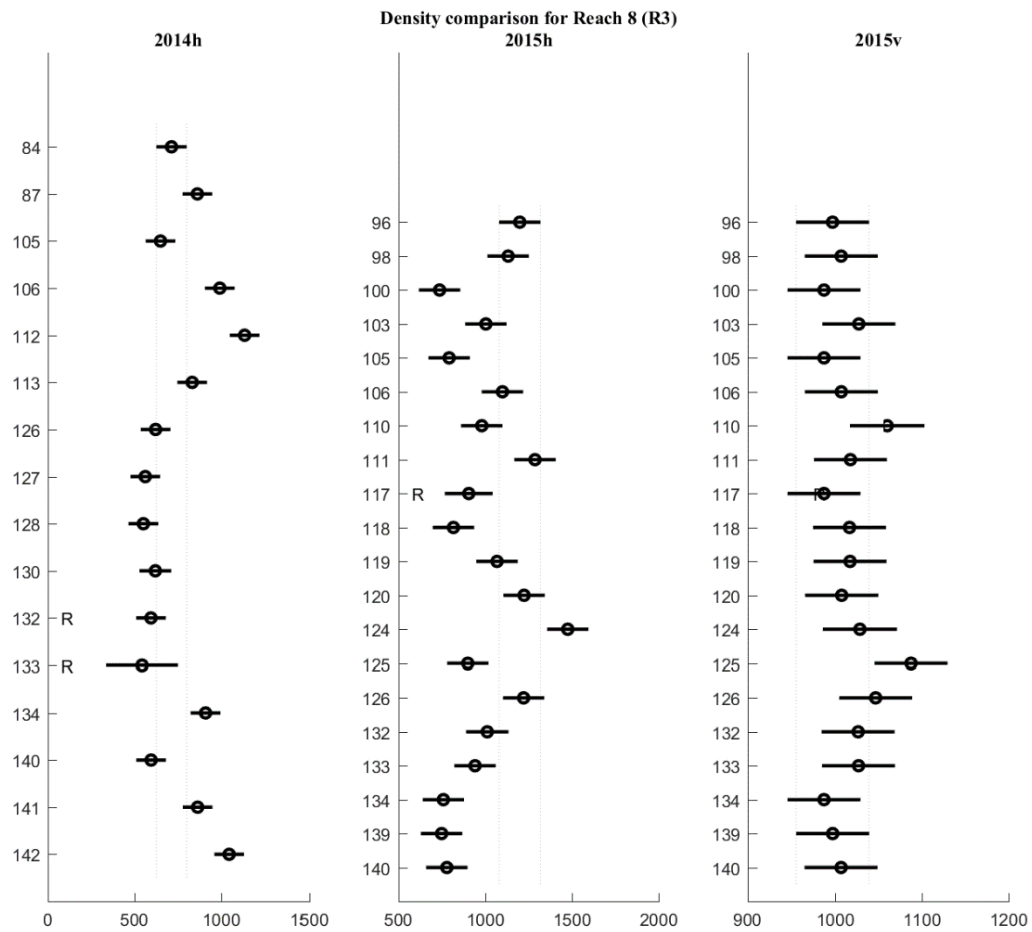


Figure 57. Multiple comparison test of fish densities by time (Julian day) for reach R3 in 2014 and 2015. Predator removals are indicated by "R."

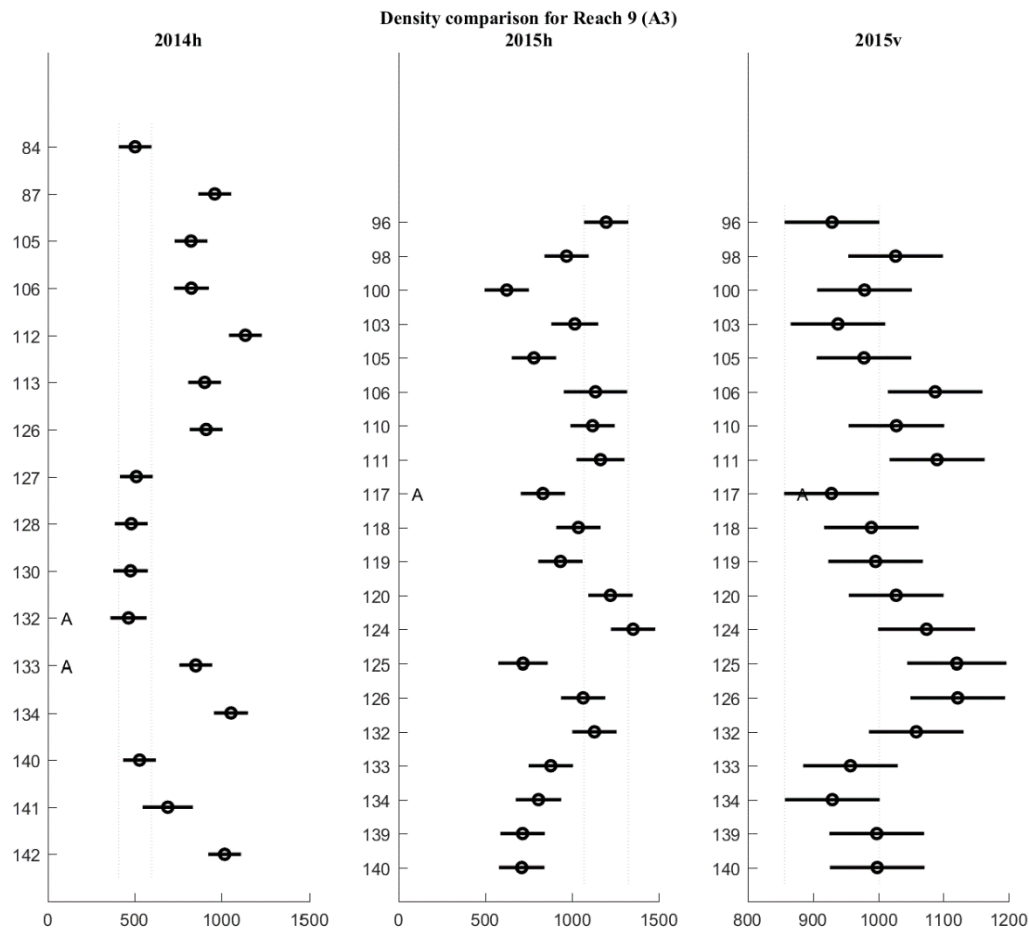


Figure 58. Multiple comparison test of fish densities by time (Julian day) for reach A3 in 2014 and 2015. Predator additions are indicated by "A."

Density comparison over space and time

Densities from the 2015 forward sonar, summarized by 1-km river segments and survey day, were compared (multiple comparison tests on Kruskal-Wallis statistics) for differences over space and time. The results are shown as a matrix of 'pixels' representing 1-km river segments, where the blocks of 26 rows by 26 columns separated by grid lines contain comparison results for each survey day (Figure 59). Significantly higher densities are indicated by the hot colors (yellow to red), non-significant differences are gray, and significantly lower densities are greens and blues. For example, densities over the entire river on survey day 14 (4 May, 2015) were significantly higher than densities throughout the river on almost all other days, and densities on days 3 and 6 (10 and 15 April, 2015) were significantly lower than those on most other days.

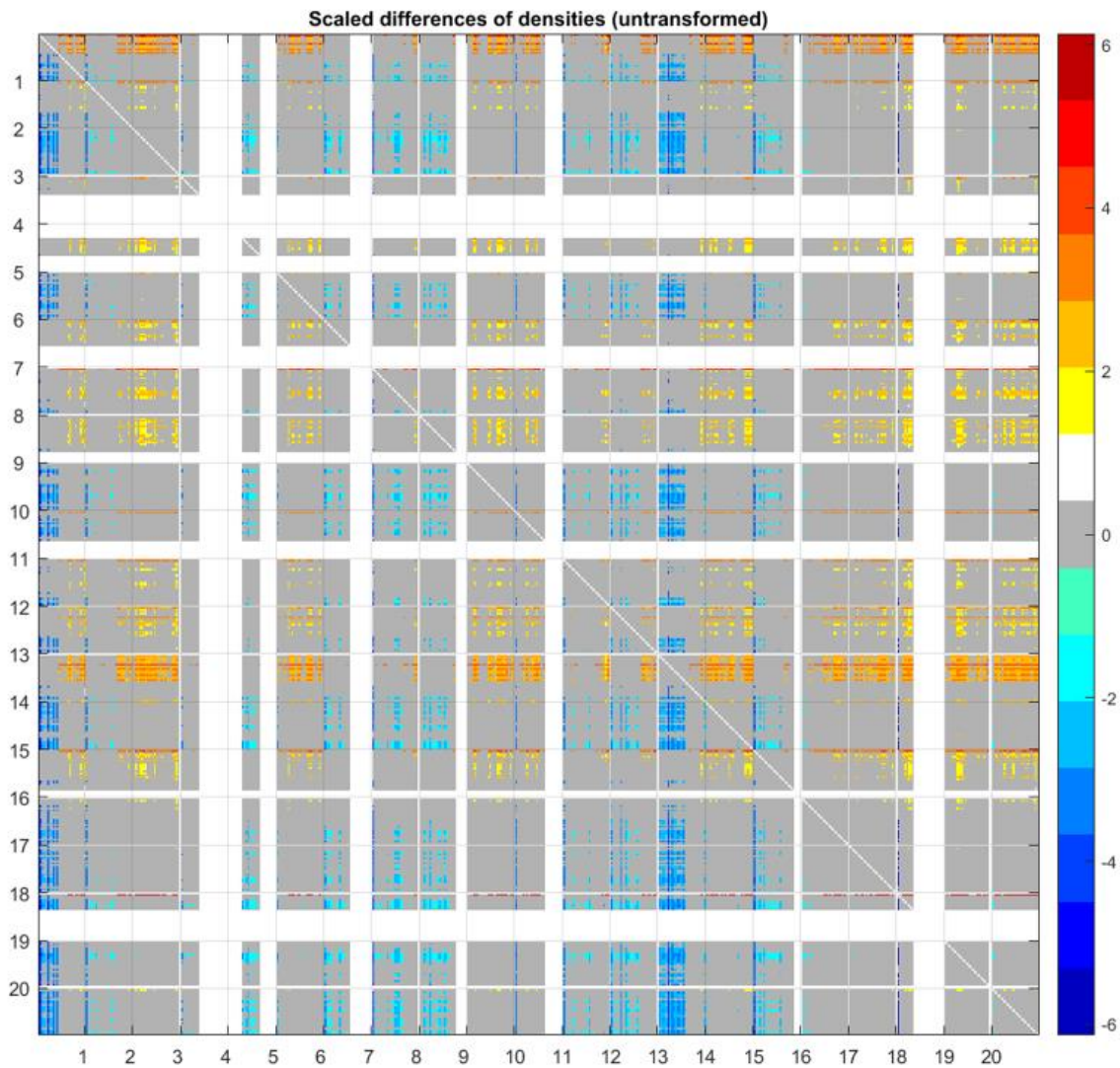


Figure 59. Space-time comparison of fish densities from forward sonar, for the 21 survey days of 2015.

TS spatial distribution

Values of *TS* measured over the entire 2015 study period were non-uniformly spatially distributed throughout the SJR (Figure 60). Considering *TS* as a proxy for target size, larger fish were found more often near bends in the river, perhaps in association with deep pools.

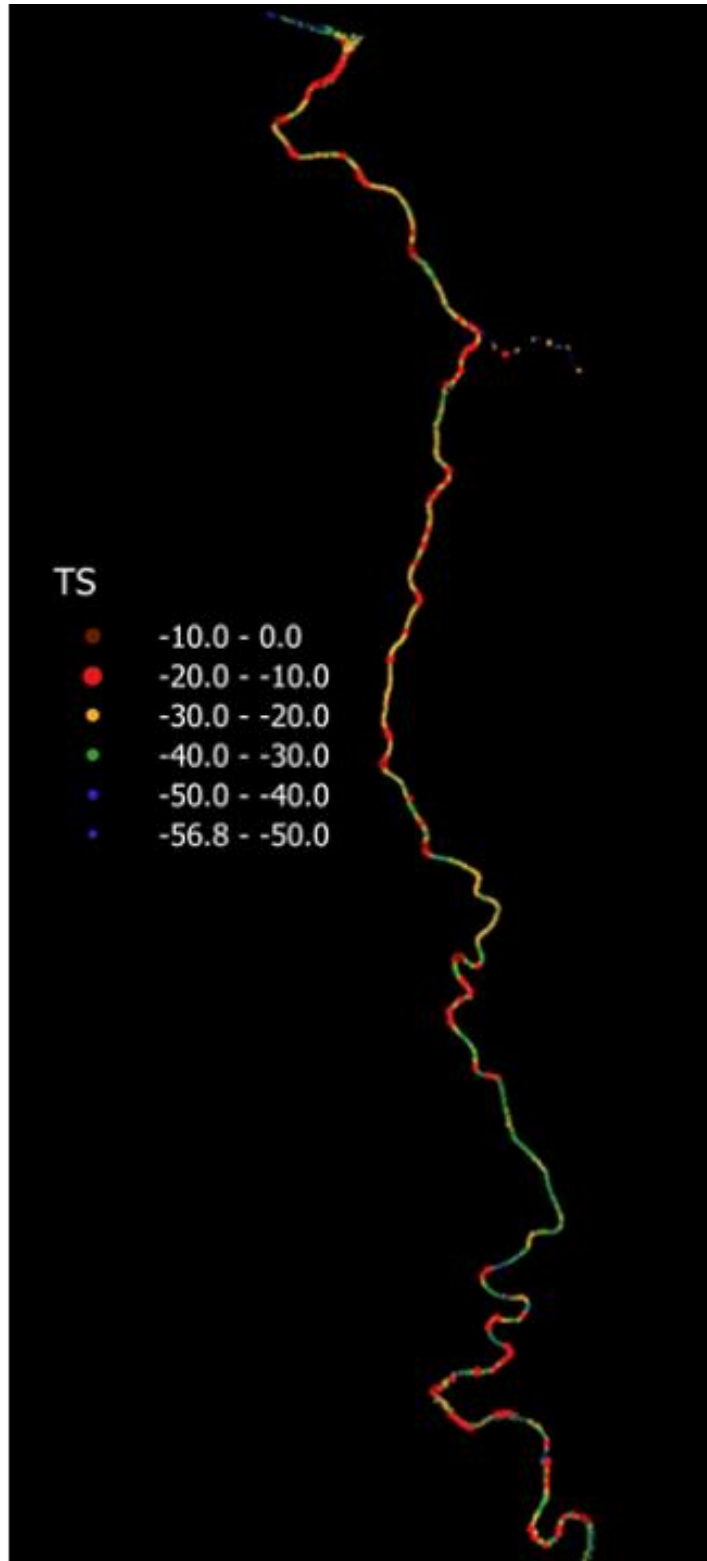


Figure 60. Spatial distributions of fish target strengths.

River conditions

Water temperature from three river monitoring stations (SJG, BDT, SJL) ranged from lows between 15° and 16° to highs of 23°C during 2014 and 2015, respectively (Figure 61). The maximum water temperature occurred two weeks earlier during the 2014 study period. During the 2014 survey period, water temperature quickly increased from near lowest to highest temperatures between 1 and 11 April, decreased to 15° by 26 April, and then increased to 21° by 22 May 2014 (end of study period). During the 2015 survey period, water temperature increased from 16° on 6 April to > 23° on 3 May, then decreased to 20° by 20 May 2015.

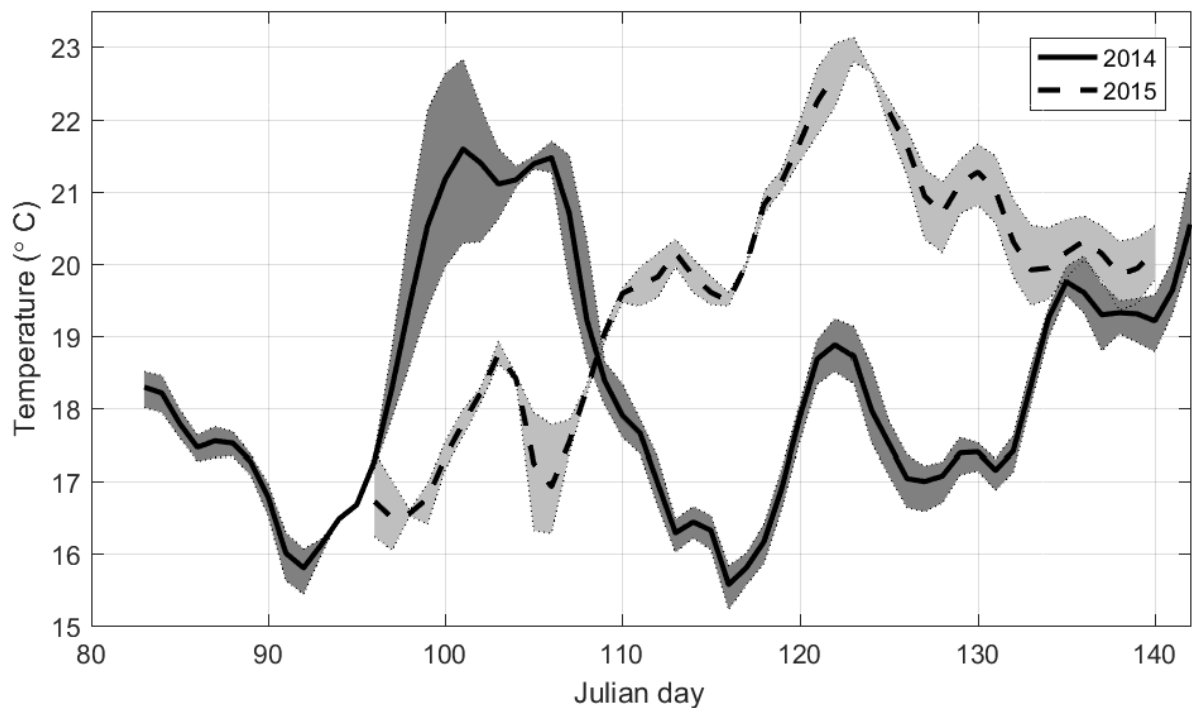


Figure 61. 2014 and 2015 mean (dark solid and dashed lines), minimum, and maximum daily temperatures (shaded) from three river monitoring stations.

Water temperature measured by the CTD varied throughout the river and season (Figure 62) and agreed well with the daily mean or median values from the river monitoring stations (Figure 63).

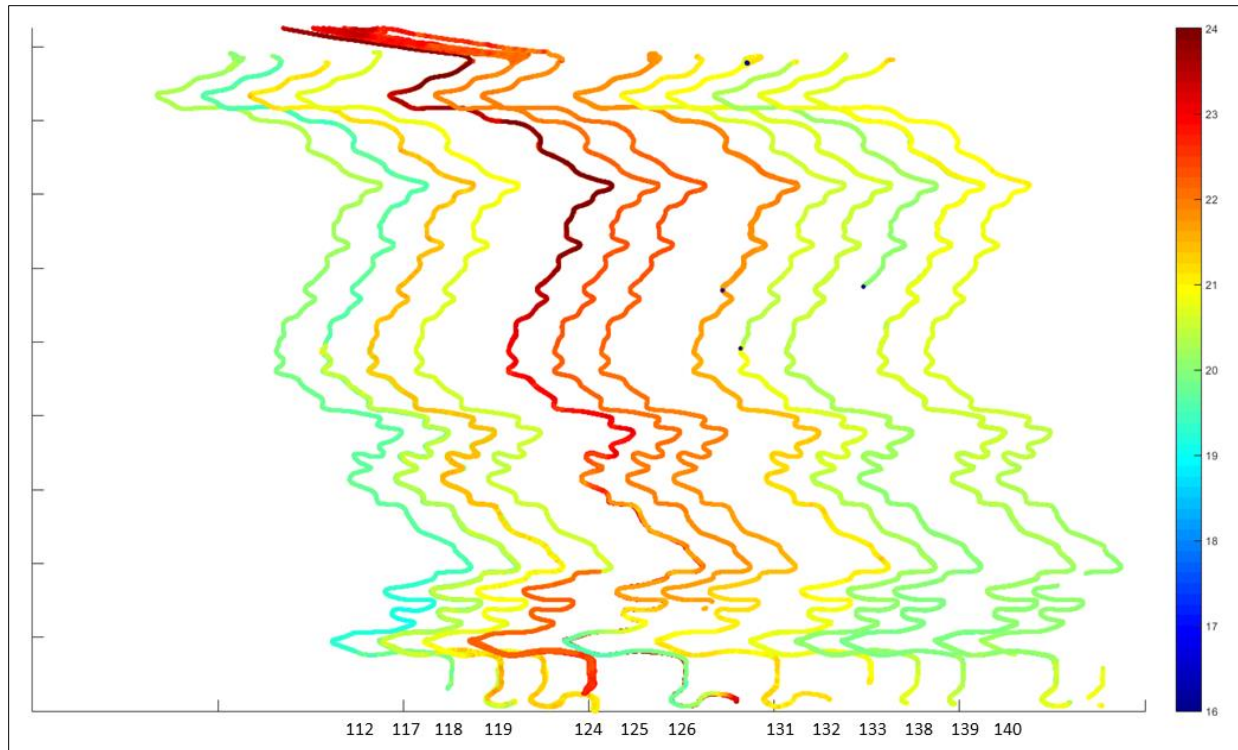


Figure 62. 2015 river water temperature ($^{\circ}\text{C}$) measured from a CTD mounted on the vessel, by Julian day.

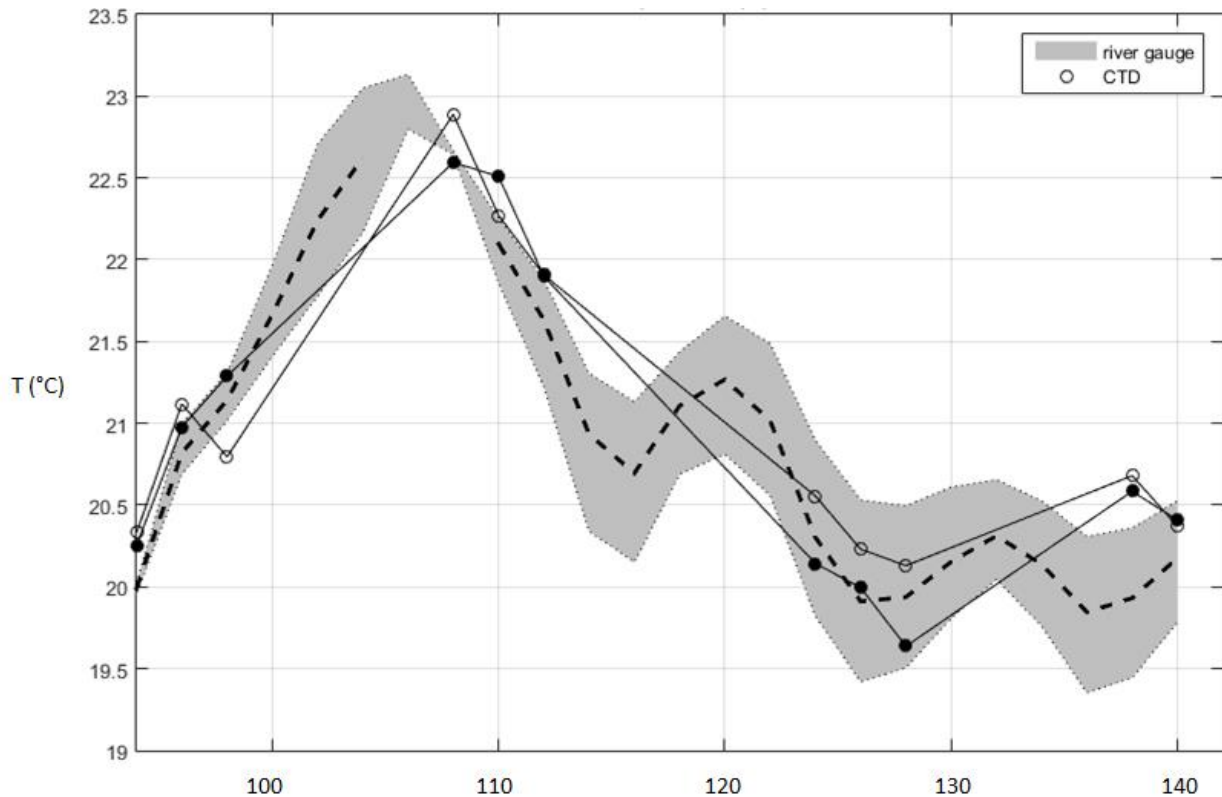


Figure 63. Comparison of river water temperature (T ; $^{\circ}\text{C}$) values (CTD vs river monitoring station). The dashed line is the mean T of the stations (SJG, BDT, SJL) bounded by the shaded area representing the minimum and maximum T . The solid lines are mean T (solid circles) and median T (open circles) from the vessel-mounted CTD.

Fish density in conjunction with tide, flow and lunar phase

Mean fish densities from the 2014 side sonar were mostly lower in the southern block, (C1, R1, A1) and higher in the northern block (C3, R3, A3), but varied throughout the season (Figure 64). There were no obvious patterns relating block-wide fish densities to temperature, flow, or lunar cycle.

Mean fish densities from the 2015 forward sonar were mostly lower in the southern block (C1, R1, A1), and higher in the northern block (C3, R3, A3), and varied temporally (Figure 65). In all blocks, densities increased between JD 117 and 124, coinciding with increased river water temperature and waxing moon phase (full on JD 123). Besides that trend, there is no obvious pattern relating block-wide fish densities to temperature, flow, or lunar cycle.

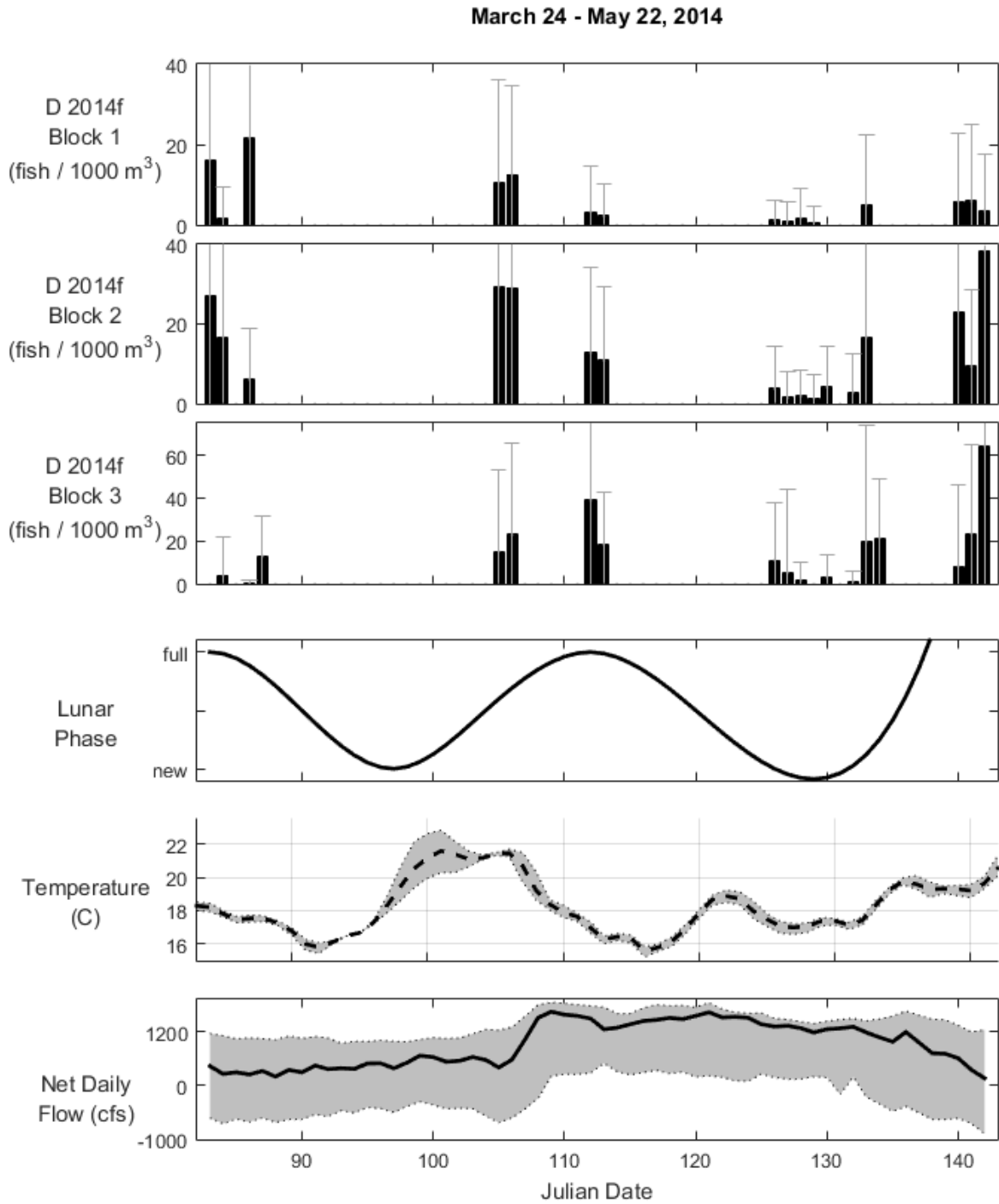


Figure 64. Fish density (fish 1000 m⁻³) from 2014 side sonar by block (1 in the south, 2 middle, and 3 north), lunar phase, mean daily temperature (°C), and net daily flow (cfs) bounded by minimum and maximum flow values (shaded area).

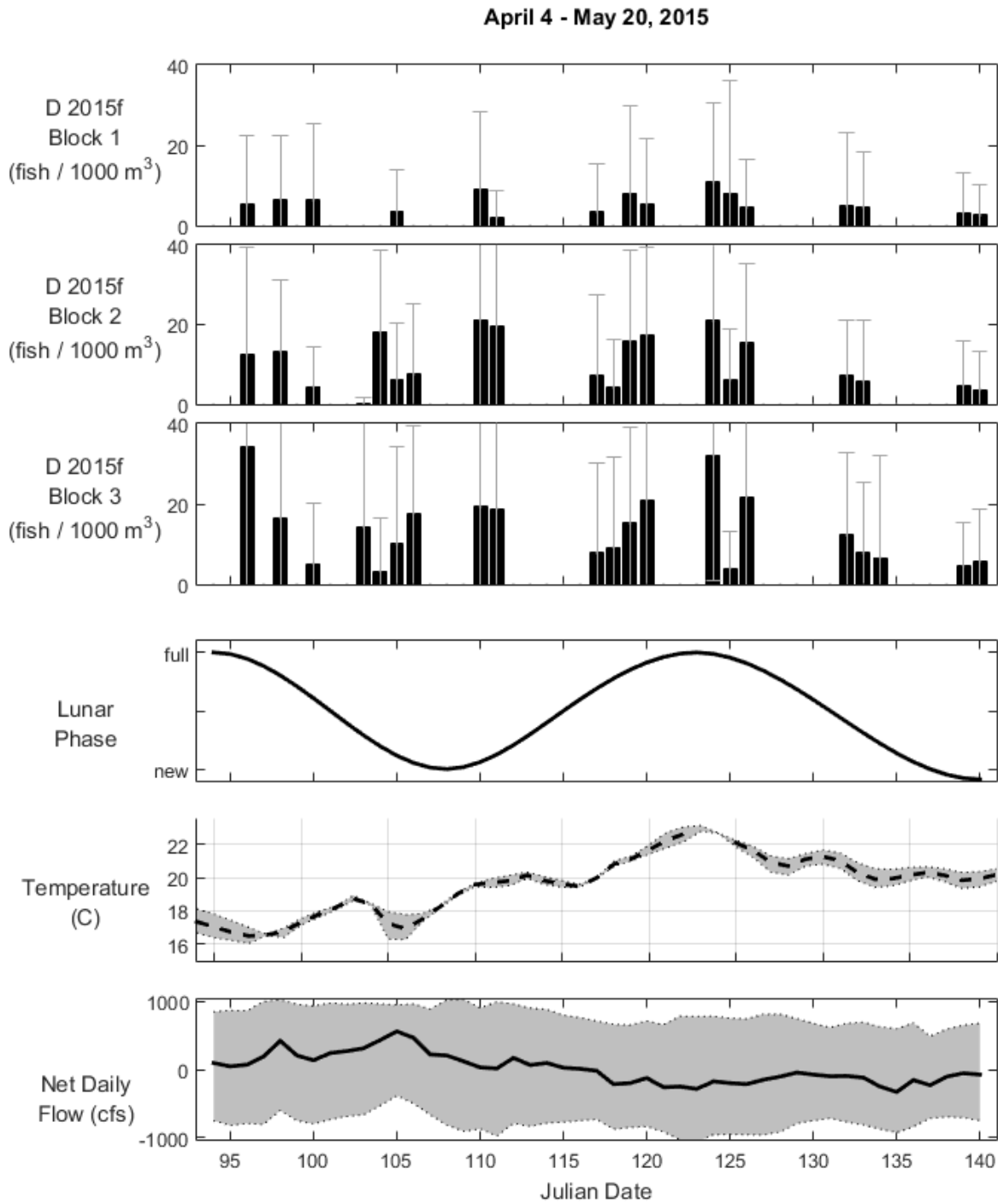


Figure 65. Fish density (fish 1000 m⁻³) from 2015 forward sonar by block (1 in the south, 2 middle, and 3 north), lunar phase, mean daily temperature (°C), and net daily flow (cfs) bounded by minimum and maximum flow values (shaded area).

Target identification and fish species composition

Acoustic targets may be assigned to species and sizes using concomitant samples of fish (Everson et al. 1996; Zwolinski et al. 2014). However, the process of assigning acoustic targets to species and sizes is complicated by the potential influence of a combination of factors such as fish orientation and size, and uncertainty in the spatially and temporally dynamic composition of the fish community.

This study included electro-fishing during both 2014 and 2015 with seven community sampling events, conducted during 3-5 days per year, where all fish caught were identified and measured. These data suggest that there were more predators in the north than the south, particularly for block 3 compared to block 1 (Figure 66), and that largemouth bass were more abundant than striped bass. However, predation event recorder (PER) data indicated a much higher incidence of predation by striped bass on tethered salmonid smolts during those experiments (Figure 67). Other fish-catch and acoustic-tag tracking data (C. Michel and J. Smith, pers. comm.) suggest that the fish composition included a higher proportion of striped bass and varied throughout the survey area over the study periods.

Differences in these results may be explained by potential sampling bias. Electro-fishing is not effective in deep water and may be biased toward species found near the water surface and river banks (e.g. largemouth bass and common carp). Striped bass are highly mobile and tend to be in deeper water. Although carp were abundant in the electro-fishing catches, the process of identifying 'in-bounds' targets should have excluded most fish that reside close to or on the riverbed.

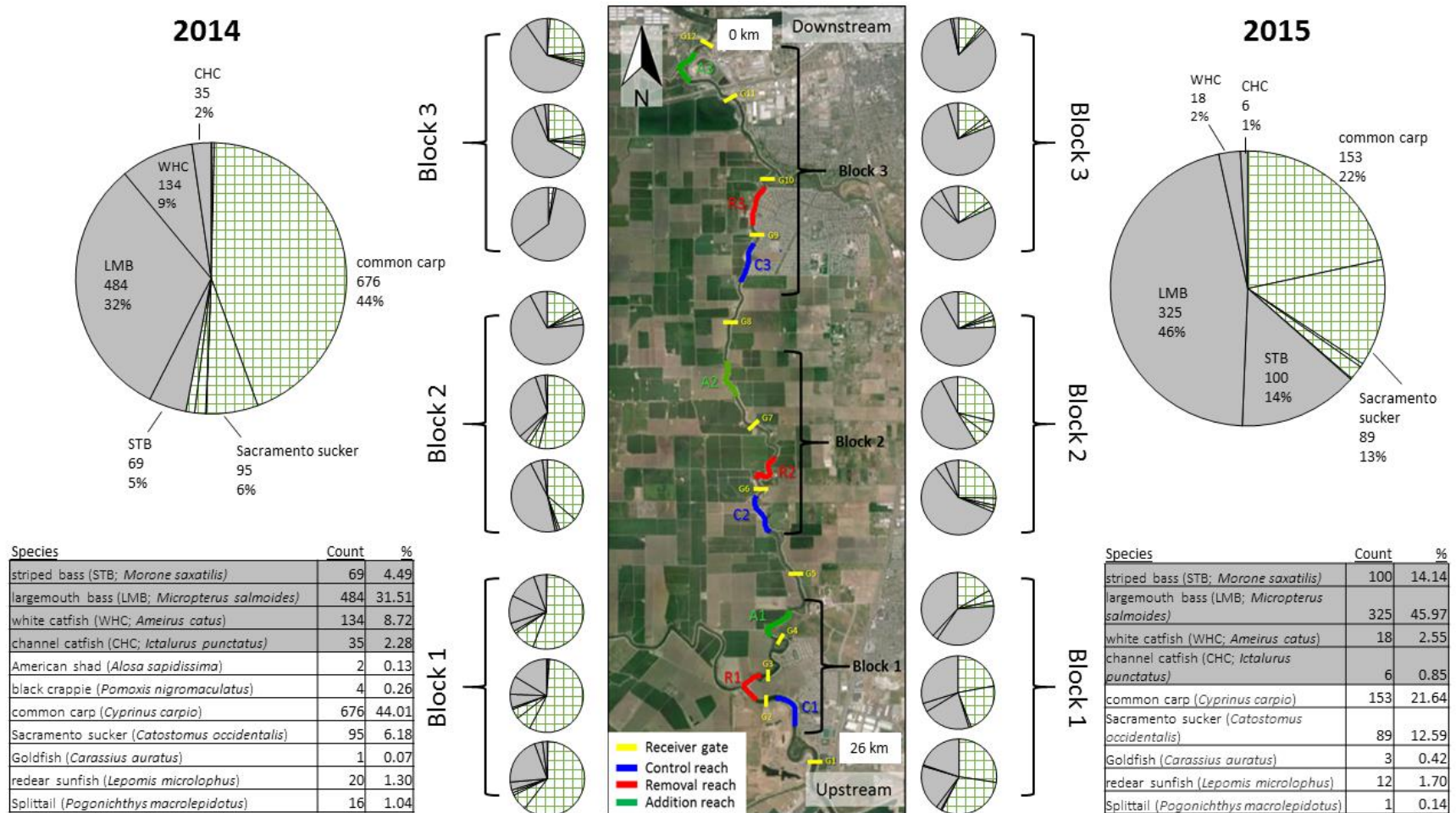


Figure 66. Proportion of predator-sized fish in the SJR by year and by reach from electro-fishing sample data on community sampling days (19, 20, and 27 May 2014, and 13-16 April 2015).

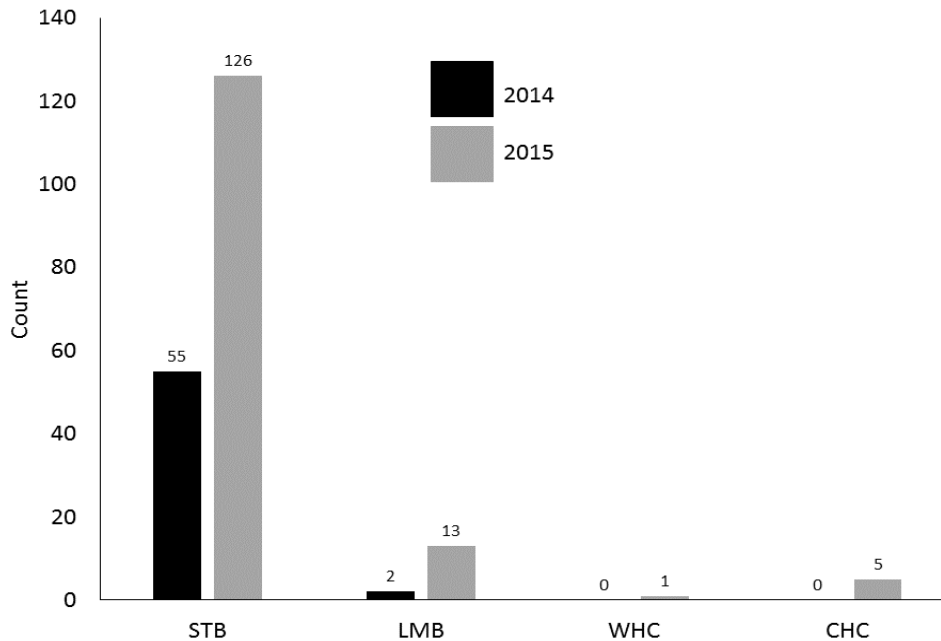


Figure 67. PER predation events with visual confirmation of predator species (LMB, STB, CHC, and WHC).

Fish habitat associations

Fish targets in context of bathymetry, terrain, and SAV

Fish targets were detected throughout the river. However, fish tended to associate with river features (Figure 68). Most of the largest fish detected by the 2015 forward sonar (Figure 68 c-d, > -22 dB) were located in or near deep pools at depths > 5 m (Figures 68 and 69). Some of these targets were near or within SAV beds, a preferred habitat for largemouth bass in the San Joaquin River (Conrad et al. 2016).

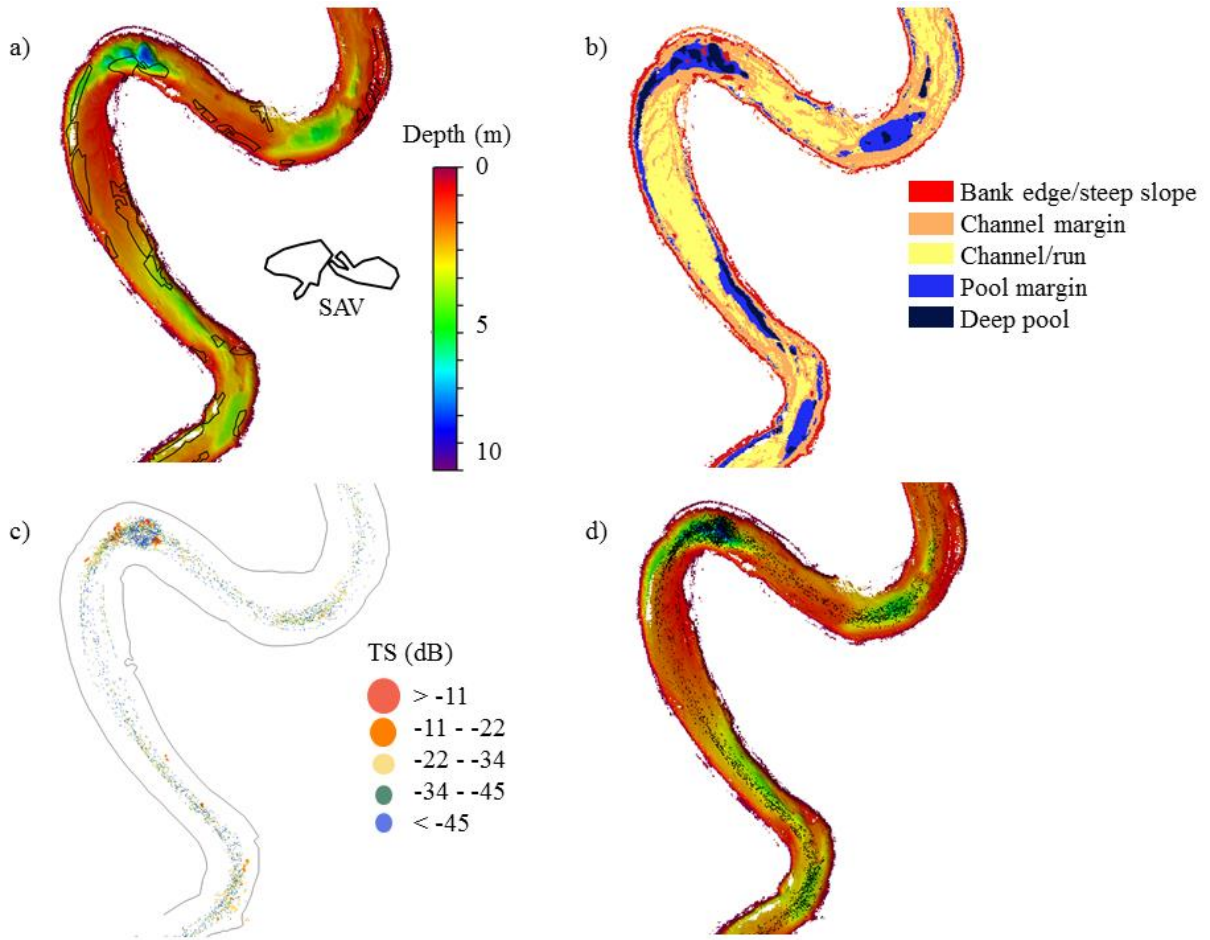


Figure 68. Associations between fish and riverbed attributes.

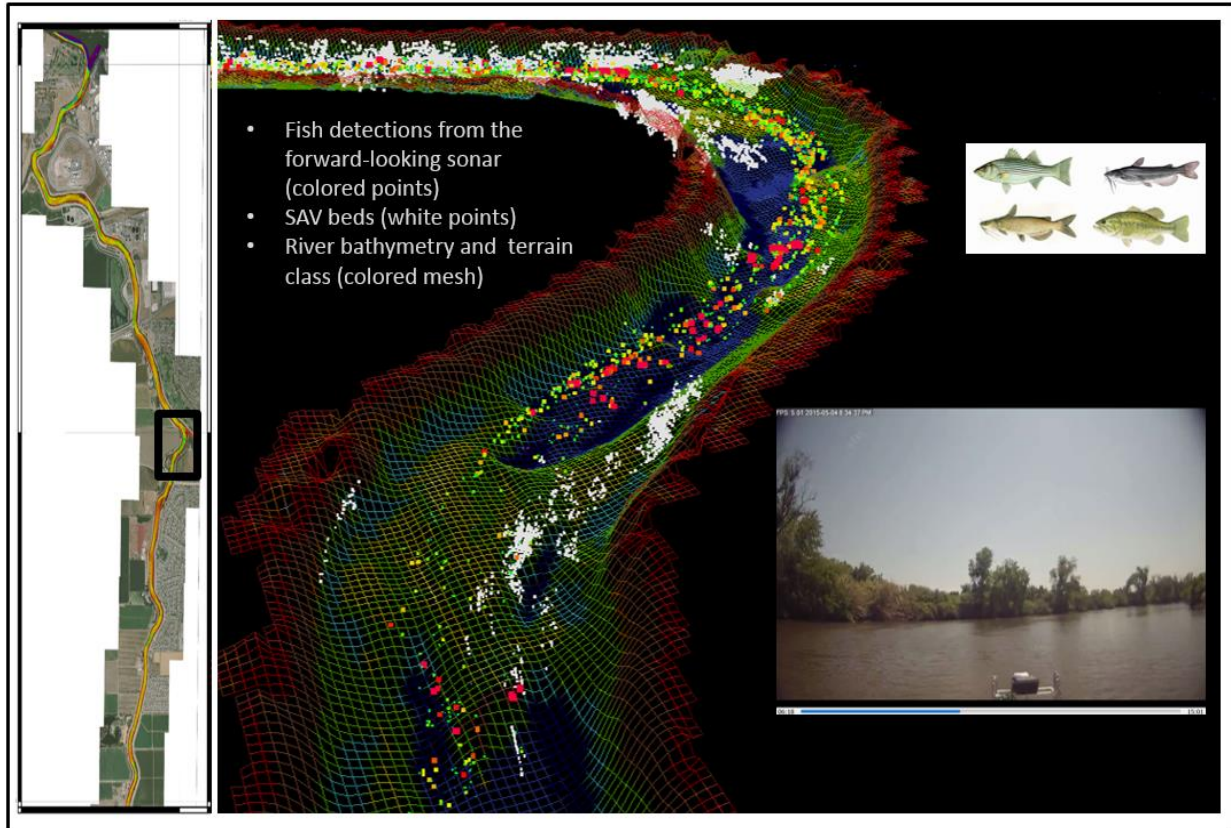


Figure 69. 3D scene of all 2015 forward sonar fish detections, SAV, and river bathymetry for the San Joaquin River near French Camp Slough, and a photo of the eastern river bank.

Conclusion

This study provides acoustically estimated densities and abundances for salmonid smolt predators and riverbed bathymetry within a 26-km stretch of the San Joaquin River, from Port of Stockton to Lathrop, California, during spring of 2014 and 2015. The results include an unprecedented level of detail of fish and their habitats in space and time. Fish densities and abundances are provided for every 10-m river interval for 19 and 21 days per year. Bank-to-bank bathymetry is mapped with 1-m resolution. Collectively, these indicate the spatial and temporal variability of fish densities, some locations with persistent high densities, and fish associations with riverbed features and submerged aquatic vegetation.

Other studies have mapped and classified riverbeds using multibeam sonars for shallow water (Montereale Gavazzi et al. 2016), but not in combination with multibeam fish-detection and simultaneous mapping of fish using fisheries sonars as implemented here. Hence, this study provides a unique data set that can be used to better define habitat suitability and utilization models for this river system. Additionally, when used in

combination with data from the accompanying predation experiments and fish tagging studies, this dataset improves models of salmonid smolt predation risk.

Acknowledgements

We thank collaborators N. Demetras and other members of the Salmon Ocean Ecology Team at NOAA Southwest Fisheries Science Center, Santa Cruz, and M. Cane and others from California Dept. of Water Resources.

References

- Acosta, G. G., and Villar, S. A. 2015. Accumulated CA-CFAR process in 2-D for online object detection from sidescan sonar data. *IEEE J. Oceanic Engr.* 40(3): 558-569.
- Brown, L. R., and D. Michniuk. 2007. Littoral fish assemblages of the alien-dominated Sacramento-San Joaquin Delta, California, 1980-1983 and 2001-2003. *Estuaries and Coasts* 30: 186-200.
- Carey, M.P., Sanderson, B.L., Barnas, K.A., and Olden, J.D. 2012. Native invaders - challenges for science, management, policy, and society. *Frontiers in Ecology and the Environment* 10(7): 373-381.
- Conrad, J. L., Andrew J. Bibian, Kelly L. Weinersmith, Denise De Carion, Matthew J. Young, Patrick Crain, Erin L. Hestir, Maria J. Santos & Andrew Sih (2016) Novel Species Interactions in a Highly Modified Estuary: Association of Largemouth Bass with Brazilian Waterweed *Egeria densa*, *Transactions of the American Fisheries Society*, 145:2, 249-263, DOI: 10.1080/00028487.2015.1114521.
- Conrad, O., Bechtel, B., Bock, M., Dietrich, H., Fischer, E., Gerlitz, L., Wehberg, J., Wichmann, V., and Böhner, J. (2015): System for Automated Geoscientific Analyses (SAGA) v. 2.1.4, *Geosci. Model Dev.*, 8, 1991-2007, [doi:10.5194/gmd-8-1991-2015](https://doi.org/10.5194/gmd-8-1991-2015).
- Conti, S.G., and Demer, D.A. 2003. Wide-bandwidth acoustical characterization of anchovy and sardine from reverberation measurements in an echoic tank. *ICES Journal of Marine Science: Journal du Conseil* 60(3): 617-624.
- S. G. Conti, D. A. Demer, M. A. Soule, and J. H. E. Conti, An improved multiple-frequency method for measuring in situ target strengths. *ICES J. Mar. Sci.*, vol. 62, no. 8, pp. 1636-1646, 2005.
- Cox, M.J., Demer, D.A., Warren, J.D., Cutter, G.R., and Brierley, A.S. 2009. Multibeam echosounder observations reveal interactions between Antarctic krill and air-breathing predators. *Mar Ecol Prog Ser* 378: 199-209.

- Cox, M.J., Warren, J.D., Demer, D.A., Cutter, G.R., and Brierley, A.S. 2010. Three-dimensional observations of swarms of Antarctic krill (*Euphausia superba*) made using a multi-beam echosounder. *Deep-Sea Res Pt II* 57(7-8): 508-518.
- Cutter, G.R., and Demer, D.A. 2007. Accounting for scattering directivity and fish behaviour in multibeam-echosounder surveys. *ICES Journal of Marine Science: Journal du Conseil* 64(9): 1664-1674.
- Cutter, G. R., and Demer, D. A. 2010. Multifrequency biplanar interferometric imaging. *IEEE Geoscience and Remote Sensing Letters* 7: 171-175.
- De Robertis, A., McKelvey, D.R., and Ressler, P.H. 2010. Development and application of an empirical multifrequency method for backscatter classification. *Can J Fish Aquat Sci* 67(9): 1459-1474.
- Demer, D.A., and Conti, S.G. 2003. Validation of the stochastic distorted-wave Born approximation model with broad bandwidth total target strength measurements of Antarctic krill (vol 60, pg 625, 2003). *ICES J Mar Sci* 61(1): 155-156.
- Demer, D.A., Cutter, G.R., Renfree, J.S., and Butler, J.L. 2009. A statistical-spectral method for echo classification. *ICES Journal of Marine Science: Journal du Conseil* 66(6): 1081-1090.
- Ehrenberg, J.E., and Lytle, D.W. 1972. Acoustic Techniques for Estimating Fish Abundance. *Ieee T Geosci Elect Ge10*(3): 138-&.
- Everson, I., Bravington, M., Goss, C. 1996. Combined acoustic and trawl survey for efficiently estimating fish abundance. *Fisheries Research* 26: 75-91.
- Graham, T.R., Harvey, J.T., Benson, S.R., Renfree, J.S., and Demer, D.A. 2010. The acoustic identification and enumeration of scyphozoan jellyfish, prey for leatherback sea turtles (*Dermochelys coriacea*), off central California. *ICES Journal of Marine Science: Journal du Conseil* 67(8): 1739-1748.
- Grossman, G.D., Essington, T.E., Johnson, B., Miller, J., Monsen, N.E., and Pearsons, T.N. 2013. Effects of fish predation on salmonids in the Sacramento River-San Joaquin Delta and associated ecosystems, p. 71.
http://deltacouncil.ca.gov/sites/default/files/documents/files/Fish_Predation_Final_Report_9_30_13.pdf.
- Hartman, K. J., and Nagy, B. W. 2005. A target strength and length relationship for striped bass and white perch. *Transactions of the American Fisheries Society* 134: 375-380.
- Hateley, J., and Gregory, J. 2006. Evaluation of a multi-beam imaging sonar system (DIDSON) as Fisheries Monitoring Tool: Exploiting the Acoustic Advantage. Environment Agency, Richard Fairclough House, Knutsford Road, Warrington, WA4 1HG, United Kingdom.
- Iwahashi, J. and R. J. Pike. 2007. Automated classifications of topography from DEMs by an unsupervised nested-means algorithm and a three-part geometric signature. *Geomorphology* 86: 409-440.

- Kayanda, R., Everson, I, Munyaho, T., and Mgaya, Y. 2012. Target strength measurements of Nile perch (*Lates niloticus*: Linnaeus, 1758) in Lake Victoria, East Africa. *Fisheries Research* 113: 76-83
- Korneliussen, R.J., Heggelund, Y., Eliassen, I.K., Oye, O.K., Knutsen, T., and Dalen, J. 2009. Combining multibeam-sonar and multifrequency-echosounder data: examples of the analysis and imaging of large euphausiid schools. *ICES J Mar Sci* 66(6): 991-997.
- Kubecka, J., and Wittingerova, M. 1998. Horizontal beaming as a crucial component of acoustic fish stock assessment in freshwater reservoirs. *Fisheries Research* 35: 99-106.
- Lindley, S. T., and Mohr, M. S., 2003. Modeling the effect of striped bass (*Morone saxatilis*) on the population viability of Sacramento River winter-run chinook salmon (*Oncorhynchus tshawytscha*). *Fish. Bull.*, 101: 321-331.
- Lyons, J. 1998. A hydroacoustic assessment of fish stocks in the River Trent, England. *Fisheries Research* 35: 83-90.
- Montereale Gavazzi, G., Madricardo, F., Janowski, L., Kruss, A., Blondel, P., Sigovini, M., and Foglini, F. 2016. Evaluation of seabed mapping methods for fine-scale classification of extremely shallow benthic habitats – Application to the Venice Lagoon, Italy, *Estuarine, Coastal and Shelf Science*, Volume 170(5): 45-60.
- Michel, C. 2010. River and estuarine survival and migration of yearling Sacramento River Chinook Salmon (*Oncorhynchus tshawytscha*) smolts and the influence of environment. Master of Arts, Ecology and Evolutionary Biology, University of California, Santa Cruz.
- Mulligan, T. J. and Kieser, R. 1996. A split-beam echo-counting model for riverine use. - *ICES Journal of Marine Science*, 53: 403-406.
- Nobriga, M, Chotkowski, M, Baxter, R. 2003. Baby steps toward a conceptual model of predation in the Delta: preliminary results from the Shallow Water Habitat Predator-Prey Dynamics Study. *Interagency Ecological Program for the San Francisco Estuary Newsletter* 16(1): 19-27.
- Nobriga, Matthew L. and Frederick Feyrer 2007. Shallow-Water Piscivore-Prey Dynamics in California's Sacramento-San Joaquin Delta. *San Francisco Estuary and Watershed Science*. Vol. 5, Issue 2. Article 4. <http://repositories.cdlib.org/jmie/sfews/vol5/iss2/art4>
- Patel, R., and Ona, E. 2009. Measuring herring densities with one real and several phantom research vessels. *ICES J Mar Sci* 66(6): 1264-1269.
- Renfree, J.S., Hayes, S.A., and Demer, D.A. 2009. Sound-scattering spectra of steelhead (*Oncorhynchus mykiss*), coho (*O. kisutch*), and Chinook (*O. tshawytscha*) salmonids. *ICES Journal of Marine Science: Journal du Conseil* 66(6): 1091-1099.
- Steig, T. W., and Jonhston, S. V. 1996. Monitoring fish movement patterns in a reservoir using horizontally scanning split-beam techniques. *ICES J. Mar Sci.* 53: 435-441.

Stockwell, J.D., Weber, T.C., Baukus, A.J., and Jech, J.M. 2013. On the use of omnidirectional sonars and downwards echosounders to assess pelagic fish distributions during and after midwater trawling. *ICES Journal of Marine Science: Journal du Conseil* 70(1): 196-203.

Tuser, M. Kubecka, J., Frouzova, J., and Jarolim, O. 2009. Fish orientation along the longitudinal profile of the Rimov reservoir during daytime: consequences for horizontal acoustic surveys. *Fisheries Research* 96: 23-29.

Warner, D.M., Claramunt, R.M., Hanson, D., and Farha, S.A. 2012. Status of pelagic prey fishes in Lake Michigan, 2011. A report to the Great Lakes Fishery Commission, Lake Michigan Committee Meeting, Windsor, Ontario, March 19, 2012.

Zwolinski, J.P., Demer, D. A., Cutter Jr., G.R., Stierhoff, K., and Macewicz, B.J. 2014. Building on fisheries acoustics for marine ecosystem surveys. *Oceanography* 27(4): 68-79, <http://dx.doi.org/10.5670/oceanog.2014.87>.

Appendix

Table A01. Calendar date (yyyymmdd) and Julian date of 2014 and 2015 acoustic surveys of the San Joaquin River between Port of Stockton and Lathrop.

	Survey Day	Calendar Date	Julian Date
2014	1	20140324	2014 - 083
	2	20140325	2014 - 084
	3	20140327	2014 - 086
	4	20140328	2014 - 087
	5	20140415	2014 - 105
	6	20140416	2014 - 106
	7	20140422	2014 - 112
	8	20140423	2014 - 113
	9	20140506	2014 - 126
	10	20140507	2014 - 127
	11	20140508	2014 - 128
	12	20140509	2014 - 129
	13	20140510	2014 - 130
	14	20140512	2014 - 132
	15	20140513	2014 - 133
	16	20140514	2014 - 134
	17	20140520	2014 - 140
	18	20140521	2014 - 141
	19	20140522	2014 - 142
2015	1	20150406	2015 - 096
	2	20150408	2015 - 098
	3	20150410	2015 - 100
	4	20150413	2015 - 103
	5	20150414	2015 - 104
	6	20150415	2015 - 105
	7	20150416	2015 - 106
	8	20150420	2015 - 110
	9	20150421	2015 - 111
	10	20150427	2015 - 117
	11	20150428	2015 - 118
	12	20150429	2015 - 119
	13	20150430	2015 - 120
	14	20150504	2015 - 124
	15	20150505	2015 - 125
	16	20150506	2015 - 126
	17	20150512	2015 - 132
	18	20150513	2015 - 133
	19	20150514	2015 - 134
	20	20150519	2015 - 139
	21	20150520	2015 - 140

Table A02. Midpoint locations of study reaches / river sections; northing and easting (m) coordinates from UTM zone 10 north projection (WGS84 ellipsoid).

Reach id (string)	Reach id (numeric)	Midpoint Easting (m)	Midpoint Northing (m)
0.1	0.1	648705	4184289
C1	1	648525	4185318
1.1	1.1	647940	4185605
R1	2	647247	4185855
2.3	2.3	648065	4186443
A1	3	647796	4187224
3.5	3.5	648410	4188647
C2	4	647680	4189928
4.1	4.1	647624	4190539
R2	5	647750	4190892
5.5	5.5	647532	4192077
A2	6	646697	4193122
6.5	6.5	646785	4194636
C3	7	647161	4196001
7.1	7.1	647402	4196593
R3	8	647282	4197283
8.5	8.5	647127	4199055
A3	9	645434	4200551
9.1	9.1	646136	4201408

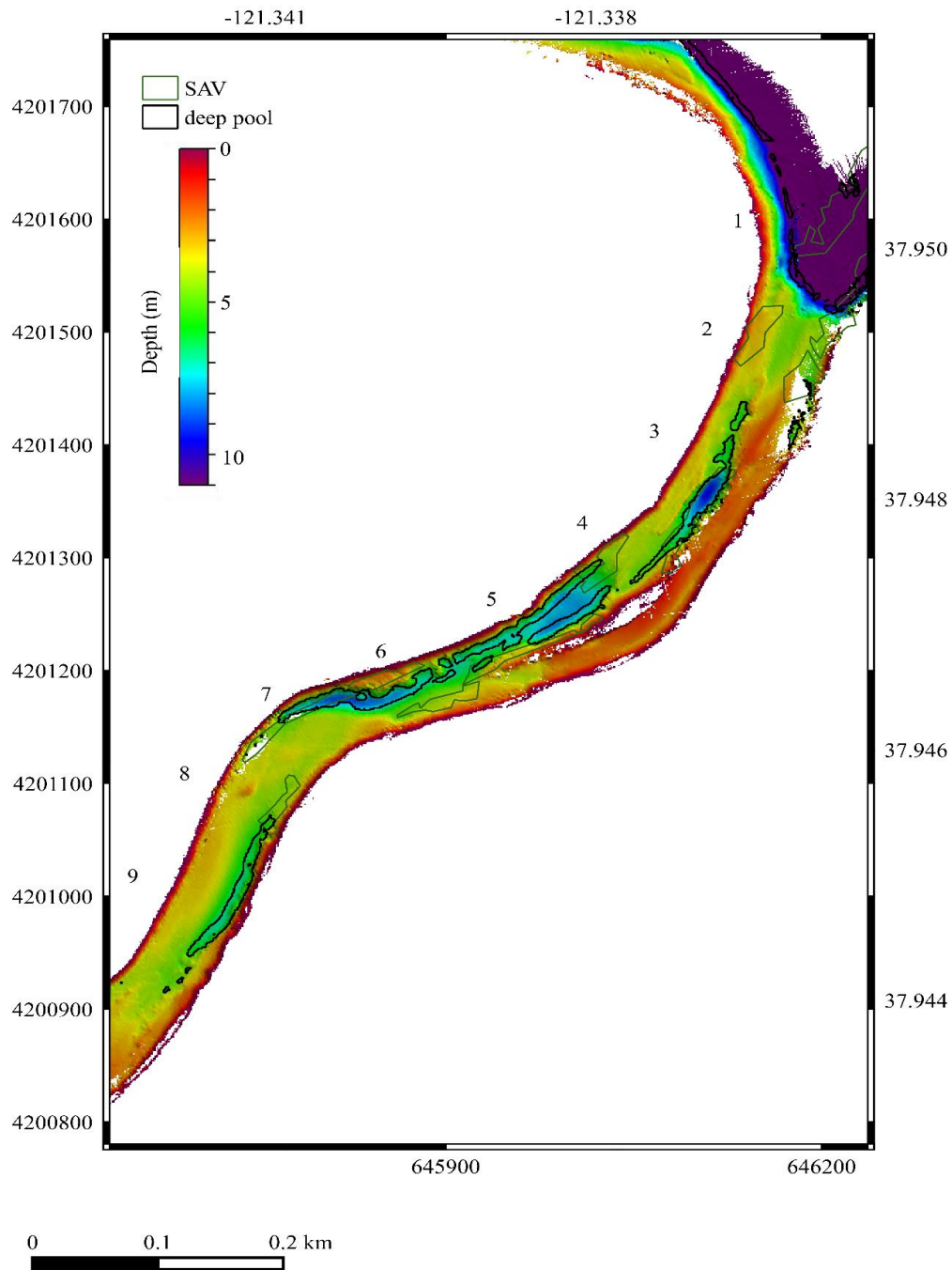


Figure A01. Bathymetry, pool classification (black polygon), and submerged aquatic vegetation (SAV, green polygon). Each 100m along-river segment noted with number. Not to be used for navigation.

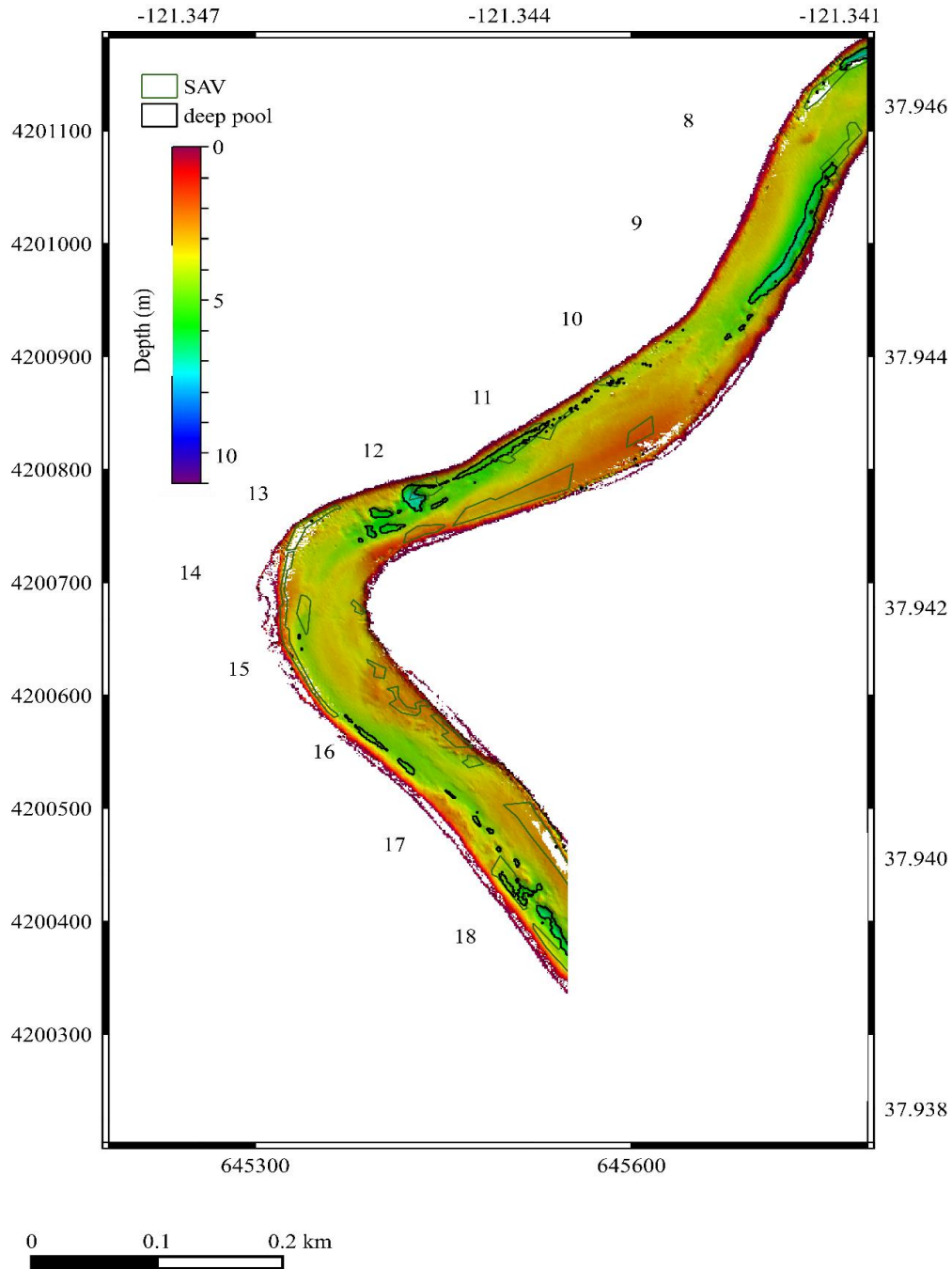


Figure A02. Bathymetry, pool classification (black polygon), and submerged aquatic vegetation (SAV, green polygon). Each 100m along-river segment noted with number. Not to be used for navigation.

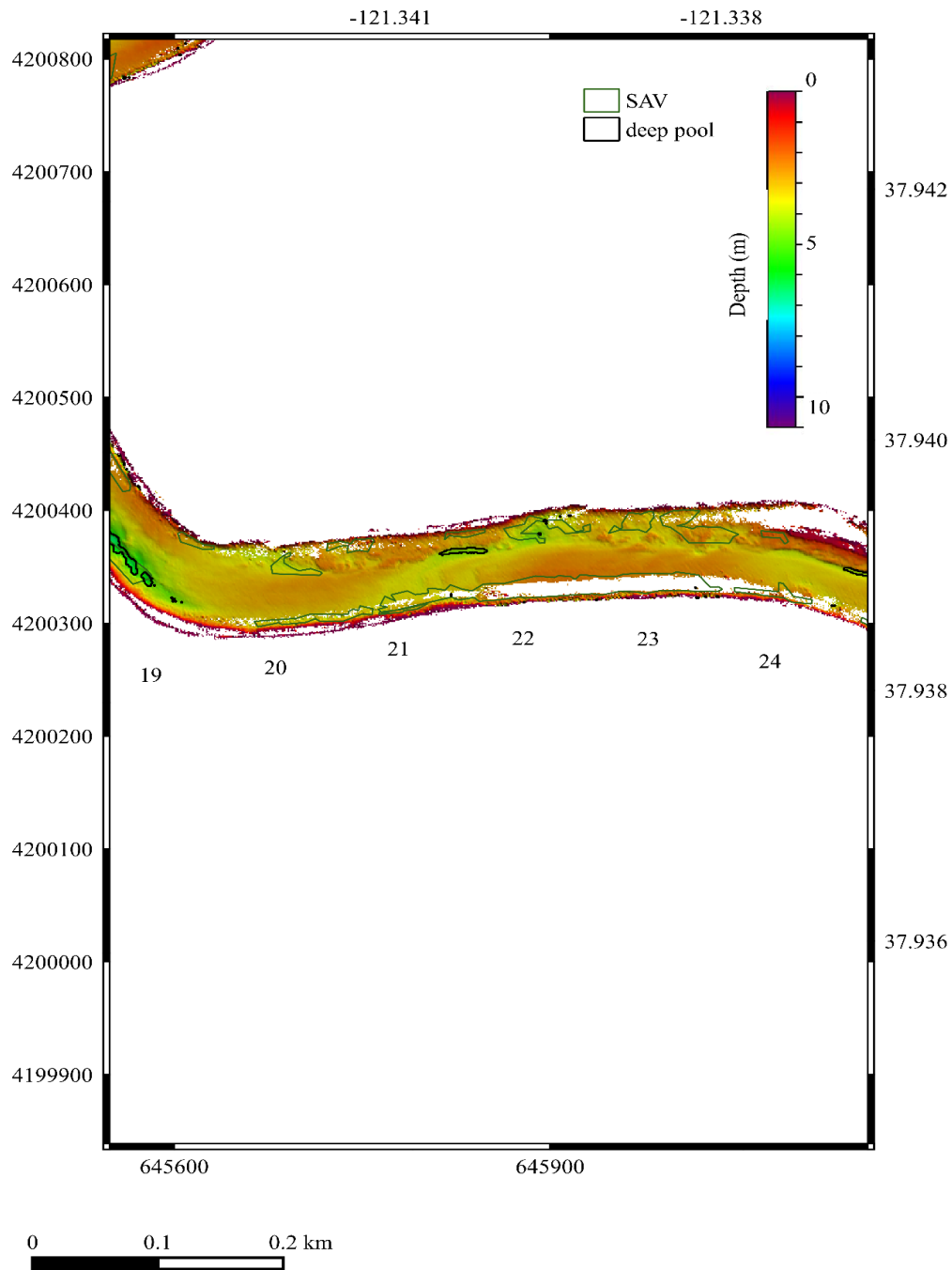


Figure A03. Bathymetry, pool classification (black polygon), and submerged aquatic vegetation (SAV, green polygon). Each 100m along-river segment noted with number. Not to be used for navigation.

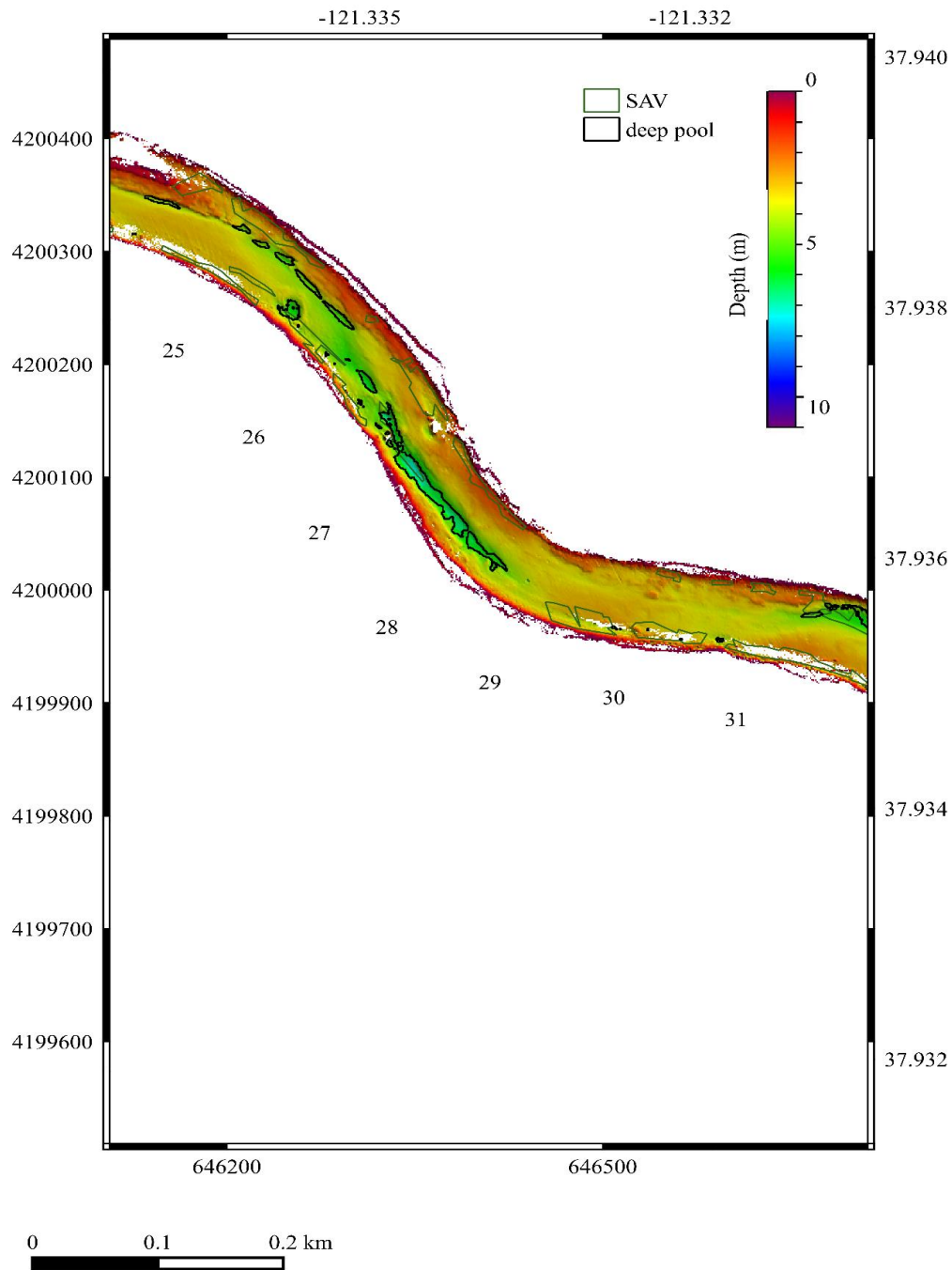


Figure A04. Bathymetry, pool classification (black polygon), and submerged aquatic vegetation (SAV, green polygon). Each 100m along-river segment noted with number. Not to be used for navigation.

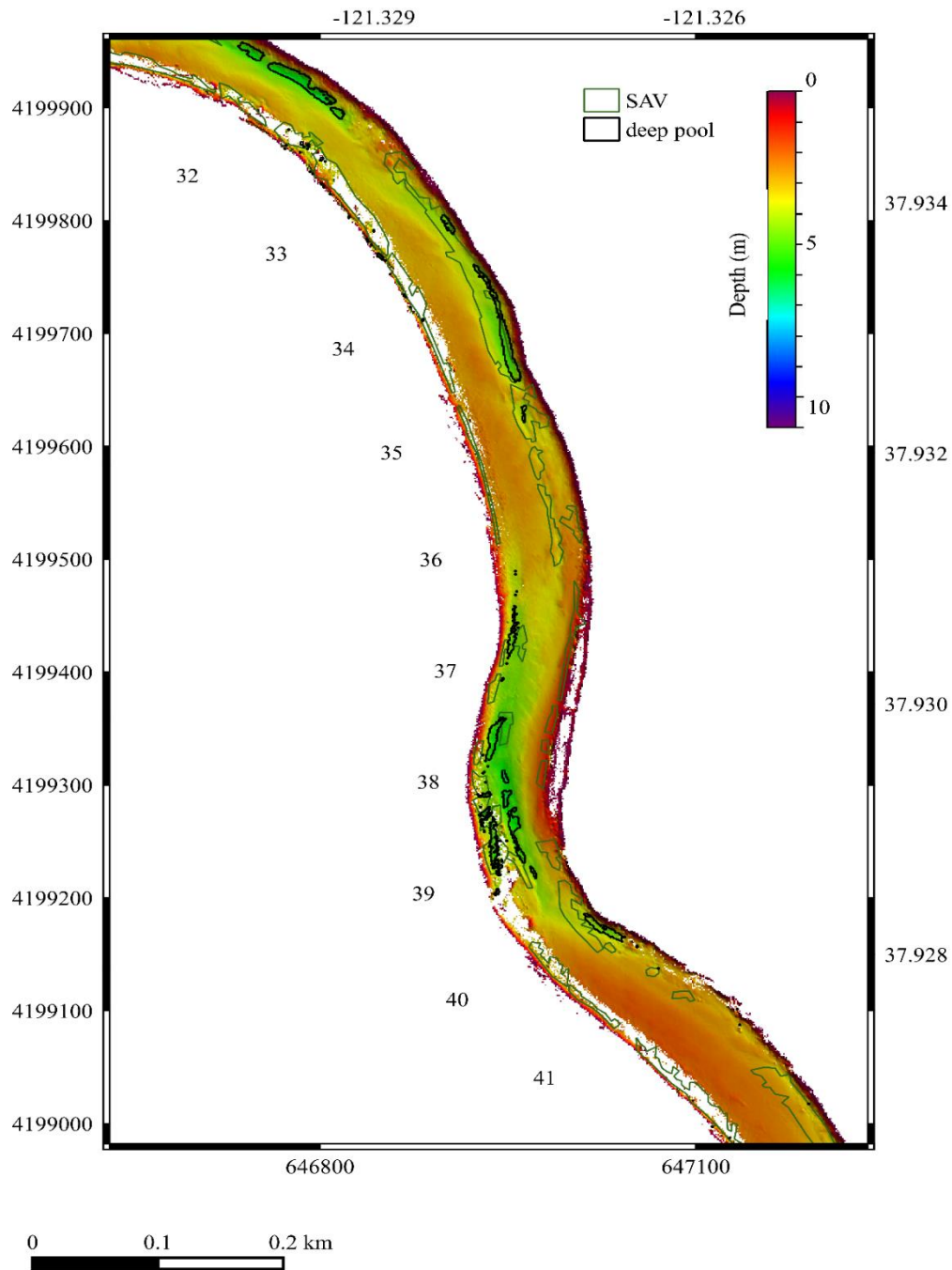


Figure A05. Bathymetry, pool classification (black polygon), and submerged aquatic vegetation (SAV, green polygon). Each 100m along-river segment noted with number. Not to be used for navigation.

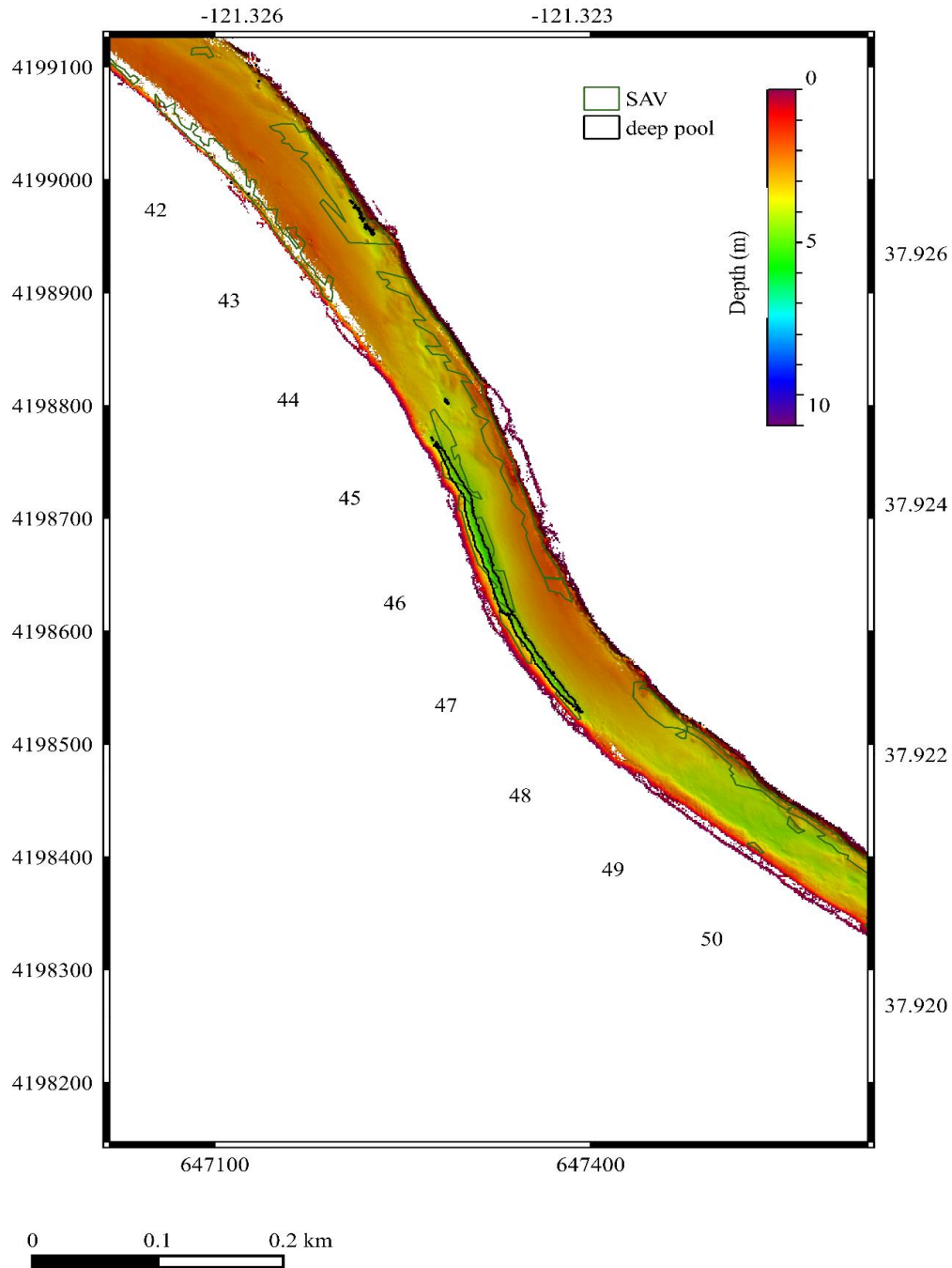


Figure A06. Bathymetry, pool classification (black polygon), and submerged aquatic vegetation (SAV, green polygon). Each 100m along-river segment noted with number. Not to be used for navigation.

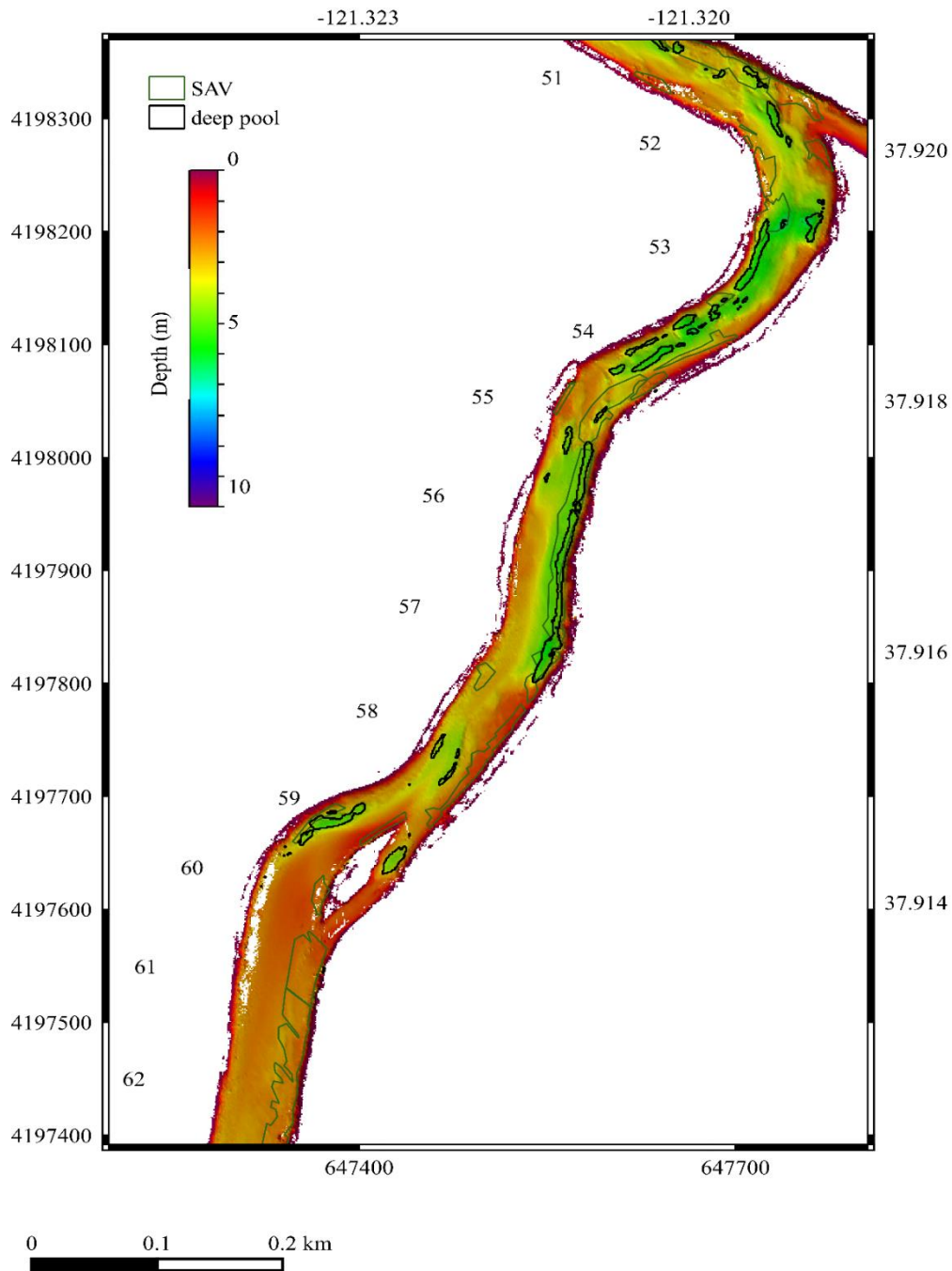


Figure A07. Bathymetry, pool classification (black polygon), and submerged aquatic vegetation (SAV, green polygon). Each 100m along-river segment noted with number. Not to be used for navigation.

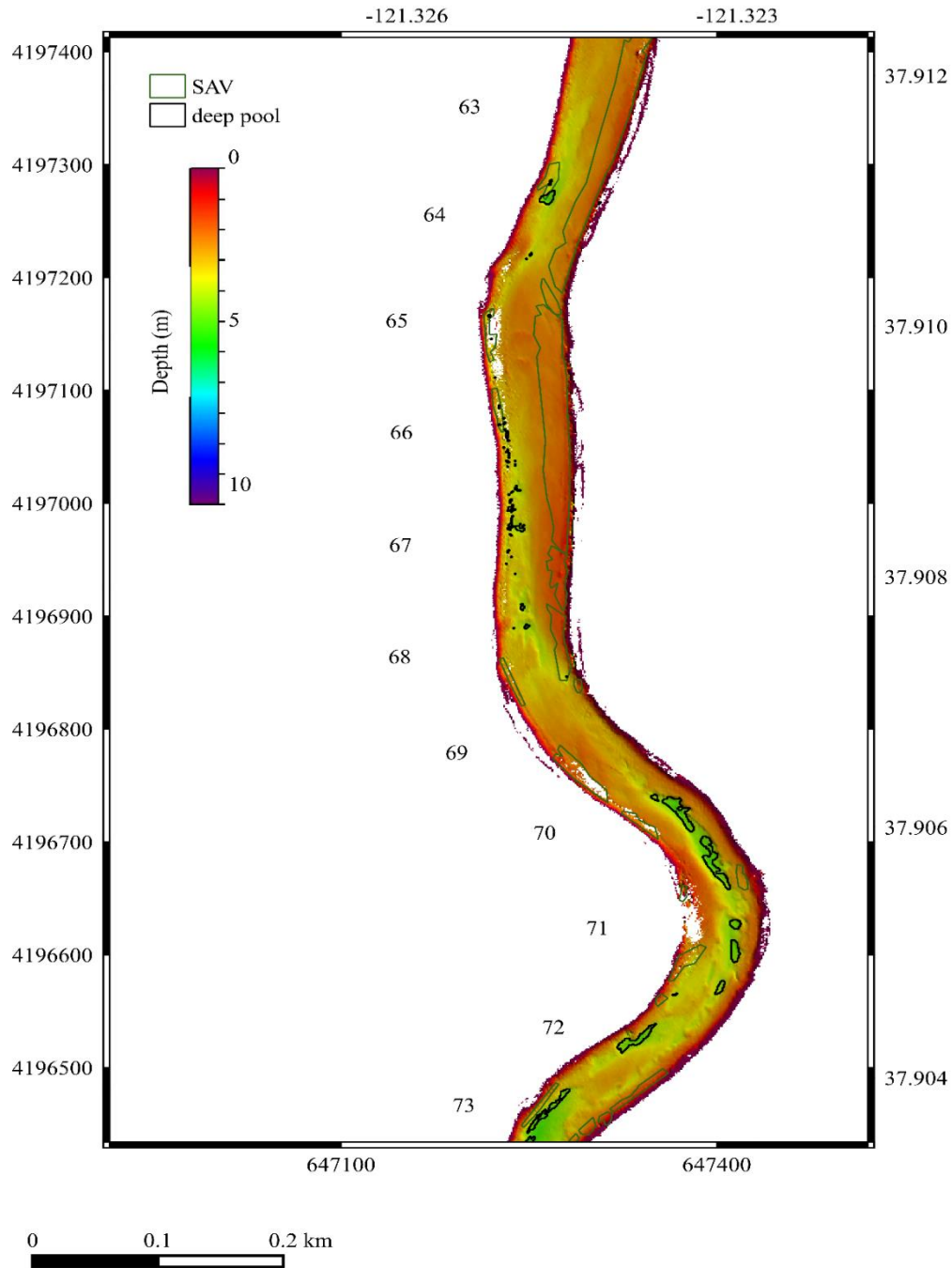


Figure A08. Bathymetry, pool classification (black polygon), and submerged aquatic vegetation (SAV, green polygon). Each 100m along-river segment noted with number. Not to be used for navigation.

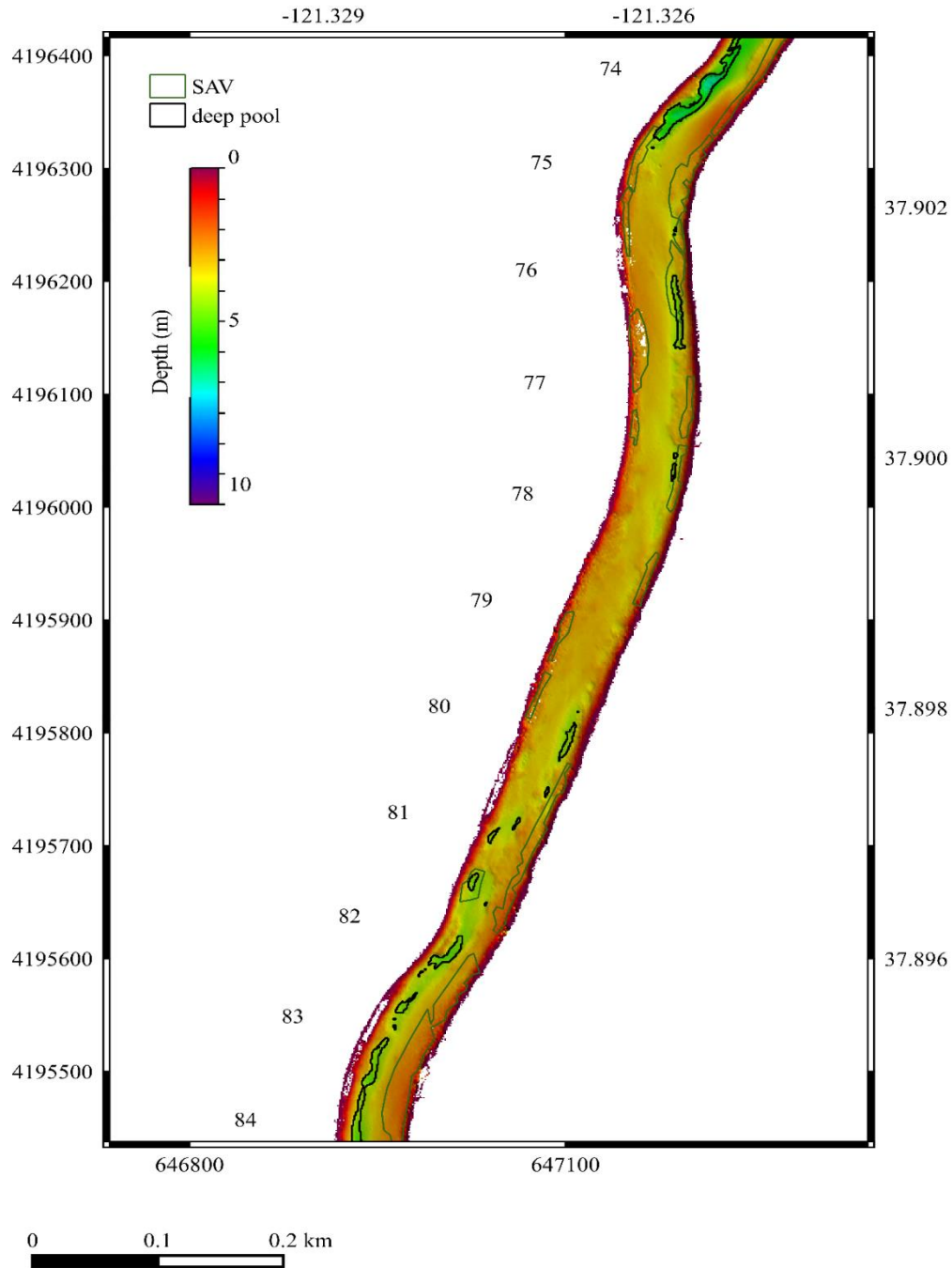


Figure A09. Bathymetry, pool classification (black polygon), and submerged aquatic vegetation (SAV, green polygon). Each 100m along-river segment noted with number. Not to be used for navigation.

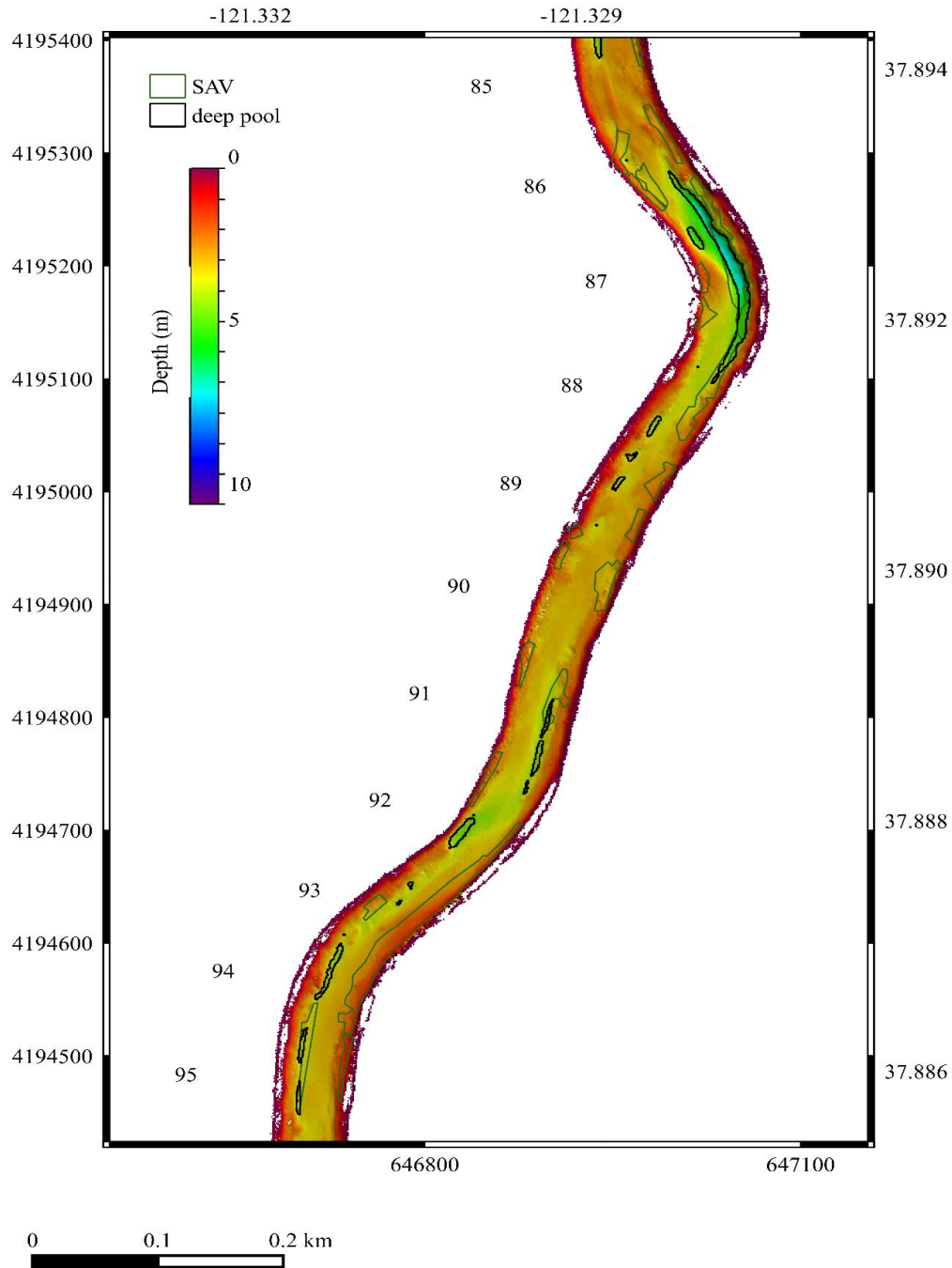


Figure A10. Bathymetry, pool classification (black polygon), and submerged aquatic vegetation (SAV, green polygon). Each 100m along-river segment noted with number. Not to be used for navigation.

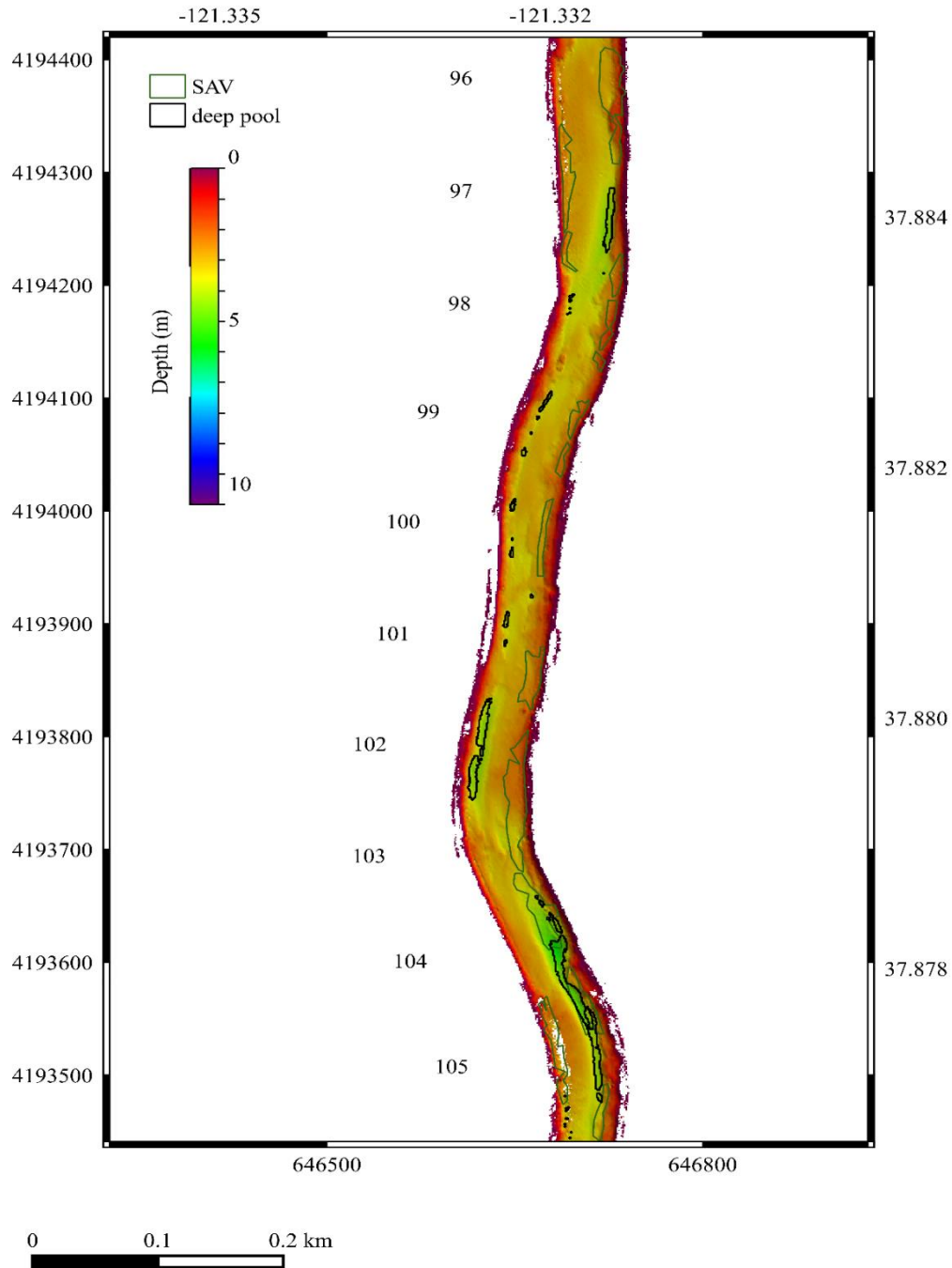


Figure A11. Bathymetry, pool classification (black polygon), and submerged aquatic vegetation (SAV, green polygon). Each 100m along-river segment noted with number. Not to be used for navigation.

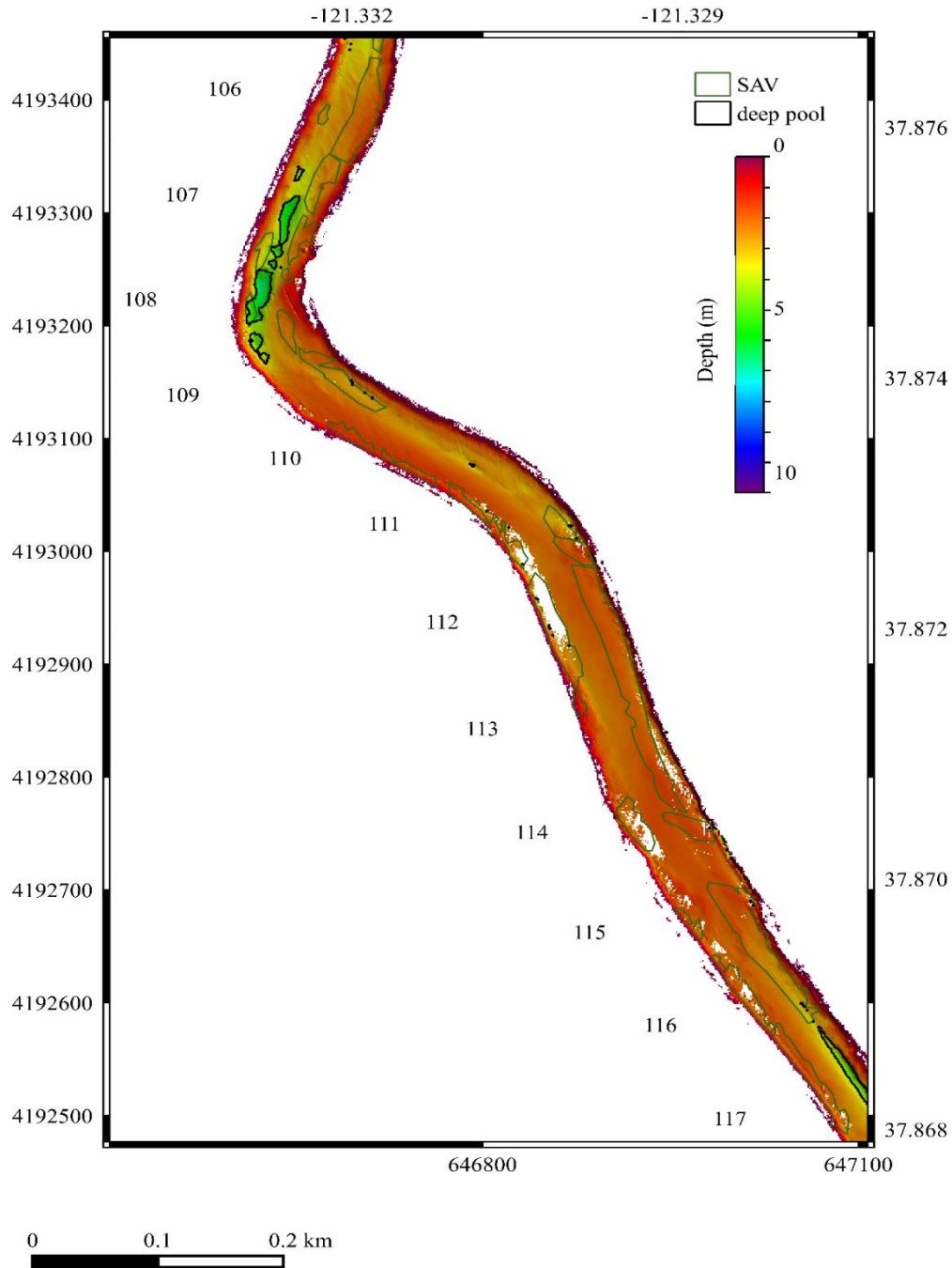


Figure A12. Bathymetry, pool classification (black polygon), and submerged aquatic vegetation (SAV, green polygon). Each 100m along-river segment noted with number. Not to be used for navigation.

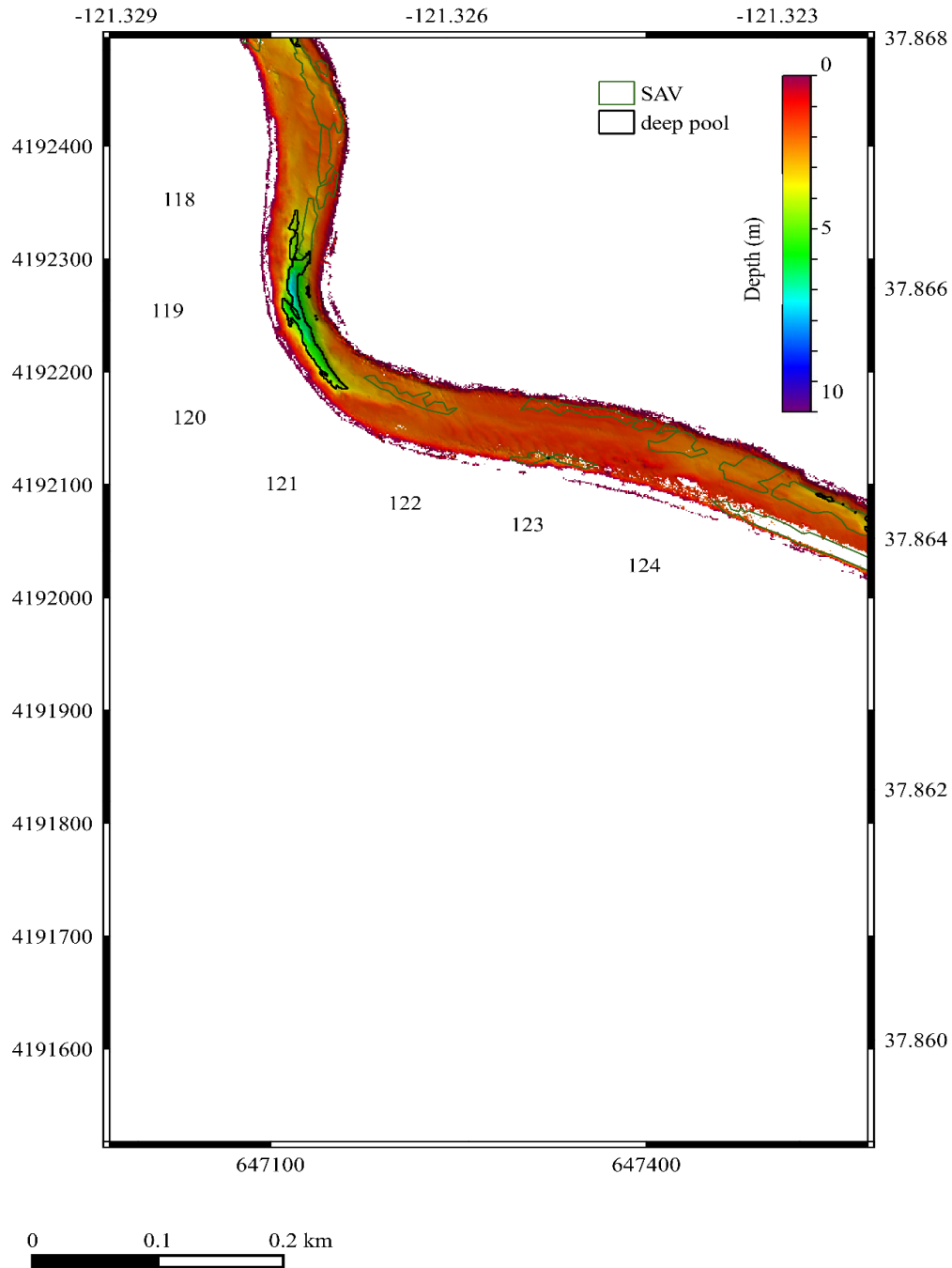


Figure A13. Bathymetry, pool classification (black polygon), and submerged aquatic vegetation (SAV, green polygon). Each 100m along-river segment noted with number. Not to be used for navigation.

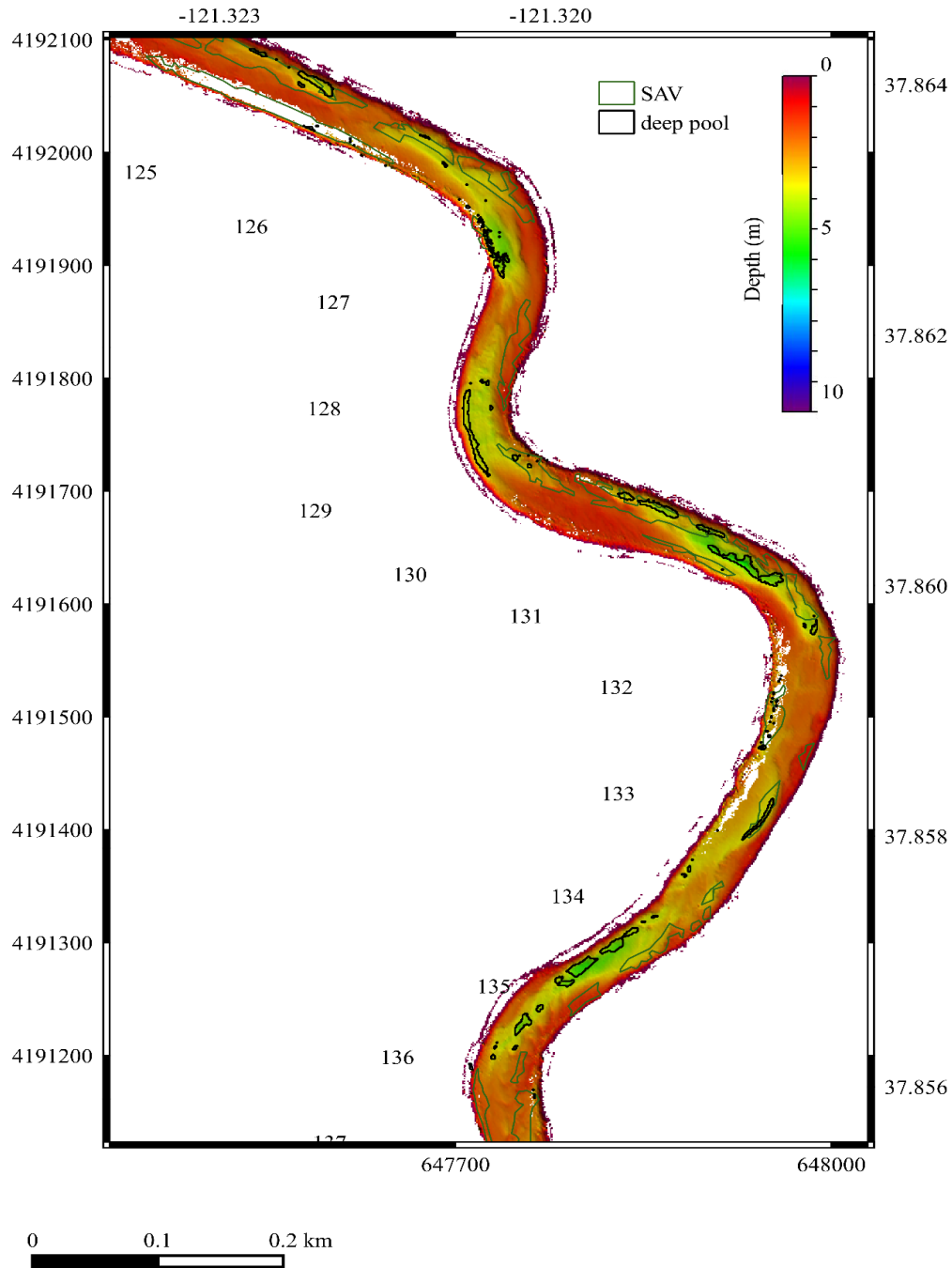


Figure A14. Bathymetry, pool classification (black polygon), and submerged aquatic vegetation (SAV, green polygon). Each 100m along-river segment noted with number. Not to be used for navigation.

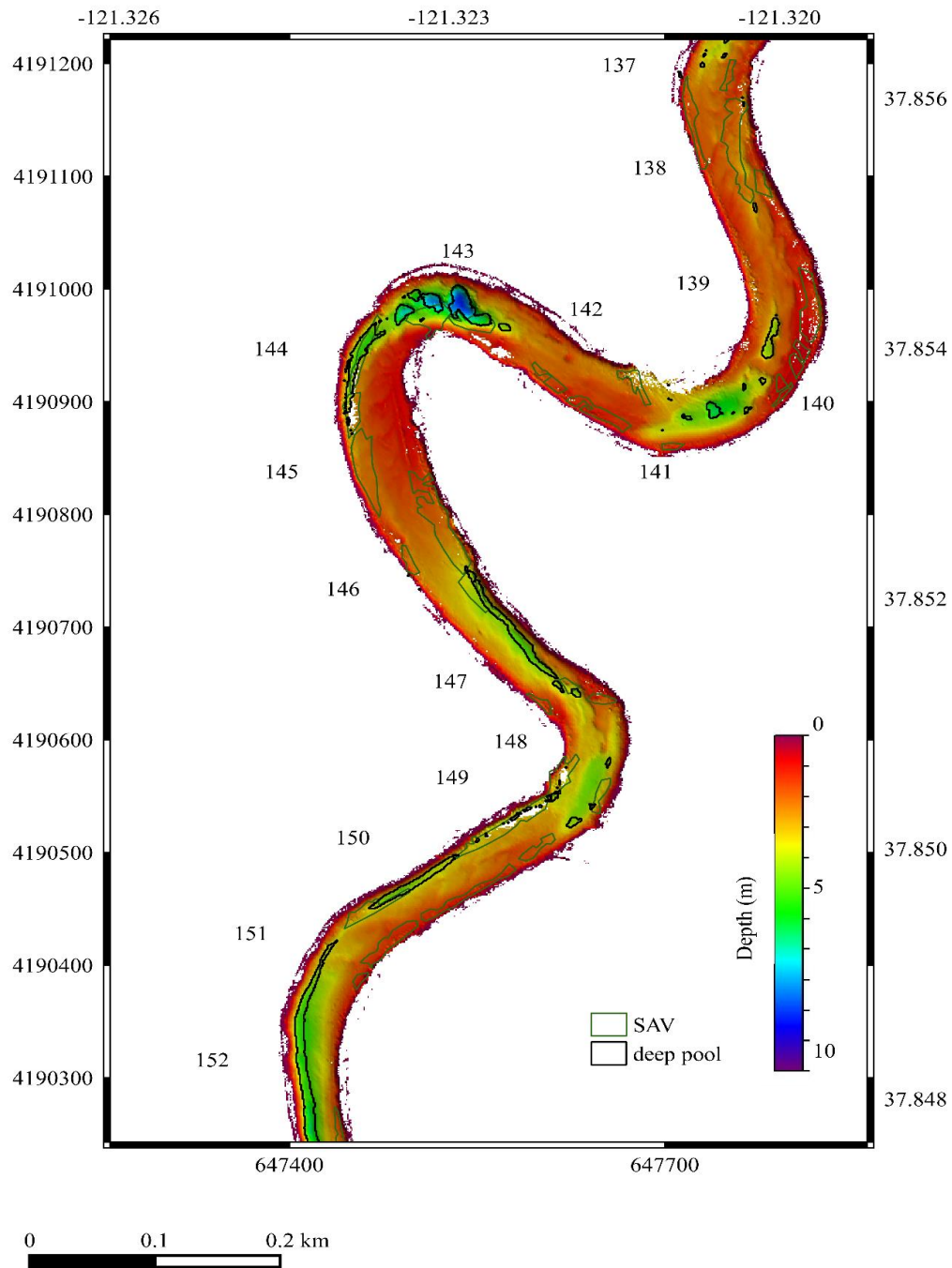


Figure A15. Bathymetry, pool classification (black polygon), and submerged aquatic vegetation (SAV, green polygon). Each 100m along-river segment noted with number. Not to be used for navigation.

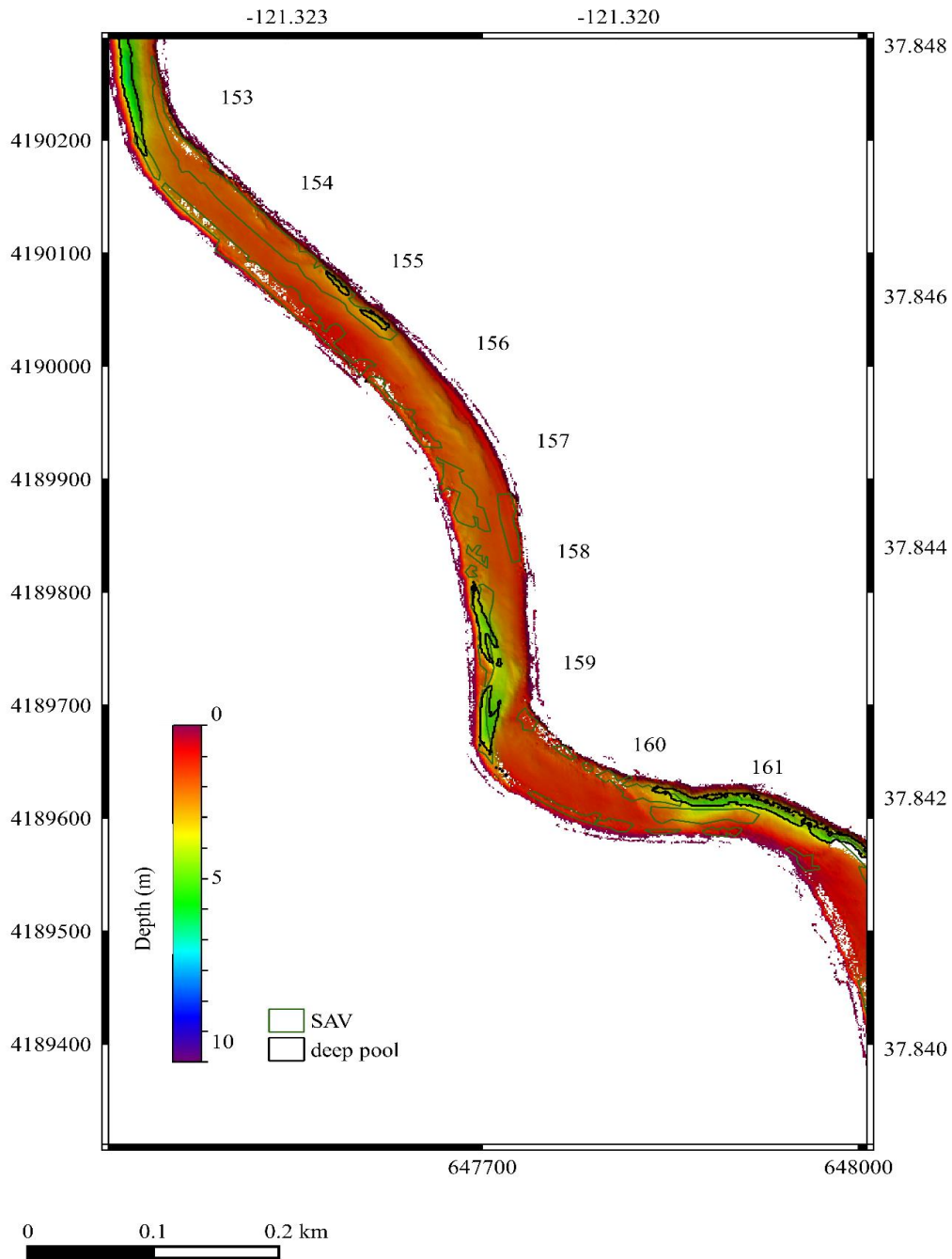


Figure A16. Bathymetry, pool classification (black polygon), and submerged aquatic vegetation (SAV, green polygon). Each 100m along-river segment noted with number. Not to be used for navigation.

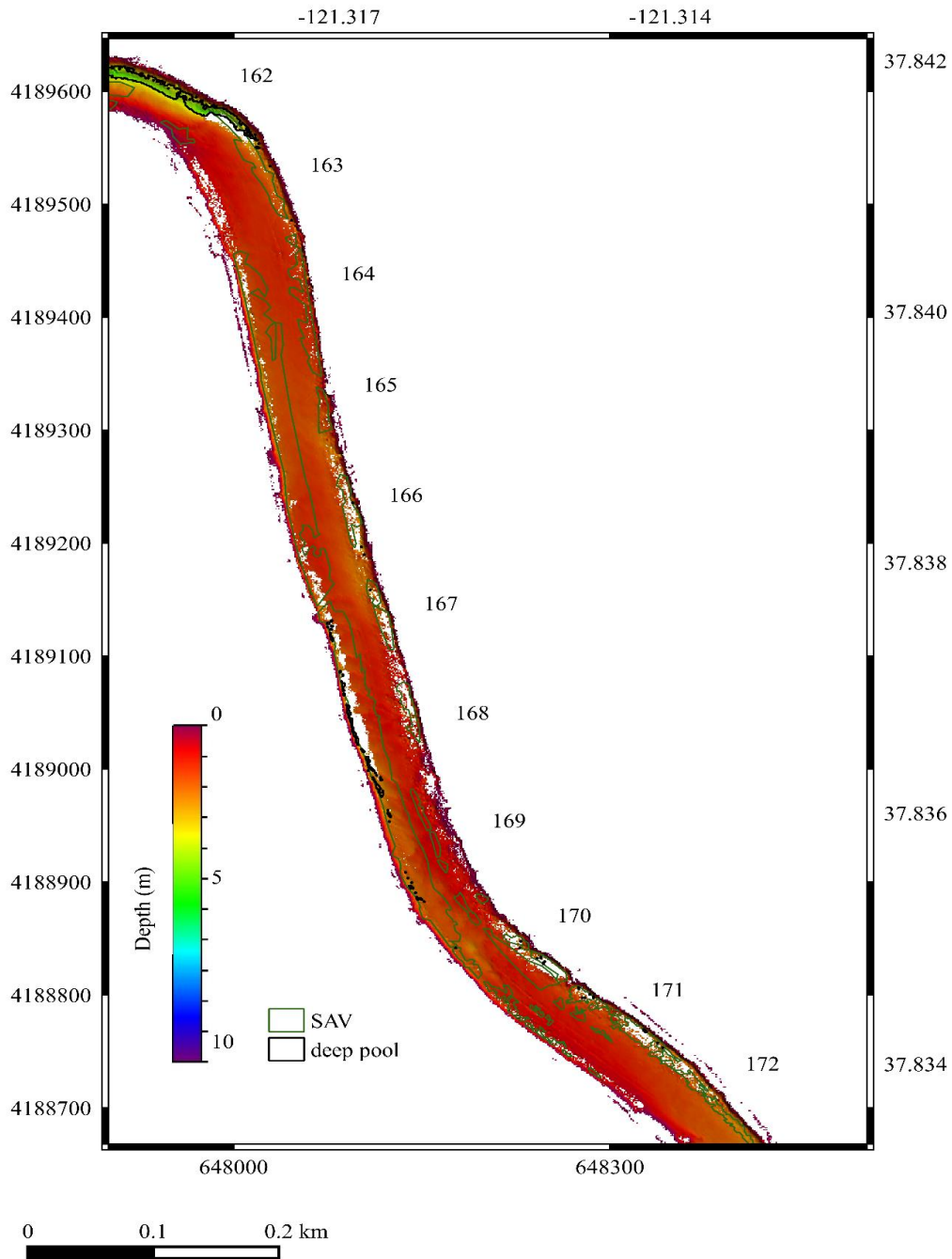


Figure A17. Bathymetry, pool classification (black polygon), and submerged aquatic vegetation (SAV, green polygon). Each 100m along-river segment noted with number. Not to be used for navigation.

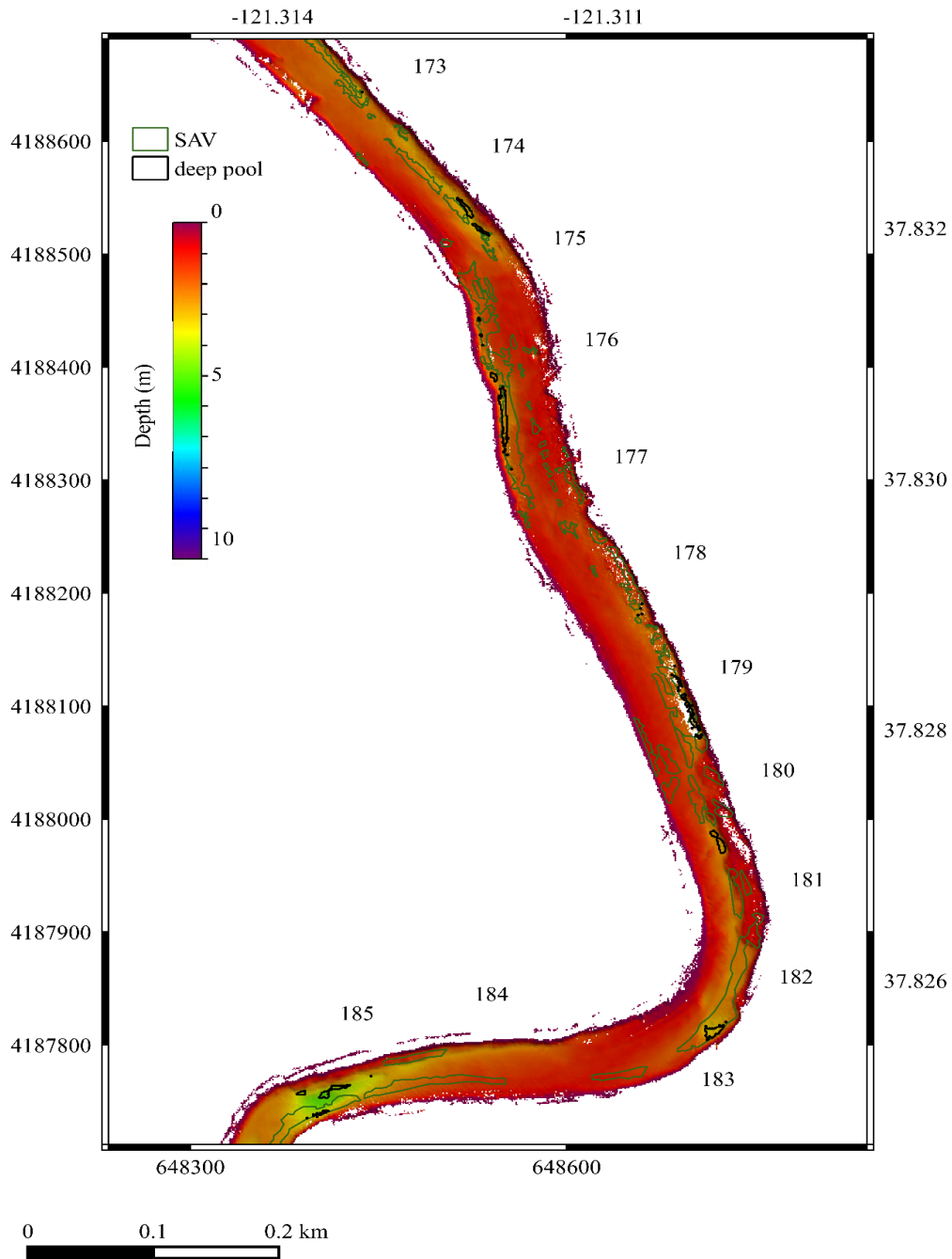


Figure A18. Bathymetry, pool classification (black polygon), and submerged aquatic vegetation (SAV, green polygon). Each 100m along-river segment noted with number. Not to be used for navigation.

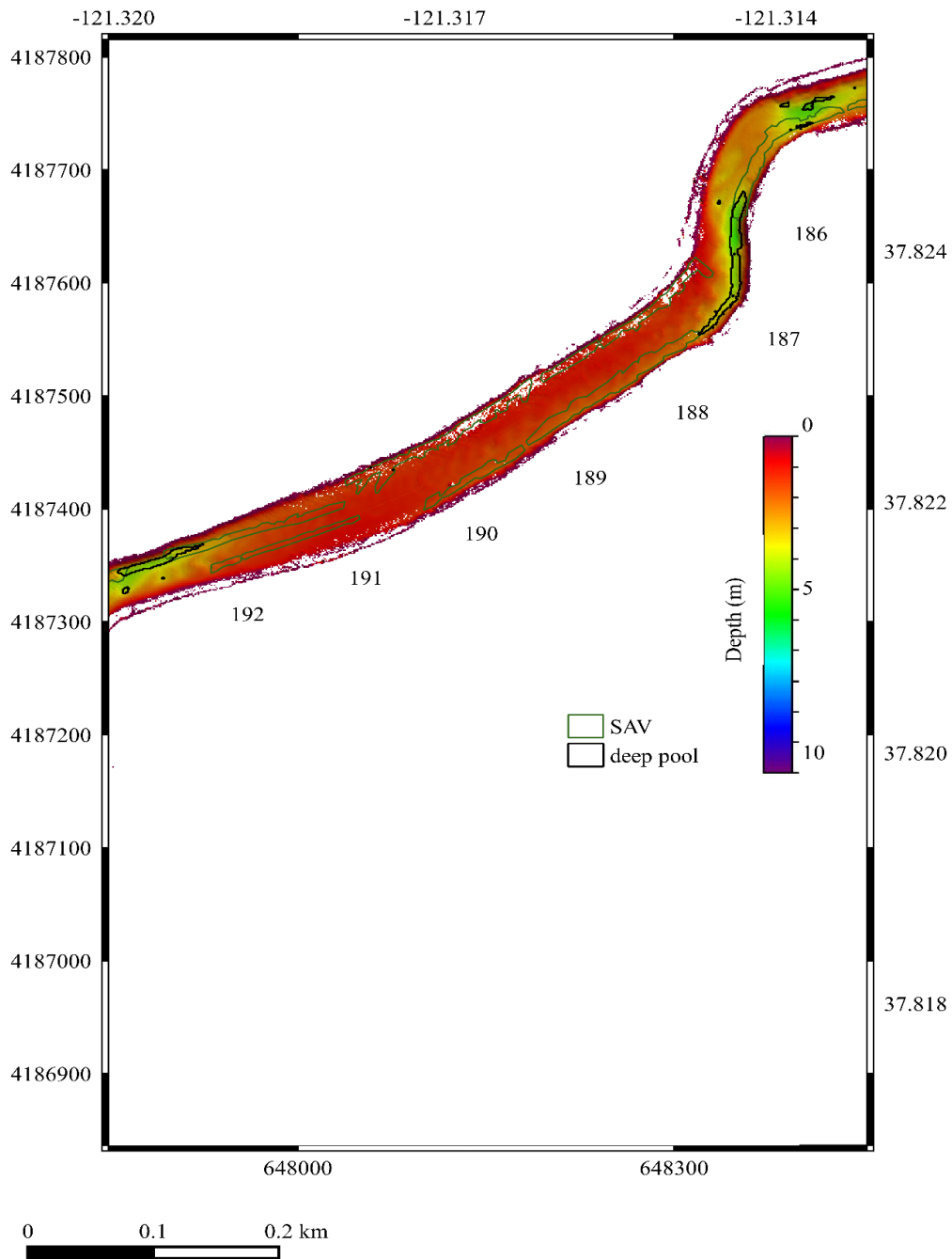


Figure A19. Bathymetry, pool classification (black polygon), and submerged aquatic vegetation (SAV, green polygon). Each 100m along-river segment noted with number. Not to be used for navigation.

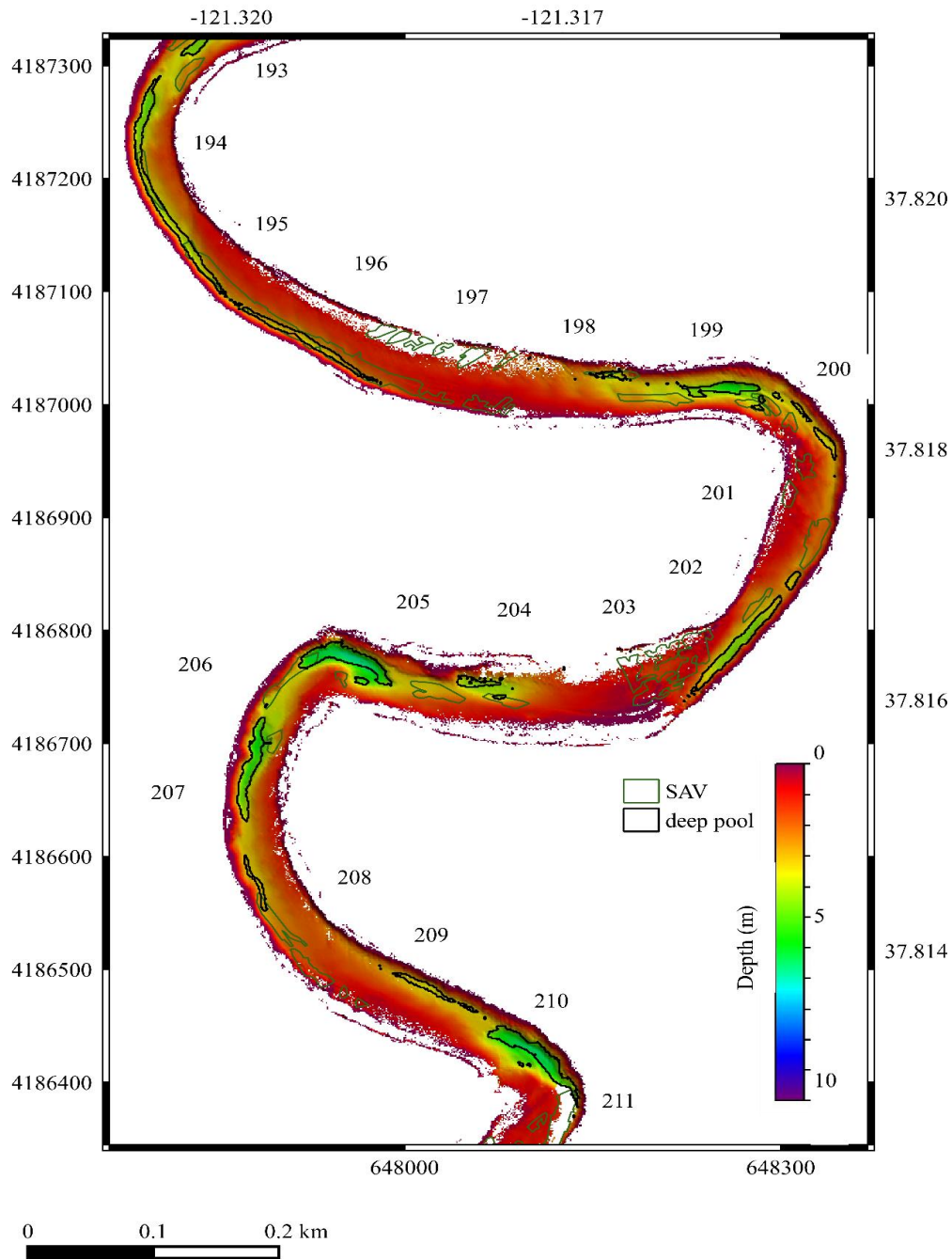


Figure A20. Bathymetry, pool classification (black polygon), and submerged aquatic vegetation (SAV, green polygon). Each 100m along-river segment noted with number. Not to be used for navigation.

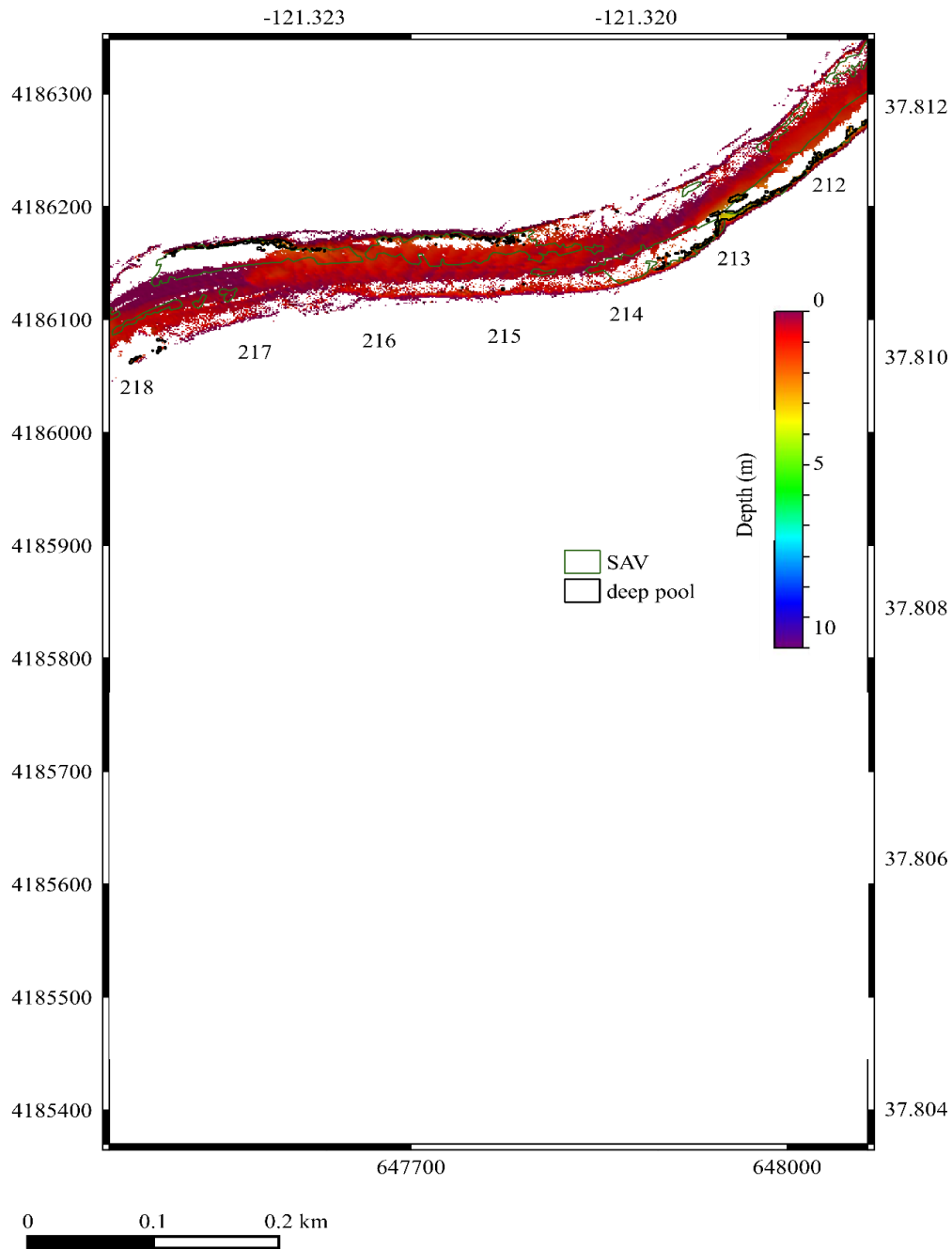


Figure A21. Bathymetry, pool classification (black polygon), and submerged aquatic vegetation (SAV, green polygon). Each 100m along-river segment noted with number. Not to be used for navigation.

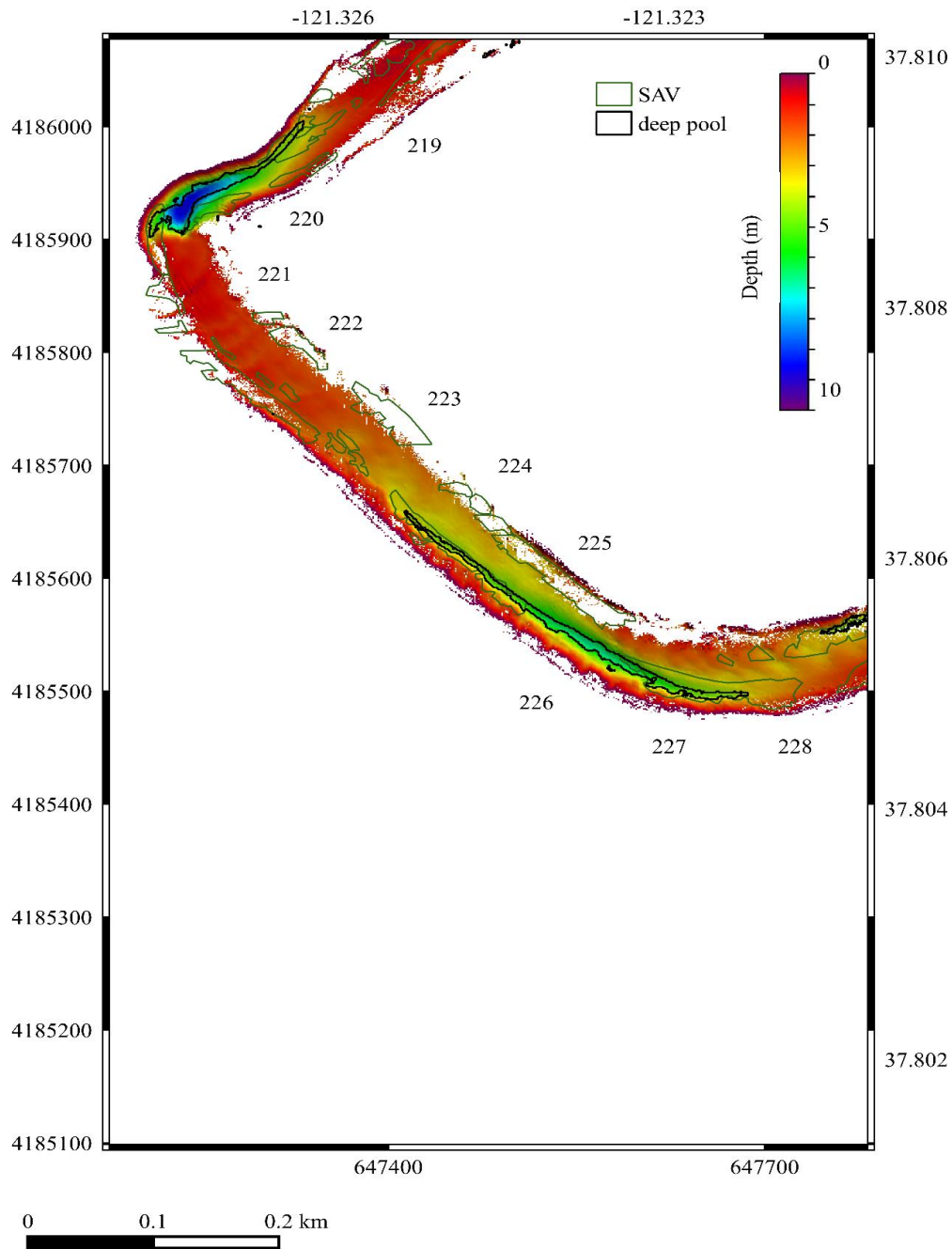


Figure A22. Bathymetry, pool classification (black polygon), and submerged aquatic vegetation (SAV, green polygon). Each 100m along-river segment noted with number. Not to be used for navigation.

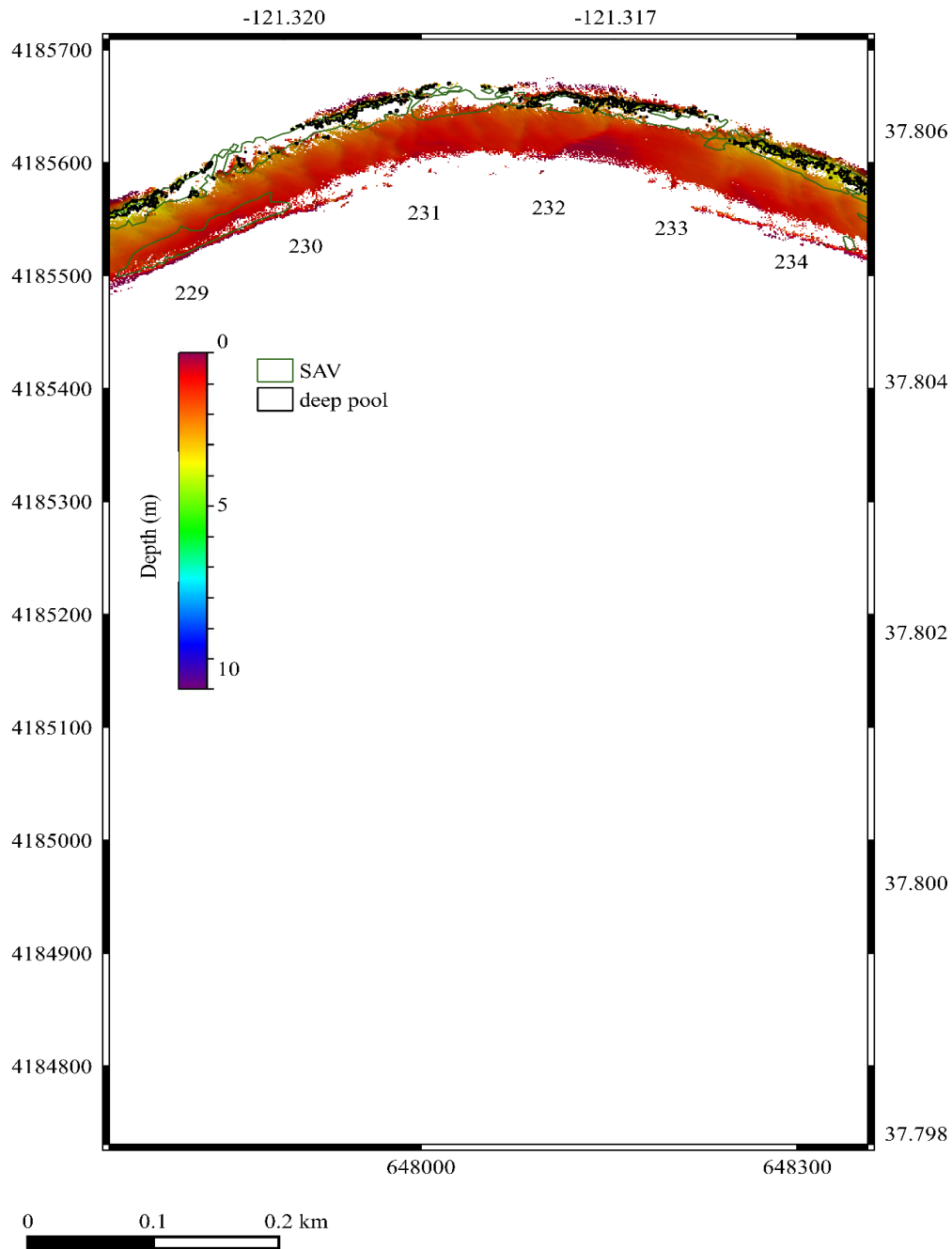


Figure A23. Bathymetry, pool classification (black polygon), and submerged aquatic vegetation (SAV, green polygon). Each 100m along-river segment noted with number. Not to be used for navigation.

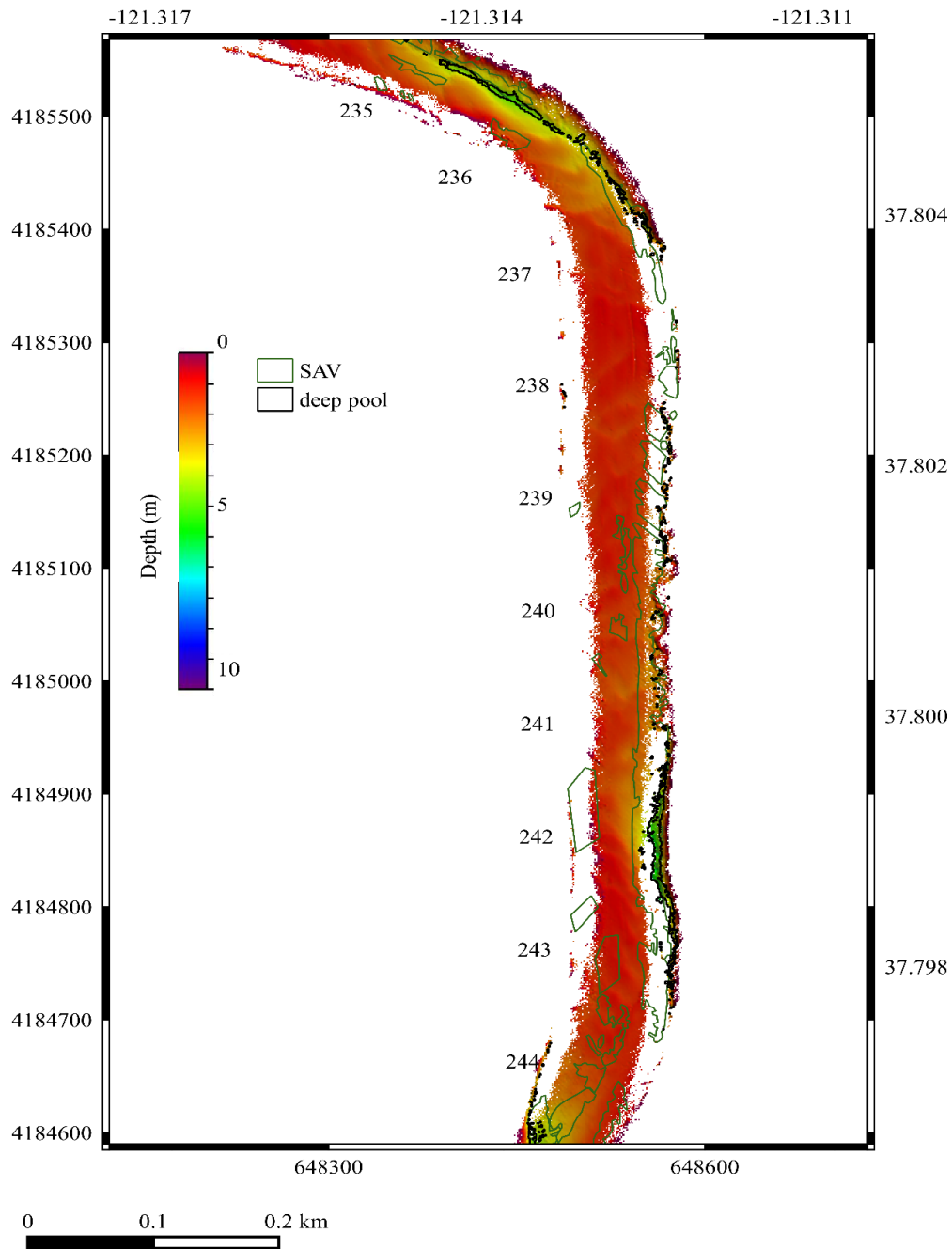


Figure A24. Bathymetry, pool classification (black polygon), and submerged aquatic vegetation (SAV, green polygon). Each 100m along-river segment noted with number. Not to be used for navigation.

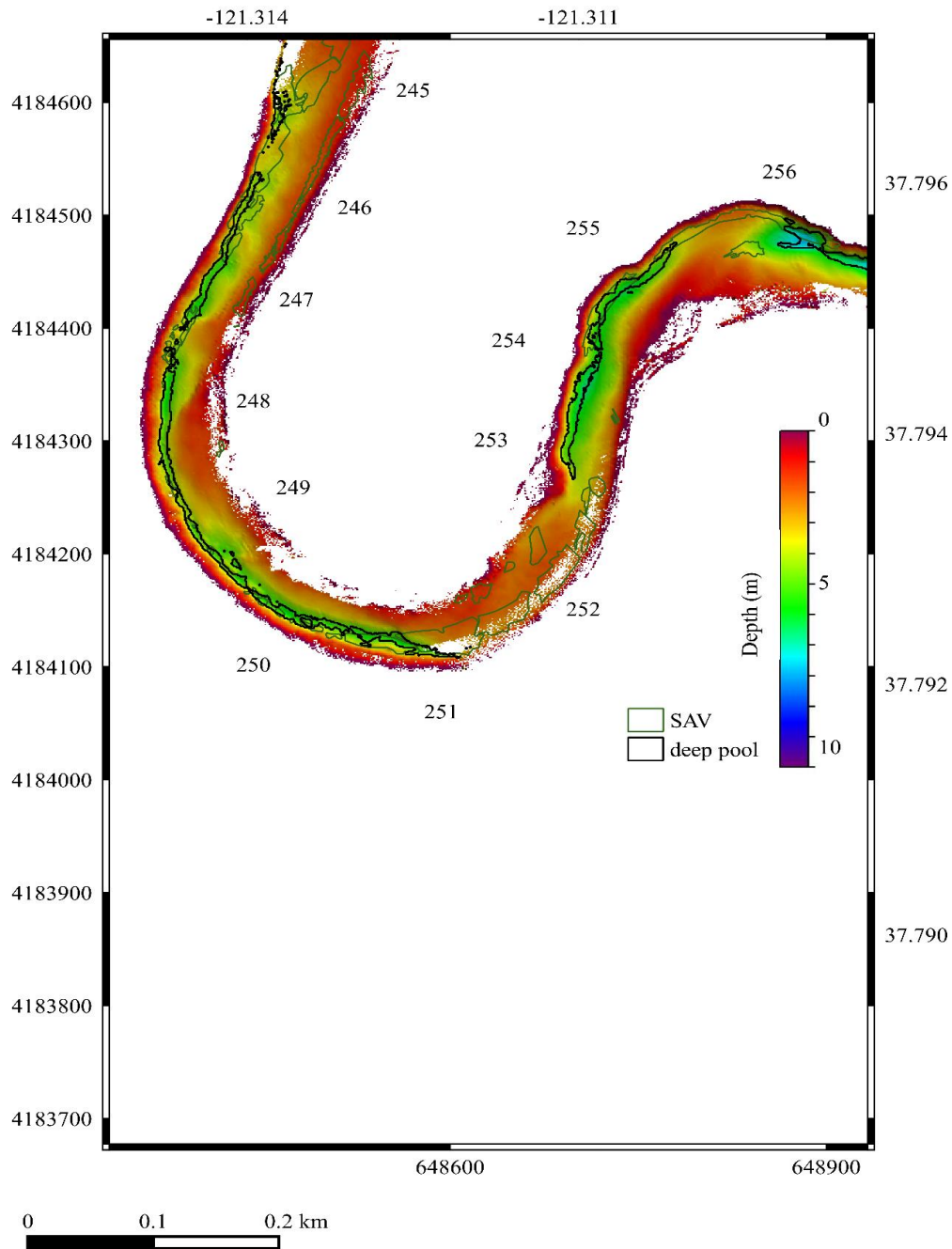


Figure A25. Bathymetry, pool classification (black polygon), and submerged aquatic vegetation (SAV, green polygon). Each 100m along-river segment noted with number. Not to be used for navigation.

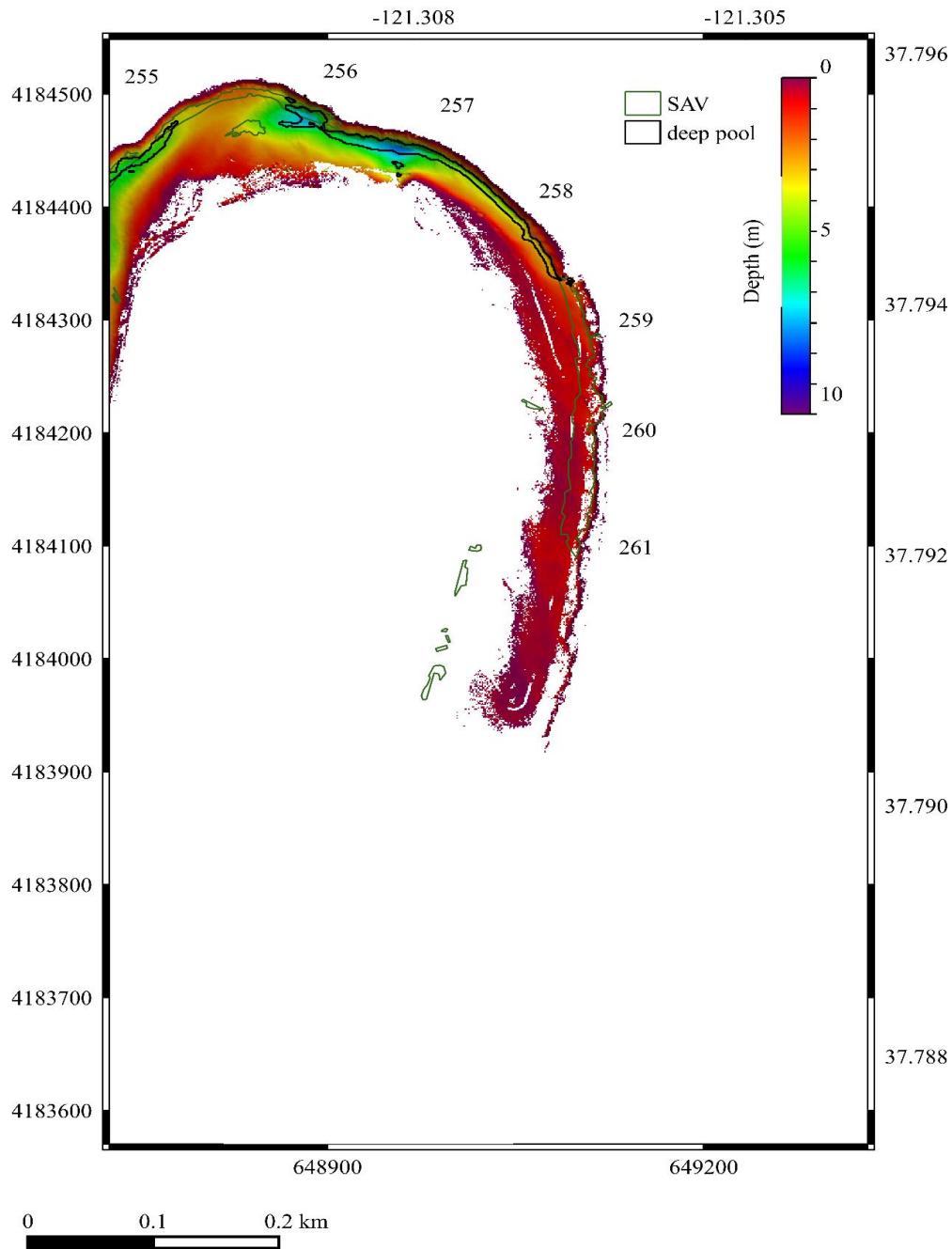


Figure A26. Bathymetry, pool classification (black polygon), and submerged aquatic vegetation (SAV, green polygon). Each 100m along-river segment noted with number. Not to be used for navigation.

Figure A27. Proportion of zeros in density data summarized by 10-m river segments.

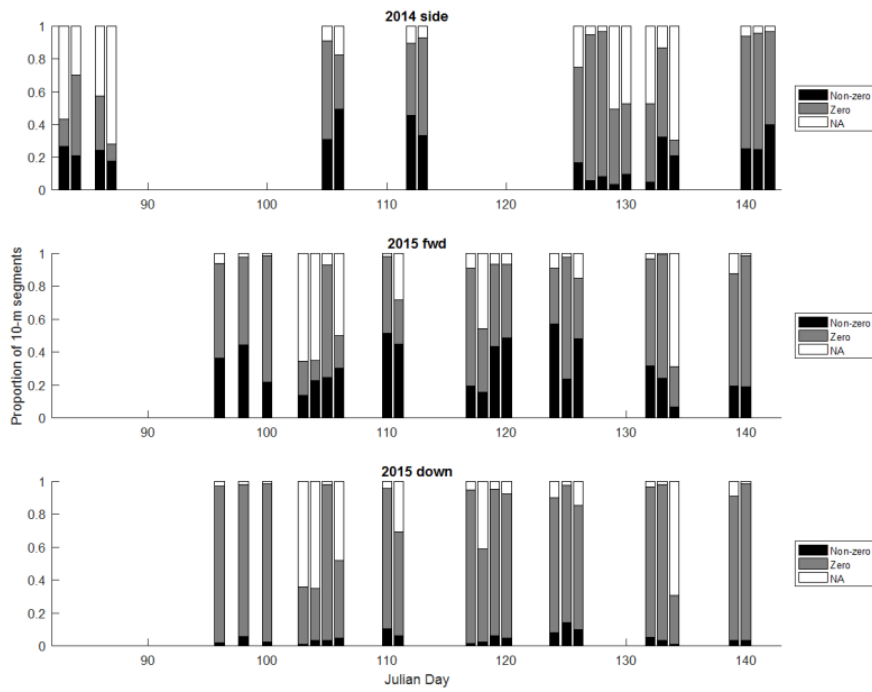


Figure A28. Proportion of zeros in density data summarized by 20-m river segments.

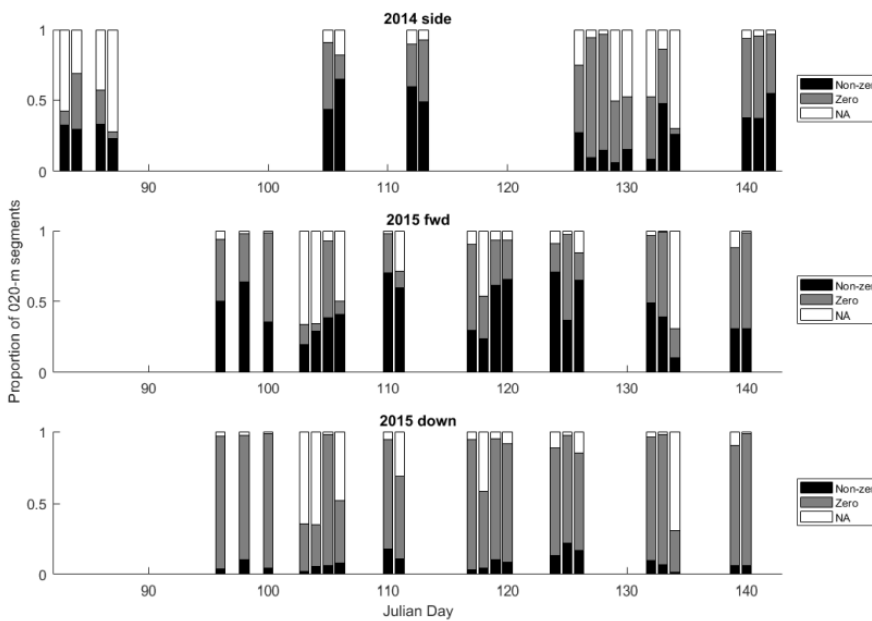


Figure A29. Proportion of zeros in density data summarized by 50-m river segments.

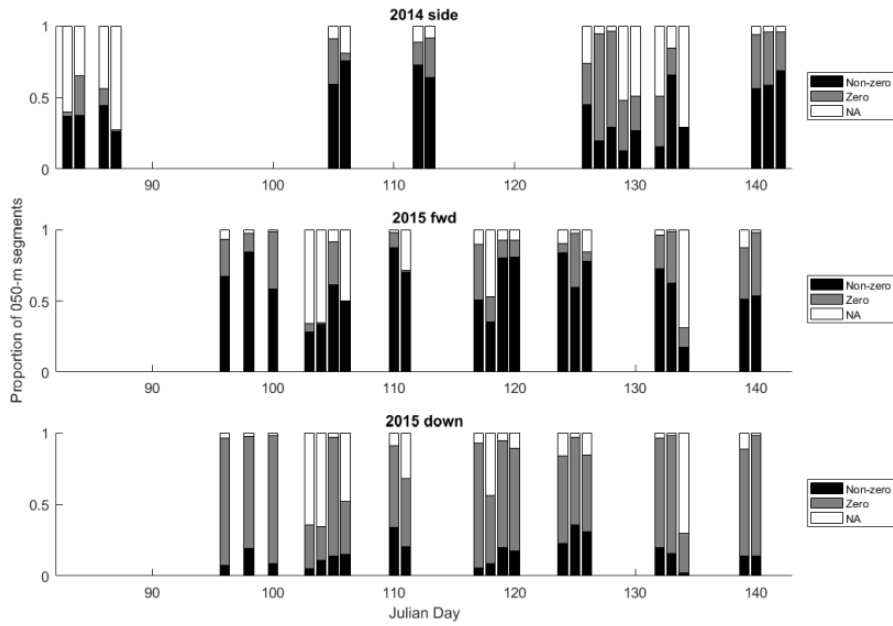


Figure A30. Proportion of zeros in density data summarized by 100-m river segments.

